

Response to Associate Editor Comments

An observational constraint on stomatal function in forests: evaluating coupled carbon and water vapor exchange with carbon isotopes in the Community Land Model (CLM 4.5)

Brett Raczka, Henrique F. Duarte, Charles D. Koven, Daniel Ricciuto, Peter E. Thornton, John C. Lin, David R. Bowling

Manuscript #: doi:10.5194/bg-2016-73, submitted Mar 22, 2016

Thank you to the associate editor, Dr. Sonke Zaehle for an exceptionally thorough review. We have organized the editor's comments with our responses in order from 1 through 37 below. In our opinion the three most important comments from the editor are, first, a need for a description in the methods of the photosynthetic parameters A_j (J_{\max}) and A_p . We address this in editor comments 1, 19 and 29. Second, the description of our $V_{c\max}$ adjustment procedure as a calibration procedure, and the impact of this calibration upon our results in editor comments 5, 6 and 29. Third, the description of our unlimited nitrogen formulation within CLM as analogous to a foliar nitrogen model in editor comments 4, 31 and 33. All pages and line numbers refer to the most recent version of the manuscript, and therefore the page and line numbers referred to by the editor comments are no longer valid.

In addition to the editors concerns, we identified a small error in the previous manuscript draft which required edits to Figure 8, Figure S4 and sections 3.2.2 and 3.2.3 (page 1, line 26; page 19, line 11; page 20, lines 2-4). We sent an email to the editor on 7/28/16 notifying him of this correction which we paraphrase here: The modeled photosynthetic discrimination should have been approximately 2 ‰ lower than what was shown in the previous manuscript draft. This does not change the overall discussion or implications within the manuscript --the model simulation still overestimates the observed photosynthetic discrimination.

Thank you for the opportunity to publish in Biogeosciences.

On behalf of all authors,

Dr. Brett Raczka

brett.raczka@utah.edu

University of Utah

Response to general comments of editor:

Editor: Overall I feel that the manuscript has improved. However, I have a list of comments that require addressing before this manuscript can be published in Biogeosciences. While most of these are mostly editorial matters, some require some further attention and clarification.

Author: We thank the editor for his attention to detail and for providing comments that have improved the clarity of the manuscript.

Editor 1: - P6 Why is only A_c explained, but not A_j or A_p ? Are they not relevant for the study? I think these should be mentioned, though for the sake of the paper, eq 2 and 3, as well as their A_j and A_p counterparts could become part of an methodological Appendix.

Author 1: We made a judgment call on where to make a cutoff for equations. Our goal was to include those that were most relevant to our analysis. We defined (through text) A_j and A_p (page 5, lines 19-23), and also provide the reader Oleson et al. (2013) as a source for further details—a manuscript freely available on the CLM website without a journal subscription. We included equation (2) to define A_c (instead of A_j and A_p) because 1) this links V_{cmax} to net assimilation (A_n) 2) V_{cmax} becomes important later on because of our calibration procedure. In this way we think we achieved a good balance of brevity and clarity relevant to our main focus. In an effort to better address A_j and A_p we add text to page 6, lines 5-6 and page 13, line 12-14 that explains our calibration procedure influences not only V_{cmax} but A_j and A_p as well.

As suggested we could create a methods appendix for equations (2) and (3) but feel inclusion in the main text was necessary given the importance of our calibration procedure, and also feedback from the first line of reviews including from Ralph Keeling that requested some of these equations in the main text.

Editor 2: - Eq 11: Explain why A_n is assumed to be reduced, but g_s not. This violates eq 4.

Author 2: Just to be sure we are on the same page, technically, within Eq. 11 A_n is NOT assumed to be reduced. Both A_n and g_s within eq. 11 directly follow from the coupling in eq. 5. However, and this is a critical point, the coupling between A_n - g_s in equation (5) happened BEFORE the nitrogen limitation step in eq. (9). The fundamental reason for why the $(1-f_{dreg})$ is necessary in equation (11) is because this version of CLM only has partial or temporary coupling between A_n - g_s . As described on page 8-9, lines 16-32 and 1-2 and page 16 lines 16-22 and also in previous reviewer/editor responses the stomatal conductance (eq. 5) is solved prior to the nitrogen downregulation step eq. (9). Therefore prior to the nitrogen downregulation the model is still fully coupled between A_n - g_s . However, once the GPP is downregulated through nitrogen limitation, the model is technically un-coupled, because the reduced A_n (call it A_n^*) is no longer consistent with g_s in equation (5), hence partially-coupled, or as you say eq 5 is violated. In

order to account for this within the discrimination part of the model (eq 11) the $(1-f_{dreg})$ term adjusts the A_n (solved for in Equation 5). In effect the $(1-f_{dreg})$ artificially reduces A_n to A_n^* therefore artificially boosting c_i to c_i^* .

We apologize if this was already clear and what you may actually be asking is: why does ONLY A_n have the $(1-f_{dreg})$ coefficient and not g_s in (eq. 11)? In other words why is A_n adjusted to A_n^* and g_s not adjusted to g_s^* ? This is admittedly a potential weakness in the model and we believe one of our key findings. The allocation downscaling approach to nitrogen limitation, in effect, forces a decoupling between A_n - g_s , and the impact of that decoupling has implications upon the discrimination, which in part is accounted for with the inclusion of the $(1-f_{dreg})$ expression in equation 11. Based upon our findings in this manuscript the $(1-f_{dreg})$ is not sufficient. We believe it is worth testing a foliar nitrogen model (which allows for a dynamic nitrogen budget linked to V_{cmax} and full coupling between A_n - g_s) within the framework of CLM (Ghimire et al. 2016) and we say this in pages 22-23 lines 28-31; 1-2 and in the conclusions on page 26, lines 13-16. We hope to test this another manuscript, but it is out of the scope for this manuscript.

Editor 3: Also verify scaling coefficients for g_b and g_s . My textbook says the diffusion correction factors are 1.37 for boundary layer and 1.6 for stomate's whereas your equation suggests the inverse. This will obviously have a fairly significant effect on the predicted c_i and thus discrimination!

Author 3: We double-checked and this is how the coefficients are defined in equation (25.10) of Oleson et al. (2013), and also the way they are implemented within the source code of CLM 4.5. Equation (25.10) comes directly from equation (8.31) in Oleson by solving for c_i . The terms 1.4 and 1.6 are the ratios of diffusivity of CO_2 to H_2O for the leaf boundary layer resistance and stomatal resistance respectively, however because equation (25.10) is expressed in terms of conductances ($1/resistance$) the coefficients are reversed and therefore 1.4 is multiplied by the leaf stomatal conductance and 1.6 is multiplied by the leaf boundary layer conductance.

Editor 4: - P8 L10: It is unclear where this nitrogen is then coming from? Does this not break the logic of CLM 4.5's closed N budget and introduce an unknown source of N? Or is this only assumed in eq 11 (then be more precise as to how this is implemented, and what happens to the extra C assimilation).

Author 4: It is important to distinguish between the two different model formulations, the *limited nitrogen* formulation and the *unlimited nitrogen* formulation, which are two entirely separate CLM simulations. As we have described on page 8-9 lines 16-32, 1-2 and also illustrated in Figure 1 the *limited nitrogen* formulation calculates a potential amount of allocated carbon (CF_{avail_alloc} , Eq. 8) and then the actual amount of allocated carbon (CF_{avail} , Eq. 8) based upon nitrogen availability. This 'extra' carbon as you call it (i.e. the difference between $GPP_{pot} - GPP$) is instantaneously 'lost' to the system (i.e. does not show up as a respiration flux etc.) We state this on page 8, line 27-29.

The unlimited nitrogen formulation ignores the nitrogen budget entirely and assumes that there is an unlimited amount of nitrogen in the system (i.e. nitrogen does not impose a limit on the allocation at all). We described this in page 8 lines 8-15. CLM 4.5's closed N budget is not considered in this case, and your intuition is correct to ask: when this 'extra' nitrogen is provided are the results realistic? The answer is no. If provided unlimited nitrogen CLM is much too productive (See Figure S2; uncalibrated run for unlimited nitrogen formulation). That is why we performed a separate V_{cmax} calibration for the *unlimited nitrogen* simulation to provide reasonable productivity (see page 13, lines 3-10). In this way although the *unlimited nitrogen* formulation ignores CLM 4.5's closed N budget, it still parameterizes the effect of nitrogen limitation within the V_{cmax} calibration. This is more similar to a foliar nitrogen style model as we discuss on page 22, lines 28-31, 1-2. We have added text to clarify that although the *unlimited nitrogen* formulation ignores CLM 4.5's nitrogen budget, it still accounts for nitrogen limitation through the V_{cmax} parameterization (page 8 line 8-12).

We recognize this is a difficult point to grasp, but hopefully the above explanation and manuscript edits have made it clearer.

Editor 5: A further point needing attention is that I think labelling your V_{cmax} tuning a calibration is misleading, because the calibration directly includes the observed and simulated GPP as a factor, depends on time-varying site-data, and is not useful outside without site-data. This approach does override a lot of the model's internal dynamics and exceeds what is conventionally called "calibration". It is not surprising that the "calibrated" model performs better, because you prescribe the seasonal course of GPP. Section heading 2.4 and associated text is hence misleading.

Author 5: We agree with the editor that the V_{cmax} calibration approach is limited in its applicability given it was created based on simulated/observed GPP at Niwot Ridge. We state this in the manuscript on page:14 lines: 1-4 '*.....within the confines of our study area*, our calibration approach was sufficient to provide a skillful representation of photosynthesis and provided a sufficient testbed for evaluating carbon isotope behavior.' To further clarify this point we have added an additional line cautioning against the application of this calibration outside of the study area. Page: 14, lines 3-4.

Although our calibration approach may not be as common, it is a time-varying parameter optimization approach that falls under the general umbrella of calibration where the end goal is to use observations to adjust parameters to reduce model-observation mismatch. Just like any other calibration approach it can correct for inaccurate parameters, and sometimes (both directly/indirectly) for structural errors within the model. For example, the approach to force the winter-time GPP to zero, in effect compensating for structural errors, is a more aggressive approach, however has been done before (Kolari et al. 2007). Therefore we suggest we keep the calibration title in 2.4 as this is well recognized within the community, and add the new text that emphasizes the limitation in our approach.

Editor 6: Because this is the case, I don't think that there is a need to emphasize differences between the off-the-shelf CLM 4.5 and your improved version. This is particularly the case as

this manuscript focusses on the use of ^{13}C as a constraint. I therefore don't see the relevance of presenting the off-the-shelf parameterisation in 3.1. specifically if the model behind the seasonal dynamics of GPP are fundamentally different between the two. The discussion of how to improve the seasonal representation of GPP also seems off topic as it does not involve the use of isotopes, and I would therefore suggest to drop this.

Author 6: We agree, and eliminated detailed discussion (~8 lines) that compared the difference between the calibrated and uncalibrated model runs in an effort to focus on isotope results. We also cut approximately 6 lines of discussion concerning the seasonal representation of GPP in an attempt to stay on topic. We kept the discussion about how our calibration approach could be improved by addressing the underlying structural problems within the model. This is useful because it emphasizes the limitations of our calibration approach (as the editor pointed out earlier) and also provides other modelers with insights on how to improve model performance.

Editor 7: The results section contains large stretches of classical discussion (Sections 3.3 and 3.4). They should be part of a discussion section and not the results, as such as no new evidence is presented and they distract the reader from the results you present.

Author 7: We moved Sections 3.3 and 3.4, previously a part of the Results & Discussion section, to the Discussion section. They are now Section 4.1 and 4.2.

Editor 8: The abstract is currently very long. Please try shortening it a bit. Pre- and post-photosynthetic N limitation are CLM construct and thus not clear to the general readership. I would reformulate this to read that the default An-gs coupling of CLM failed, but a revised formulation coupling An and gs did successfully capture the observed dynamics without mentioning the CLM-terms, which are ok to use (though still awkward) in the manuscript).

Author 8: We reduced the abstract by removing 2 non-essential sentences concerning soil moisture and WUE/discrimination trends. We also included the coupling terminology suggested by the editor. In addition we have explicitly stated in the Methods on page 8-9 lines 29-32, 1-2 that the limited nitrogen formulation has partial coupling between the carbon-water cycle and that, the unlimited nitrogen formulation is fully-coupled. Before it would not have been clear until the discussion that this was the case. We also use the partial/fully coupled terminology in the conclusions for consistency (page: 25 line: 17-19), and add An-gs coupling as a column in Table 2 where we thought this was more descriptive than the previous column heading in Table 2 which was 'Impact upon An-gs'.

Response to detailed comments of editor:

Editor 9: P3 L 11 (add "depending on for instance" to both brackets).

Author 9: This change was made.

Editor 10: P3 L 17 Provide a reference for the fact that discrimination is indeed affected by nutrient availability in the real world.

Author 10: We added Cernusak et al. (2013).

Editor 11: P4L7ff can be removed.

Author 11: We removed this line.

Editor 12: P4 L20: It does not really become clear here why you would think this is an issue that needs particular addressing. Isn't it logical that the offset between the $\delta^{13}\text{CO}_2$ at site and global mean values must be important when looking at the absolute $\delta^{13}\text{CO}_2$ values? So why would one use a global mean value to start with?

Author 12: We intended to mean that given site specific boundary conditions (including for instance site-level atmospheric $\delta^{13}\text{CO}_2$) and the stable carbon isotope sub-model within CLM, could the observed $\delta^{13}\text{CO}_2$ of carbon pools be simulated. We clarified this sentence in the text. (page: 4 line: 17-21)

Editor 13: P4 L24: water-use efficiency

Author 13: Changes were made here and elsewhere in text.

Editor 14: P6 L 14ff: Include β_t into eq 3 if it's used there. Otherwise the current paper reads as if only the intercept of the Ball&Berry relationship is affected by soil moisture. While doing this, clarify whether β_t also affects A_p and A_j ?

Author 14: Yes, β_t is applied to V_{cmax} , but is applied much later in the CLM source code, hence we left it out of eq. 3 originally. We include it now. β_t only influences V_{cmax} and A_c , not A_p and A_j within CLM.

Editor 15: P6: Equation 6 define $\text{LAI}_{\text{sunlit/shade}}$ how calculated or provide a reference.

Author 15: We added Oleson et al. (2013) as reference.

Editor 16: P7 L22: Provide a reference for these values. Explain how c_i depends on shaded and sunlit leaves, and how this affects the leaf c_i calculations and total discrimination of the A_n flux?

Author 16: We add the Farquhar et al. (1989) reference for the diffusional and enzymatic values. We add text (page: 8 lines: 1-4) describing that the c_i is calculated for shaded and sunlit portion of the leaves separately, therefore discrimination is calculated separately. What we show in the equation (11) is a simplified, general expression for simplicity and brevity.

Editor 17: P8 L7: should this not read nitrogen-limited rather than limited nitrogen? Assuming that the actual N-limitation of the ecosystem is identical between the runs, and its only a question of whether GPP is assumed to be down-regulated with N limitation or not? It seem so because that's what is said later?

Author 17: We fail to see the difference between nitrogen-limited vs. limited nitrogen. The N-limitation is in fact, not identical between the two runs. The limited nitrogen simulation downregulates GPP by tracking nitrogen within CLM, whereas the unlimited nitrogen has no downregulation of GPP, but instead depends upon V_{cmax} calibration. We discuss this in detail in page 8 lines 5-32.

Editor 18: P8 L13: Add a note that all this is very specific to the set-up of CLM and not representative of the wider class of biosphere models.

Author 18: The unlimited nitrogen formulation of CLM is specific to this analysis only, whereas the limited nitrogen formulation is the default version of CLM. We state this specifically now in the text to reinforce this point (page: 8 line: 8-15).

Editor 19: P12 L28: What happened to J_{max} ?

Author 19: We added text (page: 13, lines: 12-14) stating that both A_j (and J_{max}) and A_p defined in equation 1, are also calibrated in the same way as V_{cmax} described in Section 2.4.

Editor 20: P13 L14-22. Not necessary

Author 20: This section was removed.

Editor 21: P15 L31. The FLUXNET data do not provide evidence for the response of stomates to CO_2 , they simply suggest a trend in WUE with time, which may (or may not) be related to increasing CO_2 . I would rather recommend to quote a study relating stomatal conductance to elevated CO_2 experiments.

Author 21: We replaced the Keenan et al (2013) citation with Ward et al (2013), a Duke FACE site experiment.

Editor 22: P16 L 1 Is this change in $c_i:ca$ really a consequence of changes in CO_2 , or concurrent climatic changes? Because eq 4 should imply constant $c_i:ca$...

Author 22: Yes, because on a multi-decadal time scale the meteorology we used in the model was constant –that is we repeatedly cycled the site-level meteorology between 1998-2013 for the

time period of 1850-2013. We state this in the methods (page: 11 lines: 24-29) and also within the discussion in the preceding section (page: 15 lines 15-19) and afterwards (page: 16, 2-5).

Editor 23: P17 L 7: In the model, or in the data? Explain briefly how VPD is affected by your model formulation - not everybody will get this.

Author 23: We intended to mean in general, both in the real world and for the model. We add in parentheses how VPD influences the stomatal conductance within the model (page: 16-17 lines: 28-31, 1-2).

Editor 24: P17 L12: This is a good example of a paragraph that would be better suited in a different, separate discussion section, as it is distracting from the line of results presented. This is particularly true because another discussion of gm is on P19 L3ff

Author 24: As suggested earlier we have created a designated Discussion (Section 4) that is separate from the Results & Discussion (Section 3) which should help the organization and focus overall. In the case of mesophyll conductance as the editor mentions above, we agree that if one is interested in the results all at once, or if one would prefer the discussion of mesophyll conductance to be combined in one section, then a designated discussion section for mesophyll conductance would be best. However, if instead, one prefers fully developed, coherent sections based on concepts such as in Section 3.2.1 where we discuss trends in photosynthetic discrimination, and Section 3.2.2 where we discuss the magnitude/bias in photosynthetic discrimination, then our existing organization would be best. One might find it distracting to be presented trends and biases in photosynthetic discrimination, then have to scan through the rest of the results/discussion before returning to the concept of mesophyll conductance again. It is not clear to us one method of organization is more advantageous than the other, therefore, at the editor's discretion, we prefer to keep it as is.

Editor 25: P17 L30: I must have missed this: which global simulation. So far, you only talked about Niwot ridge.

Author 25: We introduce the global CESM simulation at the end of the previous paragraph: 'These trends in iWUE and discrimination have also been found in a fully-coupled, isotope enabled, global CESM simulation (Figure S3).' (Page 17, Lines 12-14)

Editor 26: P18 L 3. Why is this equation introduced here and not in the Methods?

Author 26: We felt it was logical to include this equation only after we had fully developed the discussion between discrimination and iWUE. Otherwise, if introduced in the methods, it would be premature. In addition it also may present some confusion to the reader to put the equation in the Methods, given that it is not an equation found in CLM, but a simplification of a CLM equation used as a diagnostic for model behavior. We also felt the manuscript would be easier to read if we introduced this equation as the clincher to this discussion section, rather than have the reader have to jump way back to the Methods section.

Editor 27: P19 L18. which mixing model?

Author 27: We mean the mixing model approach employed by Bowling et al. (2014) which we introduce at the beginning of this section (page 18: line 3-4). We add the citation again here, to remind the reader where this is coming from (page 19: lines 7-8).

Editor 28: P19 L30ff This may either be the introduction to this section or removed, because at this stage, you are simply repeating what's been said before.

Author 28: Yes, it was our intent to summarize the key points given the complexity of the discussion. From personal experience we have found a condensed summary helps reinforce the points, and at the editor's discretion we prefer to keep this.

Editor 29: P20 L6 ff: Isn't this all simply a consequence of the model tuning via a time-dependent V_{cmax} while not touching leaf respiration? This must yield unrealistically high $c_i:c_a$ and thus discrimination values. Given that this is an artefact of the way you've matched the seasonal cycle and it will be specific to CLM 4.5, is it really worth discussing this here?

Author 29: Not only is V_{cmax} (A_c) adjusted in our time dependent calibration approach, but also for A_j , A_p and the maintenance leaf respiration. We have added text clarifying this point (page 13: lines 12-14). Both the limited nitrogen and unlimited nitrogen formulations undergo similar V_{cmax} calibrations, therefore the difference in seasonal discrimination performance between the two formulations being an artifact of the calibration seems unlikely. Instead, as we state in the manuscript we believe the difference in behavior is likely the result of the nitrogen downregulation approach used in the default model, and the method for accounting for the downregulation approach within the c_i equation (eq. 11). Furthermore, the fact that the nitrogen downregulation also forces the model to be partially-coupled where g_s is no longer consistent with A_n may also play a role.

Editor 30: P22 L25. Please define what you mean by "categorical differences." It is not correct to state that CLM4 did not capture the NPP response only because it had too little initial N availability. We have demonstrated clearly that it was lacking important functional features of the response such as the too strong carbon-nitrogen coupling of biomass production (Zaehle et al. 2014). CLM4 had the lowest WUE response in the ensemble (de Kauwe et al, 2013).

Author 30: Thank you for the correction. We have changed the text to say that the poor NPP response was from both initial N availability and too strong carbon-nitrogen coupling. (page 22: line: 20-21)

Editor 31: P23 L4. This is not correct, because you do not update foliar N to calculate V_{max} (with all the consequences for the N requirement of biomass etc.), but prescribed a time-dependent V_{cmax} scaled to the observed GPP independent of foliar N (unless your description in Sect 2.4 is inaccurate).

Author 31: We have changed the wording to say there are only ‘similarities’ between the unlimited nitrogen formulation and a true foliar nitrogen model. We then point out that a true foliar nitrogen model would link a dynamic nitrogen cycle with leaf nitrogen (Ghimire et al. 2016) (page: 22-23 line: 28-31, 1-2)

Editor 32: P25 L22: No land surface model qualifies as highly mechanistic.

Author 32: We removed the word ‘highly’.

Editor 33: P25 L22L What you have shown is that if employing eq 4 on the "true" A_n , all is fine, but if you follow the standard CLM approach, the results are not as good. What you have not shown is that if one uses foliar N to diagnose V_{cmax} , this improves the simulation of discrimination. You have not, because you calibrate for each day V_{cmax} based on its difference to the observed GPP, implying that there are variations of V_{cmax} on a day-to-day basis unrelated to any changes in foliar N. The latter would be what "foliar-N" models do. Therefore, your claim that you are mimicking the functionality of a foliar N model is unsubstantiated.

Author 33: We agree that the unlimited nitrogen formulation of CLM and a foliar nitrogen model are not the same thing, although there are similarities. We remove the text ‘mimic the functionality of a foliar nitrogen model’ to clarify this. (page 25, line 14-16).

Editor 34: Figures: Please label all sub-plots with consecutive letters and refer to these in the caption.

Author 34: We made these changes for all figures.

Editor 35: Figure caption 1: “The N-limitation is determined by required N availability to meet demand from C:N ratio based on CF.” Isn’t the available soil N determining whether or not the growth is N limited?

Author 35: We agree that what you have suggested is a better wording. We have updated the caption in Figure 1 to say ‘N-limitation is applied if the available N cannot meet the demand determined by the available carbon for allocation () and the C:N biomass ratio’.

Editor 36: I wonder if this Figure could be made clearer by having two arrows between the box of eq 8 and eq2 indicating for both scheme the direction of information (ie is it growth or V_{cmax} determining photosynthesis and conductance?).

Author 36: Not sure if this is exactly what you mean, but we like the idea of a backwards arrow linking the downregulation nitrogen box to the photosynthesis-stomatal conductance box (feedback loop), to indicate that photosynthesis is reduced. We have made this change.

Editor 37: General remark: carefully revise writing and punctuation

Author 37: We have carefully revised the entire document. Thank You.

An observational constraint on stomatal function in forests: evaluating coupled carbon and water vapor exchange with carbon isotopes in the Community Land Model (CLM 4.5)

Brett Raczka¹, Henrique F. Duarte², Charles D. Koven³, Daniel Ricciuto⁴, Peter E. Thornton⁴, John C. Lin², David R. Bowling¹

[1]{Dept. of Biology, University of Utah, Salt Lake City, Utah}

[2]{Dept. of Atmospheric Sciences, University of Utah, Salt Lake City, Utah}

[3]{Lawrence Berkeley National Laboratory, Berkeley, California}

[4]{Oak Ridge National Laboratory, Oak Ridge, Tennessee}

Correspondence to: B. Raczka (brett.raczka@utah.edu)

Abstract

Land surface models are useful tools to quantify contemporary and future climate impact on terrestrial carbon cycle processes, provided they can be appropriately constrained and tested with observations. Stable carbon isotopes of CO₂ offer the potential to improve model representation of the coupled carbon and water cycles because they are strongly influenced by stomatal function. Recently, a representation of stable carbon isotope discrimination was incorporated into the Community Land Model component of the Community Earth System Model. Here, we tested the model's capability to simulate whole-forest isotope discrimination in a subalpine conifer forest at Niwot Ridge, Colorado, USA. We distinguished between isotopic behavior in response to a decrease of $\delta^{13}\text{C}$ within atmospheric CO₂ (Suess effect) vs. photosynthetic discrimination (Δ_{canopy}), by creating a site-customized atmospheric CO₂ and $\delta^{13}\text{C}$ of CO₂ time series. We implemented a seasonally-varying V_{cmax} model calibration that best matched site observations of net CO₂ carbon exchange, latent heat exchange and biomass. The model accurately simulated observed $\delta^{13}\text{C}$ of needle and stem tissue, but underestimated the $\delta^{13}\text{C}$ of bulk soil carbon by 1-2 ‰. The model overestimated the multi-year (2006-2012) average Δ_{canopy} relative to prior data-based estimates by ~~2-45-6~~ ‰. The amplitude of the average seasonal cycle of Δ_{canopy} (i.e. higher in spring/fall as compared to summer) was correctly modeled but only when using ~~a revised fully-coupled $A_{\text{net-g}}$ (net assimilation rate,~~

Formatted: Not Highlight

Formatted: Font: Italic

Formatted: Font: Italic, Subscript

Formatted: Font: Italic

Formatted: Font: Italic, Subscript

1 stomatal conductance) version of the model ~~pre-photosynthetic nitrogen limitation~~ in contrast to
2 the ~~partially-coupled A_n - g_s version~~ ~~post-photosynthetic nitrogen limitation~~ used in the default
3 ~~version of the~~ model. The model attributed most of the seasonal variation in discrimination to
4 ~~the net assimilation rate (A_n)~~, whereas inter-annual variation in simulated Δ_{canopy} during the
5 summer months was driven by stomatal response to vapor pressure deficit. ~~Soil moisture did~~
6 ~~not influence modeled Δ_{canopy} .~~ The model simulated a 10% increase in both photosynthetic
7 discrimination and water-use efficiency (WUE) since 1850 ~~as a result of CO_2 fertilization,~~
8 ~~forced by constant climate conditions. This increasing trend in discrimination which~~ is counter
9 to ~~well~~-established relationships between discrimination and WUE. The isotope observations
10 used here to constrain CLM suggest 1) the model overestimated stomatal conductance and 2)
11 the default CLM approach to representing nitrogen limitation (~~partially-coupled model~~ ~~post-~~
12 ~~photosynthetic limitation~~) was not capable of reproducing observed trends in discrimination.
13 These findings demonstrate that isotope observations can provide important information related
14 to stomatal function driven by environmental stress from VPD and nitrogen limitation. Future
15 versions of CLM that incorporate carbon isotope discrimination are likely to benefit from
16 explicit inclusion of mesophyll conductance.

19 1 Introduction

20 The net uptake of carbon by the terrestrial biosphere currently mitigates the rate of
21 atmospheric CO_2 rise and thus the rate of climate change. Approximately 25% of
22 anthropogenic CO_2 emissions are absorbed by the global land surface (Le Quéré et al., 2015),
23 but it is unclear how projected changes in temperature and precipitation will influence the future
24 of this land carbon sink (Arora et al., 2013; Friedlingstein et al., 2006). A major source of
25 uncertainty in climate model projections results from the disagreement in projected strength of
26 the land carbon sink (Arora et al., 2013). Thus, it is critical to reduce this uncertainty to improve
27 climate predictions, and to better inform mitigation strategies (Yohe et al., 2007).

28 An effective approach to reduce uncertainties in terrestrial carbon models is to constrain
29 a broad range of processes using distinct and complementary observations. Traditionally,
30 terrestrial carbon models have relied primarily upon observations of land-surface fluxes of
31 carbon, water and energy derived from eddy-covariance flux towers to calibrate model
32 parameters and evaluate model skill. Flux measurements best constrain processes that occur at

Formatted: Font: Italic

Formatted: Font: Italic, Subscript

Formatted: Font: Italic

Formatted: Font: Italic, Subscript

Formatted: Font: Italic

Field Code Changed

1 diurnal and seasonal time scales (Braswell et al., 2005; Ricciuto et al., 2008). Traditional
2 ecological metrics of carbon pools (e.g. leaf area index (LAI), biomass) are also commonly
3 used to provide independent and complementary constraints upon ecosystem processes at
4 longer time scales (Ricciuto et al., 2011; Richardson et al., 2010). However, neither flux nor
5 carbon pool observations provide suitable constraints for the model formulation of plant
6 stomatal function and the related link between the carbon and water cycles.

Field Code Changed

7 Stable carbon isotopes of CO₂ are influenced by stomatal activity in C3 plants (e.g.
8 evergreen trees, deciduous trees), and thus provide a valuable but under-utilized constraint on
9 terrestrial carbon models. Plants assimilate more of the lighter of the two major isotopes of
10 atmospheric carbon (¹²C vs. ¹³C). This preference, termed photosynthetic discrimination
11 (Δ_{canopy}), is primarily a function of two processes, CO₂ diffusion rate through the leaf boundary
12 layer and into the stomata, and the carboxylation of CO₂. The magnitude of Δ_{canopy} is controlled
13 by CO₂ supply (depending on for instance atmospheric CO₂ concentration and—stomatal
14 conductance) and demand (depending on for instance photosynthetic rate; Flanagan et al.,
15 2012). In general, environmental conditions favorable to plant productivity result in higher
16 Δ_{canopy} during carbon assimilation compared to unfavorable conditions. Plants respond to
17 unfavorable conditions by closing stomata and reducing the stomatal conductance which
18 reduces Δ_{canopy} . Most relevant here, Δ_{canopy} responds to atmospheric moisture deficit (Andrews
19 et al., 2012; Wingate et al., 2010), soil water content (McDowell et al., 2010), precipitation
20 (Roden and Ehleringer, 2007) and nutrient availability (Cernusak et al., 2013). After carbon is
21 assimilated, additional post-photosynthetic isotopic changes occur (Bowling et al., 2008;
22 Brüggemann et al., 2011), but these impose a small influence on land-atmosphere isotopic
23 exchange relative to photosynthetic discrimination.

Field Code Changed

Field Code Changed

Field Code Changed

Field Code Changed

Field Code Changed

Field Code Changed

Field Code Changed

24 The Niwot Ridge Ameriflux site, located in a sub-alpine conifer forest in the Rocky
25 Mountains of Colorado, U.S.A., has a long legacy of yielding valuable datasets to test carbon
26 and water functionality of land surface models using stable isotopes. Niwot Ridge has a 17-
27 year record of eddy covariance fluxes of carbon, water, and energy, as well as environmental
28 data (Hu et al., 2010; Monson et al., 2002) and a 10-year record of $\delta^{13}\text{C}$ of CO₂ in forest air
29 (Schaeffer et al., 2008). From a carbon balance perspective, Niwot Ridge is representative of
30 subalpine forests in Western North America that, in general, act as a carbon sink to the
31 atmosphere (Desai et al., 2011). Western forests make up a significant portion of the carbon

Field Code Changed

Field Code Changed

Field Code Changed

sink in the United States (Schimel et al., 2002), yet this sink is projected to weaken with projected changes in temperature and precipitation (Boisvenue and Running, 2010).

Field Code Changed

Field Code Changed

The Community Land Model (CLM), the land sub-component of the Community Earth System Model (CESM) has a comprehensive representation of biogeochemical cycling (Oleson et al., 2013) that can be applied across a range of temporal (hours to centuries) and spatial (site to global) scales. A mechanistic representation of photosynthetic discrimination based upon diffusion and enzymatic fractionation (Farquhar et al., 1989) was included in the latest release of CLM 4.5 (Oleson et al., 2013), and is similar to the formulation implemented in other land surface models (Flanagan et al., 2012; Scholze et al., 2003; Wingate et al., 2010; van der Velde et al., 2013). An early version of CLM simulated carbon (but not carbon isotope) dynamics at Niwot Ridge with reasonable skill (Thornton et al., 2002). ~~To date, we are not aware of any CLM-based studies that have used CO₂ isotopes at natural abundance to quantify the accuracy of the photosynthetic discrimination sub-model, or to evaluate the utility of CO₂ isotopes to constrain carbon and water cycle coupling.~~

Field Code Changed

Field Code Changed

Field Code Changed

Here, we evaluate the performance of the ¹³C/¹²C isotope discrimination sub-model within CLM 4.5 against a range of isotopic observations at Niwot Ridge, to examine what new insights an isotope-enabled model can bring upon ecosystem function. Specifically, we test whether CLM simulates the expected isotopic response to environmental drivers of CO₂ fertilization, soil moisture and atmospheric vapor pressure deficit (VPD). A previous analysis at Niwot Ridge showed a seasonal correlation between vapor pressure deficit (VPD) and photosynthetic discrimination (Bowling et al., 2014) suggesting that leaf stomata are responding to changes in VPD, and influencing discrimination. We use CLM to test whether VPD is the primary environmental driver of isotopic discrimination, as compared to soil moisture and net assimilation rate. Next we determine whether ~~including~~ site-specific ~~boundary conditions (including for instance δ¹³C of atmospheric CO₂) within the model simulation~~ combined with ~~simulated the representation of~~ long term (multi-decadal to century) photosynthetic discrimination and simulated carbon pool turnover within the model, can accurately reproduce the measured δ¹³C in leaf tissue, roots and soil carbon. We then use CLM to determine if the increase in atmospheric CO₂ since 1850 has led to an increase in water-use efficiency (WUE), and whether net assimilation or stomatal conductance is the primary driver of such a change. Finally, we ask what distinct insights site level isotope observations bring in

terms of both model parameterization (i.e. stomatal conductance) and model structure as compared to the traditional observations (e.g. carbon fluxes, biomass).

2 Methods

We focus the description of CLM 4.5 (Section 2.1) upon photosynthesis, and its linkage to nitrogen, soil moisture and stomatal conductance (Section 2.1.1). Next we describe the model representation of carbon isotope discrimination by photosynthesis (Section 2.1.2). Because preliminary simulations demonstrated that model results were strongly influenced by nitrogen limitation, we used three separate nitrogen formulations (described in Section 2.1.2) to better diagnose model performance. Next, to provide context for subsequent descriptions of site-specific model adjustments we describe the field site, Niwot Ridge, including the site level observations (Section 2.2) used to constrain and test model the model.

Patterns in plant growth and $\delta^{13}\text{C}$ of biomass are strongly influenced by atmospheric CO_2 and $\delta^{13}\text{C}$ of atmospheric CO_2 (δ_{atm}). Therefore we designed a site-specific synthetic atmospheric CO_2 product (Section 2.3.1) and δ_{atm} product (Section 2.3.2) for these simulations. The model setup and initialization procedure, intended to bring the system into steady state, is described in Section (2.3.3). This is followed by an explanation of the model calibration procedure that provided a realistic simulation of carbon and water fluxes (Section 2.4).

2.1 Community Land Model, Version 4.5

We used the Community Land Model, CLM 4.5 (Oleson et al., 2013), which is the land component of the Community Earth System Model (CESM) version 1.2 (<https://www2.cesm.ucar.edu/models/current>). Details regarding the Community Land Model can be found in Mao et al., (2016) and Oleson et al., (2013). Here, we emphasize the mechanistic formulation that controls photosynthetic discrimination (Δ_{canopy}) and factors that influence Δ_{canopy} including photosynthesis, stomatal conductance, water stress and nitrogen limitation. A list of symbols is provided in Table (1).

2.1.1 Net Photosynthetic Assimilation

The leaf-level net carbon assimilation of photosynthesis, A_n is based on Farquhar et al., (1980) as,

$$A_n = \min(A_c, A_j, A_p) - \text{Resp}_d, \quad (1)$$

Field Code Changed

Field Code Changed

1 where A_c , A_j and A_p are the enzyme (Rubisco)-limited, light-limited, and product-limited rates
 2 of carboxylation respectively, and $Resp_d$ the leaf-level respiration. The enzyme limited rate is
 3 defined as

$$4 \quad A_c = \frac{V_{cmax}(c_i - \Gamma_*)}{c_i + K_c(1 + \frac{o_i}{K_o})}, \quad (2)$$

5 where c_i is the intercellular leaf partial pressure of CO_2 , $o_i = 0.209 P_{atm}$, P_{atm} is atmospheric
 6 pressure, and K_c , K_o and Γ_* are constants. The maximum rate of carboxylation at 25°C, V_{cmax25} ,
 7 is defined as

$$8 \quad V_{cmax25} = N_a F_{LNR} F_{NR} a_{R25} \beta_t, \quad (3)$$

9 where N_a is the nitrogen concentration per leaf area, F_{LNR} the fraction of leaf nitrogen within
 10 the Rubisco enzyme, F_{NR} the ratio of total Rubisco molecular mass to nitrogen mass within
 11 Rubisco, and a_{R25} is the specific activity of Rubisco at 25°C. The V_{cmax25} is adjusted for leaf

12 temperature to provide V_{cmax} in Eq. 2, used in the final photosynthetic calculation. Both A_i and
 13 A_p are functions of V_{cmax} as well (not shown). The variable β_t represents the level of soil
 14 moisture availability, which influences both V_{cmax} (Sellers et al., 1996), and stomatal
 15 conductance (eq. 5). CLM calculates β_t as a factor (0-1, high to low stress) by combining soil
 16 moisture, the rooting depth profile, and a plant-dependent response to soil water stress as

$$17 \quad \beta_t = \sum_i w_i r_i, \quad (4)$$

18 where w_i is a plant wilting factor for soil layer i and r_i is the fraction of roots in layer i . The
 19 plant wilting factor is scaled according to soil moisture and water potential, depending on plant
 20 functional type (PFT). Soil moisture is predicted based upon prescribed precipitation and
 21 vertical soil moisture dynamics (Zeng and Decker, 2009). The root fraction in each soil layer
 22 depends upon a vertical exponential profile controlled by PFT dependent root distribution
 23 parameters adopted from Zeng (2001).

24 The carbon and water balance are linked through c_i by the stomatal conductance to CO_2 ,
 25 g_s , following the Ball-Berry model (Ball, 1987) as defined by Collatz et al., (1991),

$$26 \quad g_s = m \frac{A_n}{c_s/P_{atm}} h_s + b \beta_t, \quad (54)$$

27 where m is the stomatal slope, c_s the partial pressure of CO_2 at the leaf surface, h_s the relative
 28 humidity at the leaf surface and b the minimum stomatal conductance when the leaf stomata
 29 are closed. ~~The variable β_t represents the level of soil moisture availability, which influences~~

Formatted: Font: Italic

Formatted: Font: Italic, Subscript

Formatted: Font: Italic

Formatted: Font: Italic, Subscript

Formatted: Font: Italic

Formatted: Font: Italic, Subscript

Field Code Changed

Field Code Changed

Field Code Changed

Field Code Changed

stomatal conductance directly, but also indirectly through A_n by multiplying V_{cmax} by β_s (Sellers et al., 1996). CLM calculates β_s as a factor (0-1, high to low stress) by combining soil moisture, the rooting depth profile, and a plant dependent response to soil water stress as

$$\beta_s = \sum_i w_i r_i, \quad (5)$$

where w_i is a plant wilting factor for soil layer i and r_i is the fraction of roots in layer i . The plant wilting factor is scaled according to soil moisture and water potential, depending on plant functional type (PFT). Soil moisture is predicted based upon prescribed precipitation and vertical soil moisture dynamics (Zeng and Decker, 2009). The root fraction in each soil layer depends upon a vertical exponential profile controlled by PFT dependent root distribution parameters adopted from Zeng (2001).

The version of CLM used here has a 2-layer (shaded, sunlit) representation of the vegetation (Oleson et al. 2013). Photosynthesis and stomatal conductance are calculated separately for the shaded and sunlit portion and the total canopy photosynthesis is the potential gross primary productivity (GPP), CF_{GPPpot} :

$$CF_{GPPpot} = [(A_n + Resp_d)_{sunlit} (LAI)_{sunlit} + (A_n + Resp_d)_{shaded} (LAI)_{shaded}] * 12.011^{-6}, \quad (6)$$

where LAI is the leaf area index and 12.011^{-6} is a unit conversion factor. The total carbon available for new growth allocation (CF_{avail_alloc}) is defined as

$$CF_{avail_alloc} = CF_{GPPpot} - CF_{GPP,mr} - CF_{GPP,xs}, \quad (7)$$

where the maintenance respiration is derived either from recently assimilated photosynthetic carbon ($CF_{GPP,mr}$), or, if photosynthesis is low or zero (e.g. night), the maintenance respiration is drawn from a carbon storage pool ($CF_{GPP,xs}$). In contrast, CF_{alloc} , is the actual carbon allocated to growth calculated from the available nitrogen and fixed C:N ratios for new growth (e.g. stem, roots, leaves). The downregulation of photosynthesis from nitrogen limitation, f_{dreg} , is given by

$$f_{dreg} = \frac{CF_{avail_alloc} - CF_{alloc}}{CF_{GPPpot}}. \quad (8)$$

The actual, nitrogen-limited GPP is defined as:

$$GPP = CF_{GPPpot}(1 - f_{dreg}) \quad (9)$$

2.1.2 Photosynthetic Carbon Isotope Discrimination

The canopy-level fractionation factor α is defined as the ratio of $^{13}\text{C}/^{12}\text{C}$ within atmospheric CO_2 (R_a) and the products of photosynthesis (R_{GPP}) as $\alpha = \frac{R_a}{R_{GPP}}$. The preference of C3 vegetation to assimilate the lighter CO_2 molecule during photosynthesis is simulated in CLM with two steps: diffusion of CO_2 across the leaf boundary layer and into the stomata, followed by enzymatic fixation to give the leaf-level fractionation factor:

$$\alpha = 1 + \frac{4.4 + 22.6 \frac{c_i^*}{c_a}}{1000} \quad (10)$$

where c_i^* and c_a are the intracellular and atmospheric CO_2 partial pressure respectively. The numbers 4.4 and 22.6 represent the diffusional and enzymatic contributions to isotopic discrimination respectively. The variable c_i^* (known in CLM as the ‘revised intracellular CO_2 partial pressure’) is marked with an asterisk to indicate the inclusion of nitrogen downregulation as defined as,

$$c_i^* = c_a - A_n (1 - f_{dreg}) P_{atm} \frac{(1.4g_s) + (1.6g_b)}{g_b g_s} \quad (11)$$

where g_b is the leaf boundary layer conductance. The inclusion of the nitrogen downregulation factor f_{dreg} in the above expression reflects the two-stage process in which the potential photosynthesis (Eq. 6) and the actual photosynthesis (Eq. 9) are calculated within CLM and prevents a mismatch between the actual photosynthesis and the intracellular CO_2 . Equation 11 is a general expression for c_i^* , where within the model c_i^* and discrimination is calculated for the sunlit and shaded layer of leaves separately and subject to the local environmental conditions unique to each layer (Oleson et al. 2013).

The sensitivity of preliminary model results to nitrogen limitation led us to test three distinct discrimination formulations (Figure 1; Table 2). The *limited nitrogen* formulation was based on the default version of CLM 4.5 and included both nitrogen limitation and the nitrogen downregulation factor within the calculation of c_i^* as given in equation (11). The second, *unlimited nitrogen* formulation, which we created specifically for this analysis, also follows equation (11), however, the vegetation is allowed unlimited access to nitrogen ($CF_{GPPpot} = GPP, f_{dreg} = 0$) which ignores the nitrogen budget within CLM. We account for the increased productivity in the *unlimited nitrogen* model simulations by calibrating V_{cmax} (Section 2.4). Finally, in the *no downregulation discrimination* formulation, (also created specifically for this

Formatted: Subscript

Formatted: Font: Italic

Formatted: Font: Italic, Subscript

Formatted: Font: Italic

Formatted: Font: Italic

Formatted: Font: Italic, Subscript

Formatted: Font: Italic

Formatted: Font: Italic

Formatted: Subscript

analysis) we included nitrogen limitation, but removed the downregulation factor f_{dreg} within the isotopic discrimination equation (11).

In the *unlimited nitrogen* formulation, we use a different modifier on V_{cmax25} (Figure 1; described in section 2.4 and Fig. S1, S2) in the calibrated runs to give similar carbon flux, water flux and biomass as in the other two formulations, such that all three formulations have fluxes and biomass that are similar to what is observed at the site, and which presumably reflect nitrogen limitation. Thus the distinction between these three formulations can be viewed entirely as *when* nitrogen limitation is imposed in relation to photosynthesis: (1) *after photosynthesis* via a downregulation between potential and actual GPP (equation 9) that feeds back on the c_i^*/c_a used for isotopic discrimination but *not on* g_s or A_n in the *limited nitrogen* formulation; (2) *before photosynthesis* via V_{cmax} , which limits photosynthetic capacity affecting both c_i^*/c_a , g_s and A_n in the *unlimited nitrogen* formulation; and (3) *after photosynthesis with no effect on either* the c_i^*/c_a for isotopic discrimination or g_s or A_n in the *no downregulation discrimination* formulation. The downscaled portion of the carbon during nitrogen limitation ($CF_{GPPpot} - GPP$) is removed from the system and does not appear as a respired flux (Figure 1). In summary, the *limited nitrogen (post-photosynthetic)* formulation adjusts the photosynthetic rate by explicitly tracking N availability, whereas the *unlimited nitrogen (pre-photosynthetic)* formulation takes into account any N-limitation through the V_{cmax} parameterization. Because the *limited nitrogen* formulation reduces A_n during the nitrogen downregulation step without explicitly solving for g_s , the carbon-water cycle is ‘partially-coupled’, whereas the *unlimited nitrogen* formulation is ‘fully-coupled’.

Carbon isotope ratios are expressed by standard delta notation,

$$\delta^{13}C_x = \left(\frac{R_x}{R_{VPDB}} - 1 \right) \times 1000, \quad (12)$$

where R_x is the isotopic ratio of the sample of interest, and R_{VPDB} is the isotopic ratio of the Vienna Pee Dee Belemnite standard. The delta notation is dimensionless but expressed in parts per thousand (‰) where a positive (negative) value refers to a sample that is enriched (depleted) in $^{13}C/^{12}C$ relative to the standard. Because this is the only carbon isotope ratio we are concerned with in this paper, the ‘13’ superscript is omitted for brevity in subsequent definitions using the delta notation. The canopy-integrated photosynthetic discrimination, Δ_{canopy} , is defined as the difference between the $\delta^{13}C$ of the atmospheric and assimilated carbon,

$$\Delta_{canopy} = \delta_{atm} - \delta_{GPP}. \quad (13)$$

Formatted: Font: Italic

Formatted: Font: Italic

Formatted: Font: Italic, Subscript

Formatted: Font: Italic

Formatted: Font: Italic, Subscript

Formatted: Font: Italic

The difference between $\delta^{13}\text{C}$ of the total ecosystem respiration (ER) and GPP fluxes, called the isotope disequilibrium (Bowling et al., 2014), is defined as,

$$\text{disequilibrium} = \delta_{\text{ER}} - \delta_{\text{GPP}}. \quad (14)$$

The ecosystem-level water-use efficiency (WUE) is defined as actual carbon assimilated (GPP) per unit water transpired (E_T) per unit land surface area,

$$\text{WUE} = \frac{\text{GPP}}{E_T}. \quad (15)$$

The intrinsic water-use efficiency (*iWUE*) from leaf-level physiological ecology is defined as,

$$i\text{WUE} = \frac{A_n}{g_s}, \quad (16)$$

where A is the net carbon assimilated per unit leaf area and g_s is the stomatal conductance.

CLM calculates g_s (Equation 54) for shaded and sunlit portions of the canopy separately, therefore an overall conductance was calculated by weighting the conductance by sunlit and shaded leaf areas.

2.2 Niwot Ridge and site-level observations

Site-level observations and modeling were focused on the Niwot Ridge Ameriflux tower (US-NR1), a sub-alpine conifer forest located in the Rocky Mountains of Colorado, U.S.A. The forest is approximately 110 years old and consists of lodgepole pine (*Pinus contorta*), Engelmann spruce (*Picea engelmanni*), and subalpine fir (*Abies lasiocarpa*). The site is located at an elevation of 3050 m above sea level, with mean annual temperature of 1.5°C and precipitation of 800 mm, in which approximately 60% is snow. More site details are available elsewhere (Hu et al., 2010; Monson et al., 2002). Flux and meteorological data were obtained from the Ameriflux archive (<http://ameriflux.lbl.gov/>).

Net carbon exchange (NEE) observations were derived from flux tower measurements based on the eddy covariance method and were partitioned into component fluxes of GPP and ER according to two separate methods described by Reichstein et al., (2005) and Lasslop et al., (2010) using an online tool provided by the Max Planck Institute for Biogeochemistry (<http://www.bgc-jena.mpg.de/~MDIwork/eddyproc/>). Seasonal patterns in δ_{GPP} and δ_{ER} were derived from measurements as described by Bowling et al., (2014). Observations of $\delta^{13}\text{C}$ of biomass (Schaeffer et al., 2008) and carbon stocks (Bradford et al., 2008; Scott-Denton et al., 2003) were compared to model simulations. Schaeffer et al., (2008) reported soil, leaf and

Field Code Changed

Field Code Changed

Field Code Changed

Field Code Changed

Field Code Changed

Field Code Changed

Field Code Changed

1 root observations specific to each conifer species, however, the observed mean and standard
2 error for all species were used for comparison because CLM treated all conifer species as a
3 single PFT.

4 **2.3 Atmospheric CO₂, isotope forcing and initial vegetation state**

5 **2.3.1 Site-specific atmospheric CO₂ concentration time series**

6 Global average atmospheric CO₂ concentrations increased roughly 40% from 1850 to
7 2013 (from 280 to 395 ppm). The standard version of CLM 4.5 includes an annually and
8 globally averaged time series of this CO₂ increase, however, this does not capture the observed
9 seasonal cycle of ~10 ppm at Niwot Ridge (Troler et al., 1996). Therefore we created a site-
10 specific atmospheric CO₂ time series (Figure 2) to provide a seasonally realistic atmosphere at
11 Niwot Ridge. From 1968-2013 the CO₂ time series was fit to flask observations (Dlugokencky
12 et al., 2015) from Niwot Ridge. Prior to 1968, the CO₂ time series was created by combining
13 the average multi-year seasonal cycle based on the Niwot Ridge flask data to the annual CO₂
14 product provided by CLM. More details are located in the supplemental material.

Field Code Changed

16 **2.3.2 Customized $\delta^{13}\text{C}$ atmospheric CO₂ time series**

17 As atmospheric CO₂ has increased, the $\delta^{13}\text{C}$ of atmospheric CO₂ (δ_{atm}) has become
18 more depleted (Francey et al., 1999), and this change continues at Niwot Ridge at -0.25 ‰ per
19 decade (Bowling et al., 2014). The δ_{atm} also varies seasonally, and depends on latitude (Troler
20 et al., 1996). However, CLM 4.5 as released assigned a constant $\delta^{13}\text{C}$ of -6 ‰. We therefore
21 created a synthetic time series of δ_{atm} from 1850-2013 (Figure 2). From 1990-2013 the time
22 series was fit to the flask observations (White et al., 2015) as described in Section 2.3.1. Prior
23 to 1990 the inter-annual variation within the δ_{atm} time series was fit to the ice core data from
24 Law Dome (Francey et al., 1999; see also Rubino et al., 2013). This annual data product was
25 then combined with the average seasonal cycle at Niwot Ridge as determined by the flask
26 observations to create the synthetic product from 1850-1990. More details are located in the
27 supplemental material.

Field Code Changed

Field Code Changed

Field Code Changed

2.3.3 Model Initialization

We performed an initialization to transition the model from near bare-ground conditions to present day carbon stocks and LAI that allowed for proper evaluation of isotopic performance. This was implemented in 4 stages: 1) accelerated decomposition (1000 model years) 2) normal decomposition (1000 model years) 3) parameter calibration (1000 model years) and 4) transient simulation period (1850-2013). The first two stages were pre-set options within CLM with the first stage used to accelerate the equilibration of the soil carbon pools, which require a long period to reach steady state (Thornton and Rosenbloom, 2005). The parameter calibration stage was not a pre-set option but designed specifically for our analysis. For this we introduced a seasonally varying V_{cmax} that scaled the simulated GPP and ecosystem respiration fluxes to present day observations (Section 2.4). In the transient phase, we introduced time-varying atmospheric conditions from 1850-2013 including nitrogen deposition (CLM provided), atmospheric CO_2 , and δ_{atm} (site-specific as described above). Environmental conditions of temperature, precipitation, relative humidity, radiation, and wind speed were taken from the Niwot Ridge flux tower observations from 1998-2013 and then cycled continuously for the entirety of the initialization process. We used a scripting framework (PTCLM) that automated much of the workflow required to implement several of these stages in a site level simulation (Mao et al., 2016; Oleson et al., 2013).

Field Code Changed

2.4 Specific model details and model calibration

This version of CLM included a fully prognostic representation of carbon and nitrogen within its vegetation, litter and soil biogeochemistry. We used the Century model representation for soil (3 litter and 3 soil organic matter pools) with 15 vertically resolved soil layers (Parton et al. 1987). Nitrification and prognostic fire were turned off. Our initial simulations used prognostic fire, but we found that simulated fire was overactive leading to low simulated biomass compared to observations. Although Niwot Ridge has been subject to disturbance from fire and harvest in the past, ultimately our final simulations did not include either fire or harvest disturbance because the last disturbance occurred over 110 years ago (early 20th century logging; Monson et al., 2005).

Field Code Changed

Ecosystem parameter values (Table 3) used here were based upon the temperate evergreen needleleaf PFT within CLM. These values were based upon observations reported

by White et al., (2000) intended for a wide range of temperate evergreen forests, and by Thornton et al., (2002) for Niwot Ridge. For this analysis two site-specific parameter changes were made. First, the e-folding soil decomposition parameter was increased from 5 to 20 meters. This parameter is a length-scale for attenuation of decomposition rate for the resolved soil depth from 0 to 5 meters where an increased value effectively increases decomposition at depth, thus reducing total soil carbon and more closely matching observations. Second, we performed an empirical photosynthesis scaling (equation 17, below) that reduced the simulated photosynthetic flux, as guided by eddy covariance observations (Figure 3; Figure S1). Consequently, all downstream carbon pools and fluxes including ecosystem respiration, aboveground biomass, and leaf area index which provided a better match to present day observations. This approach also removed a systematic overestimation of winter photosynthesis. The model simulations without the photosynthetic scaling are referred to within the text and figures as the *uncalibrated* model, whereas model simulations that include the photosynthetic scaling are referred to as the *calibrated* model. We modified CLM for this scaling approach by reducing V_{cmax} at 25° C,

$$V_{cmax25} = N_a F_{LNR} F_{NR} a_{R25} \beta_t f_{df}, \quad (17)$$

where f_{df} is the photosynthetic scaling factor, and all other parameters are identical to equation (3). These parameters were constant for the entirety of the simulations except for f_{df} , an empirically derived time dependent parameter ranging from 0-1. The value was set to zero to force photosynthesis to zero between November 13th and March 23rd, consistent with flux tower observations where outside of this range $GPP > 0$ was never observed. During the growing season period ($GPP > 0$) within days of year 83-316, f_{df} was calculated as

$$f_{df} = \frac{\text{observed } GPP(\text{day of year})}{\text{simulated } GPP(\text{day of year})}, \quad 82 < \text{day of year} < 317 \quad (18)$$

where the *observed GPP* was the daily average calculated from the partitioned flux tower observations (Reichstein et al., 2005) from 2006-2013, and the *simulated GPP* was the daily average of the unscaled value during the same time. A polynomial was fit to equation (18) that represented f_{df} for 1) both the *limited nitrogen* and *no downregulation discrimination formulations* and 2) the *unlimited nitrogen* formulation (Figure S2). Note that CLM already includes a *daylength factor* that also adjusts the magnitude of V_{cmax} according to time of year, however, that default parameterization alone was not sufficient to match the observations. [The](#)

light-limited rate, product-limited rate (A_i , A_p ; eq. 1) and maintenance leaf respiration are functions of V_{cmax} (not shown) and are therefore subject to the same calibration.

Formatted: Font: Italic

Formatted: Font: Italic, Subscript

Formatted: Font: Italic

Formatted: Font: Italic, Subscript

Formatted: Font: Italic

Formatted: Font: Italic, Subscript

3 Results & Discussion

This section is organized into four parts. First the calibrated model performance is evaluated against observed bulk carbon pool and bulk carbon flux behavior (Section 3.1.1), and against the observed $\delta^{13}\text{C}$ within carbon pools (Section 3.1.2). Second, the simulated photosynthetic discrimination is evaluated for multi-decadal trends (Section 3.2.1), magnitude (Section 3.2.2) and seasonal patterns (Section 3.2.3), including the environmental factors that were most responsible for driving the seasonal discrimination (Section 3.2.4). Third, we discuss how isotope observations can be used to guide model development related to nitrogen limitation (Section 4.1.3.3). Finally, we evaluate the capability of the model to reproduce the magnitude and trends of disequilibrium (Section 4.2.3.4).

3.2.3.1 Calibrated model performance

3.2.3.1.1 Fluxes & carbon pools

The CLM model (*limited nitrogen simulation*) was successful at simulating GPP, ER, and latent heat fluxes (Fig. 3), leaf area index (LAI), and aboveground biomass (Fig. 4), but only following site-specific calibration. ~~The uncalibrated simulation (limited nitrogen formulation) overestimated LAI (39 %), aboveground biomass (48%), average peak warm season GPP (15%), and average peak warm season ER (40%) and overestimated cold season GPP by 200 g C m⁻² yr⁻¹. The calibrated simulation was much closer to the observations for LAI and aboveground biomass (Figure 4). The calibrated peak warm and cold season GPP, and warm season ER matched observations. The simulated latent heat fluxes were relatively insensitive to the calibration. Overall the simulated latent heat during the warm season overestimated the observations by 10% and underestimated by 10% during the cold season.~~ Similar improvement was observed after calibration for the *unlimited nitrogen* run (not shown).

Formatted: Font: Italic

The calibration also eliminated erroneous winter GPP. In general, terrestrial carbon models tend to overestimate photosynthesis during cold periods for temperate/boreal conifer forests (Kolari et al., 2007), including Niwot Ridge (Thornton et al., 2002). ~~One approach to~~

Formatted: Indent: First line: 0.4"

Field Code Changed

Field Code Changed

~~correct for this is to include an acclimatization temperature (e.g. Flanagan et al., 2012) that reduces photosynthetic capacity during the spring and fall. The CLM 4.5 model includes functionality to adjust the photosynthetic capacity, including both a temperature acclimatization and a day-length factor that reduces V_{cmax} (Bauerle et al., 2012; Oleson et al., 2013). However, this alone was not sufficient to match the observed fluxes.~~ Although our calibration approach forced V_{cmax} to zero during the winter, it did not solve the underlying mechanistic shortcoming. A more fundamental approach should address either cold inhibition (Zarter et al., 2006) of photosynthesis or soil water availability associated with snowmelt (Monson et al., 2005) to achieve the photosynthetic reduction. Nevertheless, within the confines of our study area, our calibration approach was sufficient to provide a skillful representation of photosynthesis and provided a sufficient testbed for evaluating carbon isotope behavior. We caution that because the f_{lk} parameter (eq. 17) was calibrated specifically for Niwot Ridge, it would not be applicable outside this study area.

3.2.23.1.2 $\delta^{13}\text{C}$ of carbon pools

The model performed better simulating $\delta^{13}\text{C}$ biomass of bulk needle tissue, roots and soil carbon (Figure 5) for the *unlimited nitrogen* and *no downregulation discrimination* cases as compared to the *limited nitrogen* case. When nitrogen limitation was included the model underestimated $\delta^{13}\text{C}$ of sunlit needle tissue (1.8 ‰), bulk roots (1.0 ‰), and organic soil carbon (0.7‰). All simulations fell within the observed range of $\delta^{13}\text{C}$ in needles that span from -28.7 ‰ (shaded) to -26.7 (sunlit). This vertical pattern in $\delta^{13}\text{C}$ of leaves is common (Martinelli et al., 1998) and results from vertical differences in nitrogen allocation and photosynthetic capacity. The model results integrated the entire canopy and ideally should be closer to sun leaves (as in Figure 5) given that the majority of photosynthesis occurs near the top of the canopy.

Model simulations of $\delta^{13}\text{C}$ of living roots were ~1 ‰ more negative as compared to the structural roots. This range in $\delta^{13}\text{C}$ results from decreasing δ_{atm} with time (Suess effect, Figure 2). The living roots had a relatively fast turnover time of carbon within the model, whereas the structural roots had a slower turnover time and reflected an older (more enriched δ_{atm}) atmosphere. The *limited nitrogen* simulation was a poor match to observations relative to the others (Figure 5, middle panel).

Field Code Changed

Field Code Changed

Formatted: Font: Italic

Formatted: Font: Italic, Subscript

Formatted: Font: Italic

Field Code Changed

There was an observed vertical gradient in $\delta^{13}\text{C}$ of soil carbon (-24.9 to -26 ‰) with more enriched values at greater depth (Figure 5, right panel). This vertical gradient is commonly observed (Ehleringer et al., 2000). Simulated $\delta^{13}\text{C}$ of soil carbon was most consistent with the organic horizon observations. There are a wide variety of post-photosynthetic fractionation processes in the soil system (Bowling et al., 2008; Brüggemann et al., 2011) that are not considered in the CLM 4.5 model, so the match with observations is perhaps fortuitous.

Field Code Changed

Field Code Changed

3.3.3.2 Photosynthetic discrimination

3.3.3.2.1 Decadal changes in photosynthetic discrimination and driving factors

All modeled carbon pools showed steady depletion in $\delta^{13}\text{C}$ since 1850 (coinciding with the start of the transient phase of simulations, Figure 5). For the *limited nitrogen* run, there was a decrease in $\delta^{13}\text{C}$ of 2.3 ‰ for needles, 2.3 ‰ for living roots, and 0.1 ‰ for soil carbon. This occurred because of 1) decreased δ_{atm} (Suess effect, Figure 2) and 2) increased photosynthetic discrimination. We quantified the contribution of the Suess effect by performing a control run with constant δ_{atm} , and kept other factors the same (Figure 6). Approximately 70% of the reduction in $\delta^{13}\text{C}$ of needles occurred due to the Suess effect, and the remaining 30% was caused by increased photosynthetic discrimination. This occurred as plants responded to CO_2 fertilization as illustrated in Figure (7). The model indicated that plants responded to increased atmospheric CO_2 (~40% increase) by decreasing stomatal conductance (Equation 54) by 20% for the *limited nitrogen* run and 30% for the *unlimited nitrogen* run (Figure 7B) with associated change in c_i^*/c_a (Figure 7A). Other influences upon stomatal conductance were less significant, including A_n (+ 10% *limited nitrogen*, -10% *unlimited nitrogen*, Figure 7D), soil moisture availability (2-3%, Figure 7E), and negligible changes in relative humidity (potential climate change effects are neglected due to methodological cycling of weather data). This finding that stomatal conductance responded to atmospheric CO_2 is consistent with both tree ring studies (Saurer et al., 2014) and [site-level experiments](#)~~flux tower measurements~~ (Ward et al., 2012)(Keenan et al., 2013).

Field Code Changed

The effect of CO_2 fertilization, and associated response of stomatal conductance and net assimilation led to a multi-decadal increase in c_i^*/c_a for all model formulations (Figure 7A). The c_i^*/c_a increased from 0.71 to 0.76, 0.67 to 0.71 and 0.66 to 0.68 for the *limited nitrogen*, *unlimited nitrogen* and *no downregulation discrimination* formulations respectively from 1850-

2013. All simulations therefore suggested an *increase* in photosynthetic discrimination. This increase in discrimination falls in between two hypotheses posed by Saurer et al., (2004) regarding stomatal response to increased CO₂: 1) reduction in stomatal conductance causes c_i to proportionally increase with c_a keeping c_i/c_a constant and 2) minimal stomatal conductance response where c_i increases at the same rate as c_a (constant $c_a - c_i$) causing c_i/c_a to increase. Our simulation generally agrees with the observed trend in c_i/c_a as estimated from tree ring isotope measurements from a network of European forests (Frank et al., 2015). When controlled for trends in climate, Frank et al. (2015) found that c_i/c_a was approximately constant during the last century. If the Niwot Ridge multi-decadal warming trends in temperature and humidity (Mitton and Ferrenberg, 2012) were included in the CLM simulations (this analysis did not consider multi-decadal climate change) the stomatal response may have been stronger thereby holding c_i/c_a constant.

The simulated stomatal closure in response to CO₂ fertilization led to an increase in iWUE and WUE of approximately 20% and 10% respectively (Figure 7F) from 1960-2000. This simulated increase in iWUE is consistent with the observation-based studies (Ainsworth and Long, 2005; Franks et al., 2013; Peñuelas et al., 2011) which indicate a 15-20% increase in iWUE for forests during that time. The overall increase in WUE suggests that the vegetation at Niwot Ridge has some ability to maintain net ecosystem productivity when confronted with low soil moisture, low humidity conditions. Ultimately, whether Niwot Ridge maintains the current magnitude of carbon sink (Figure 3; Figure S1) will depend upon the severity of drought conditions, as improvements in WUE, in general, are only likely to negate weak to moderate levels of drought (Frank et al., 2013).

The *limited nitrogen* formulation simulated larger values of A_n and g_s , and smaller iWUE as compared to the *unlimited nitrogen* formulation (Figure 7). This is because the *unlimited nitrogen* formulation was fully coupled (i.e. solved simultaneously) between A_n and g_s (Eq. 54). The *limited nitrogen* formulation, however, was only partially coupled because A_n and g_s were initially solved simultaneously through the potential A_n (Eq. 1), however, under N-limitation A_n becomes limited below its potential value (Eq. 9) through f_{dreg} . Therefore g_s is calculated through the potential A_n (Eq. 54) and not the N-limited A_n .

The simultaneous increase in both simulated photosynthetic discrimination and iWUE conflicts with previous literature where increases in iWUE are typically linked with weakening discrimination (e.g. Saurer et al., 2004) using a linear model. In general, an increase in

Field Code Changed

Field Code Changed

Field Code Changed

Field Code Changed

Field Code Changed

atmospheric CO₂ alone tends to increase iWUE because of reduced stomatal conductance, however, the impact upon discrimination is close to neutral because the increased supply of CO₂ external to the leaf is offset by reduced stomatal conductance (Saurer et al., 2004). The VPD likely plays an important role in determining the final trends for iWUE and discrimination, where an increasing VPD should further reduce stomatal conductance ($VPD \propto \frac{1}{h_s}$, eq. 5) thereby promoting the well-established relationship (increasing iWUE, decreasing discrimination). In contrast, a weak or decreasing trend in VPD should promote the opposite relationship (increasing iWUE, increasing discrimination).

Field Code Changed

The CLM model at present neglects mesophyll conductance (g_m). When Seibt et al. (2008) included g_m in a model that linked iWUE to discrimination they found there were certain conditions when iWUE and discrimination increased together. This is in part because mesophyll conductance, unlike stomatal conductance, does not respond as strongly to changes in VPD, yet has a significant impact upon c_i/c_a and discrimination (Flexas et al., 2006). Harvard Forest is an example of a site that was observed to show simultaneous increase in iWUE and discrimination over the last two decades derived from tree rings (Belmecheri et al., 2014). In our model simulation, we do not consider multi-decadal trends in climate or mesophyll conductance, therefore increasing atmospheric CO₂ must be the primary driver for the modeled simultaneous increase in discrimination and iWUE at Niwot Ridge (Figure 7). These trends in iWUE and discrimination have also been found in a fully-coupled, isotope enabled, global CESM simulation (Figure S3). Specifically, a random sample of land model grid cells representing conifer species in British Columbia (lat: 52.3° N, lon: -122.5° W) and Quebec (lat: 49.5° N, lon: -70.0° W) all showed an increase in photosynthetic discrimination and a 10% increase in WUE from 1850-2005. These randomly chosen grid cells are likely better analogs to the site-level simulations described here because they represent boreal conifer forests, whereas the grid cells that are in the Niwot Ridge area were heterogeneous in land cover (e.g. tundra, grassland, forest) and a poor representation of conifer forest.

Field Code Changed

Field Code Changed

The relationship between iWUE and discrimination in the global simulation suggest that the site level trends are not isolated to the specific conditions of Niwot Ridge, but are a function of the model formulation. There is a relationship between iWUE and c_i^*/c_a (discrimination) as derived from equation (11) within the CLM model,

$$\frac{c_i^*}{c_a} \cong 1 - \frac{1.6}{c_a} iWUE. \quad (19)$$

The full derivation is provided in the supplement. Note that according to equation (19) increasing iWUE can be consistent with weakening discrimination (decreasing c_i/c_a ($\sim\alpha$)) and therefore consistent with established understanding between trends in iWUE and discrimination. However, this can be moderated by increasing c_a . During the course of our simulation (1850-2013) iWUE increased between 15-20% (Figure 7), however, c_a increased by 40%.

3.3.2.2 Magnitude of photosynthetic discrimination

The simulated photosynthetic discrimination (Fig. 8) was significantly larger than an estimate derived from observations and an isotopic mixing model (Bowling et al., 2014). For brevity we refer to the estimates based on the Bowling et al. (2014) method as ‘observed’ discrimination but highlight that they are derived from observations and not directly measured. On average, the simulated monthly growing season mean canopy discrimination was greater than observed values by 4.06, 2.36, and 1.85‰ for the *limited nitrogen*, *unlimited nitrogen*, and *no downregulation discrimination* formulations respectively. The model-observation mismatch in discrimination, despite model-observation agreement to biomass, carbon and latent heat flux tower observations (Figure 3) highlights the independent, and useful constraint isotopic observations provide for evaluating model performance. Specifically, the overestimation of discrimination may suggest the stomatal slope in the Ball-Berry model ($m=9$ in Eq. 54) used for these simulations was too high. This is supported by Mao et al., (2016), who found a reduced stomatal slope ($m=5.6$) was necessary for CLM 4.0 to match observed $\delta^{13}\text{C}$ in an isotope labeling study of loblolly pine forest in Tennessee. The stomatal slope was also important to match discrimination behavior in the ISOLSM model (Aranibar et al., 2006), a predecessor to CLM. A global analysis of stomatal slope inferred from leaf gas exchange measurements found that evergreen coniferous species, such as those at Niwot Ridge, had near the lowest values compared to other PFTs (Lin et al., 2015). In addition, they found that low stomatal slope values were characteristic of species with low stemwood construction costs per water transpired (high WUE), low soil moisture availability, and cold temperatures.

Alternatively, discrimination may be overestimated because CLM does not consider the resistance to CO_2 diffusion into the leaf chloroplast. The ability of CO_2 to diffuse across the chloroplast boundary layer, cell wall, and liquid interface is collectively known as the

Field Code Changed

Field Code Changed

mesophyll conductance (g_m) (Flexas et al., 2008). Multiple studies suggest that g_m is comparable in magnitude to g_s , and responds similarly to environmental conditions (Flexas et al., 2008). CLM does not account for g_m , and as a result assumes the intracellular CO_2 is the same as intercellular CO_2 , when it can be significantly lower (Di Marco et al., 1990; Sanchez-Rodriguez et al., 1999). The overestimation of c_i^* could have two important impacts upon our simulation. First, this may lead to unrealistically low values of V_{cmax} in order to compensate for the overestimation of c_i^* . In fact, we reduced the default value of V_{cmax} as much as 50% in our simulation to match the eddy covariance flux tower observations (see Section 4.13.3). Second, the overestimation of c_i^* should cause an overestimation of discrimination (Eq. 10), which is also consistent with our simulations (Figure 8). To determine whether the simulated discrimination bias is a model parameter calibration issue (g_s) or from excluding g_m , we recommend a mechanistic representation of mesophyll conductance within CLM.

The mixing model approach estimate of Δ_{canopy} (17 ‰) (Bowling et al. 2014), combined with δ_{atm} (-8.25 ‰) implies a $\delta^{13}\text{C}$ of biomass between -26 to -25 ‰ (Figure 8). This range is only slightly more enriched than the observed ranges of $\delta^{13}\text{C}$ of needle and root biomass (-27 to -26 ‰). The fact that the different approaches to measure discrimination differ by only 1 ‰, whereas CLM simulates a Δ_{canopy} that is 1.8 to 4.05-6 ‰ greater than the mixing model discrimination, strongly suggests that the model has overestimated discrimination from 2006-2012. Therefore what appeared to be a successful match between the simulated and observed $\delta^{13}\text{C}$ biomass, may in fact have been fortuitous. A multi-decadal time series of discrimination inferred from $\delta^{13}\text{C}$ of tree rings (Saurer et al., 2014; Frank et al., 2015) would be useful to investigate this mismatch as a function of time, but these data are not presently available.

If the overestimation of modeled discrimination originates from a lack of response of stomatal conductance to environmental conditions this could be a result of one or several of the following within the model: 1) the stomatal slope value is too high, 2) multi-decadal trends in climate (e.g. VPD) have not been included in the simulation 3) the model neglects g_m or 4) the Ball-Berry representation of g_s is not sensitive enough to changes in environmental conditions (e.g. humidity, soil moisture). It has been shown that VPD may be an improved predictor of g_s (Katul et al., 2000; Leuning, 1995) and discrimination (Ballantyne et al., 2010, 2011) as compared to relative humidity, currently used in CLM 4.5. Future work should consider which of these scenarios is responsible for overestimation of discrimination.

Field Code Changed

Field Code Changed

Field Code Changed

Field Code Changed

Field Code Changed

3.3.3.2.3 Seasonal pattern of photosynthetic discrimination

The model formulations that did not explicitly consider the influence of nitrogen limitation upon discrimination (*unlimited nitrogen, no downregulation discrimination*) were most successful at reproducing the seasonality of discrimination (Figure 8; Figure S4). In general, the observed discrimination was stronger during the spring and fall and weaker during summer. This observed Δ_{canopy} seasonal range (excluding November) varied from 16.5 to 18 ‰ using Reichstein partitioning (Figure 8), and was more pronounced using Lasslop partitioning (16.5 to 23 ‰) (Figure S4). The nitrogen limited simulated Δ_{canopy} had no seasonal trend whereas the *unlimited nitrogen* and *no downregulation discrimination* simulations ranged from 18.4 to 21.2 and 17.8 to 20.6 ‰ respectively. ~~both ranged from 21 to 23 ‰.~~

The main driver of the seasonality of discrimination was the net assimilation (A_n) for the *unlimited nitrogen* formulation (Figure 9). This was evident given the inversely proportional relationship between the simulated fractionation factor (α) and A_n , consistent with equation (11). Stomatal conductance (g_s) also influenced the seasonal pattern. The most direct evidence for this was during the period between days 175-200 (Figure 9), where A_n descended from its highest value (favoring higher α), and g_s abruptly ascended to its highest value (favoring higher α). The α responded to this increase in g_s with an abrupt increase by approximately 0.003 (3 ‰). Similarly, the *limited nitrogen* simulation seasonal discrimination pattern was shaped by both A_n and g_s , although the magnitude for both was approximately 30% higher during the summer months as compared to the unlimited nitrogen simulation. This was because the calibrated V_{cmax} value for the *limited nitrogen* simulation was much higher than for the *unlimited nitrogen* simulation (section 4.13.3). The difference in α between the two model formulations coincided with the sharp increase in f_{dreg} between days 125 and 275, providing strong evidence that the downregulation mechanism within the *limited nitrogen* formulation led to increased discrimination during the summer. Therefore, it follows that the nitrogen downregulation mechanism was the root cause of the small range in simulated seasonal cycle discrimination for the *limited nitrogen* formulation, which was inconsistent with the observations.

3.3.4.2.4 Environmental factors influencing seasonality of discrimination

The simulated Δ_{canopy} was driven primarily by net assimilation (A_n), followed by vapor pressure deficit (VPD) (Fig. 10). The correlation between VPD and Δ_{canopy} was strongest for

1 the *unlimited nitrogen* simulation, where the range in monthly average Δ_{canopy} spanned values
2 from 22 to 18 ‰ (Figure 10, middle row). This resembled the observed range in response based
3 upon a fitted relationship from Bowling et al., (2014) that spanned from roughly 16 to 19 ‰
4 (left panels of Fig. 10), although with a consistent discrimination bias. The correlation between
5 VPD and Δ_{canopy} , however, does not demonstrate causality. If that were the case, given that g_s
6 is a function of VPD (h_s term in Eq. 54) and discrimination is a function of g_s (Eq. 10; Eq. 11),
7 a similar relationship should have existed between g_s and Δ_{canopy} . This, in fact, was not the
8 case. Overall, the influence of g_s (responding to VPD) (R-value = -0.50) was secondary to A_n
9 (R-value = -0.77) in driving changes in discrimination (Figure 10). The model suggested that
10 the range in seasonal discrimination (intra-annual variation) was driven by the magnitude of A_n
11 based on the inverse relationship between A_n and Δ_{canopy} , (equation 11) illustrated by the
12 separation between months of low photosynthesis (October, May) vs. high photosynthesis
13 (June, July, August). During times of relatively low photosynthesis A_n also drove the inter-
14 annual variation in Δ_{canopy} . On the other hand, g_s (VPD) was most influential in driving the
15 inter-annual variation of discrimination during the summer months only, judging by the directly
16 proportional relationship during the months of June, July and August. Strictly speaking, g_s is a
17 function of h_s (leaf relative humidity) and not atmospheric VPD in CLM. However, the two
18 are closely related and the relationship between either variable (atmospheric VPD or simulated
19 leaf humidity) to Δ_{canopy} was similar (Figure S5).

20 The *limited nitrogen* formulation did not produce as wide a range in discrimination as
21 compared to the observations (Figure 10, top row). Part of this result was attributed to the lack
22 of response between A_n and Δ_{canopy} . In this case, the discrimination did not decrease with
23 increasing A_n because the signal was muted by the countering effect of f_{dreg} . The *limited*
24 *nitrogen* formulation was, however, able to reproduce the same discrimination response to g_s
25 as compared to the other model formulations. The tendency for the limited nitrogen model to
26 simulate discrimination response to g_s and not to A_n may negatively impact its ability to simulate
27 multi-decadal trends in discrimination. This may not be a major detriment to sites such as
28 Niwot Ridge which have maintained a consistent level of carbon uptake during the last decade,
29 and is likely more susceptible to environmental impact upon stomatal conductance. However,
30 sites that have shown a significant increase in assimilation rate (e.g. Harvard Forest; (Keenan
31 et al., 2013)) are less likely to be well represented by this model formulation.

Field Code Changed

Given the dependence of forest productivity at Niwot Ridge on snowmelt (Hu et al., 2010), it was surprising that the model simulated minimal soil moisture stress (Fig. 9e) and therefore minimal discrimination response to soil moisture. However, this finding was consistent with Bowling et al., (2014), who did not find an isotopic response to soil moisture. In addition, lack of response to change in soil moisture may not be indicative of poor performance of the isotopic sub-model performance, but rather an effect of the hydrology sub-model (Duarte et al. (in prep)). However, a comparison of observed soil moisture at various depths at Niwot Ridge generally agrees with the CLM simulated soil moisture (not shown), suggesting the lack of model response to soil moisture was not from biases in the hydrology model.

4 Discussion

3.4.4.1 Discrimination formulations: implications for model development

The *limited* and *unlimited model* formulations tested in this study represented two approaches to account for nitrogen limitation within ecosystem models. The *limited nitrogen* formulation reduced photosynthesis, *after the main photosynthesis calculation*, so that the carbon allocated to growth was accommodated by available nitrogen. This *allocation downscaling* approach is common to a subset of models, for example, CLM (Thornton et al., 2007), DAYCENT (Parton et al., 2010) and ED2.1 (Medvigy et al., 2009). Another class of models limits photosynthesis based upon foliar nitrogen content and adjusts the photosynthetic capacity through nitrogen availability in the leaf through V_{max} (e.g. CABLE, GDAY, LPJ-GUESS, OCN, SDVGM, TECO, *see* Zaehle et al., 2014). These *foliar nitrogen* models are similar to the *unlimited nitrogen* formulation of CLM because the scaling of photosynthesis was taken into account in the V_{max} scaling methodology (see discussion in section 2.1.2 and 2.4), *prior to the photosynthesis calculation*. In general, there were no categorical differences in behavior between these two classes of models during CO₂ manipulation experiments held at Duke forest and ORNL (Zaehle et al., 2014). *However*, CLM 4.0 was one of the few models in that study to consistently underestimate the NPP response to an increase of atmospheric CO₂ due to nitrogen limitation, ~~however~~ This finding was attributed to a lower initial supply of nitrogen and too strong of a coupling between carbon and nitrogen that limited biomass production. Also within this experiment, it was found that models that had no or partial coupling (CLM 4.0, DAYCENT) between A_n and g_s , generally predicted lower than observed WUE response to increases in CO₂ (De Kauwe et al., 2013). Similar to CLM 4.0, the *limited*

Formatted: Heading 1, Indent: First line: 0"

Field Code Changed

Field Code Changed

Field Code Changed

Field Code Changed

Field Code Changed

1 *nitrogen* formulation of CLM 4.5 in this manuscript is partially coupled (see Section 3.2.1).
2 The unlimited nitrogen formulation of CLM 4.5, on the other hand, is fully coupled and similar
3 to De Kauwe et al., (2013) outperformed the partially coupled version of CLM.

4 The *unlimited nitrogen* formulation described in our study ~~has similarities to a~~ ~~simplified~~ foliar nitrogen model, in that, ~~all of the information about the influence of~~ nitrogen
5 limitation is ~~parameterized~~ ~~incorporated~~ within the V_{cmax} ~~downscaling approach~~. ~~A more~~
6 ~~versatile approach would~~ ~~A true foliar nitrogen model, however, couples~~ a dynamic
7 nitrogen cycle directly with the calculation of V_{cmax} . This capability was recently developed
8 within CLM (Ghimire et al., 2016) and is scheduled to be included in the next CLM release.
9 Future work should test its functionality.

Field Code Changed

11 The performance of the *unlimited nitrogen* formulation was nearly identical to the *no*
12 *downregulation discrimination* formulation in terms of isotopic behavior despite the
13 mechanistic differences. The *no downregulation discrimination* formulation included nitrogen
14 limitation within the bulk carbon behavior but ignored the impact of f_{dreg} upon discrimination
15 behavior. The relative high simulation skill with this formulation implied that the ‘potential’
16 GPP linked to A_n , was a more effective predictor of discrimination behavior than the
17 ‘downscaled’ GPP, which is linked to $A_n * (1 - f_{dreg})$ (equation 11). There are several potential
18 explanations for an unrealistically large value of f_{dreg} . First this could indicate that the V_{cmax}
19 parameter was too large, thereby requiring a large f_{dreg} to compensate. As noted in Section
20 (3.1) the default temperate evergreen V_{cmax25} was $\sim 62 \mu\text{mol m}^{-2} \text{s}^{-1}$, much larger than what was
21 found based on literature reviews (Monson et al., 2005; Tomaszewski and Sievering, 2007).
22 We found to match the observed GPP we had to impose f_{dreg} that had the same effect as reducing
23 V_{cmax} (Figure S2) to values of 51 and $34 \mu\text{mol m}^{-2} \text{s}^{-1}$ for the *limited nitrogen* and *unlimited*
24 *nitrogen* formulations respectively. Alternatively, it could be that there are physiological
25 processes that are acting to reduce nitrogen limitation (e.g. nitrogen storage pools or transient
26 carbon storage as non-structural carbohydrates), or that the current measurement techniques are
27 underestimating GPP due to biases within the flux partitioning methods.

28 3.54.2 Disequilibrium, possible explanations of mismatch

29 Carbon cycle models (e.g. Fung et al., 1997) indicate that the steady decrease of δ_{atm} (Suess
30 effect, Fig. 2) should lead to a positive disequilibrium between land surface processes ($\delta^{13}\text{C}$
31 difference between GPP and ER, Eq. 14). This is because the δ_{GPP} reflects the most recent ($\delta^{13}\text{C}$

Field Code Changed

1 depleted) state of the atmosphere, whereas the δ_{ER} reflects carbon (e.g. soil carbon) assimilated
2 from an older ($\delta^{13}C$ enriched) atmosphere. This positive disequilibrium pattern promoted by
3 the Suess effect was consistent with all CLM formulations for this study with an annual average
4 disequilibrium of 0.8 ‰. In contrast, a negative disequilibrium (-0.6 ‰) was identified at
5 Niwot Ridge based upon observations (Bowling et al. 2014) as well as in other forests (Flanagan
6 et al., 2012; Wehr and Saleska, 2015; Wingate et al., 2010). Bowling et al. (2014) hypothesized
7 several reasons for this: 1) a strong seasonal stomatal response to atmospheric humidity, 2)
8 decreased photosynthetic discrimination associated with CO_2 fertilization, 3) decreased
9 photosynthetic discrimination associated with multi-decadal warming and increased VPD, and
10 4) post-photosynthetic discrimination. We evaluated the first three hypotheses within the
11 context of our CLM simulations.

12 The model results suggest a seasonal variation of discrimination that is a function of both
13 VPD and A_n . The simulated seasonal range in discrimination (Figure 8; Figure S4) varied by
14 approximately 2 ‰, and this range in seasonal discrimination could contribute to a negative
15 disequilibrium provided specific timing of assimilation, assimilate storage and respiration not
16 currently considered in the model. For example, if a significant portion of photosynthetic
17 assimilation was stored during the spring with relatively high discrimination, and then respired
18 during the summer, the net effect would deplete the δ_{ER} and thereby promote negative
19 disequilibrium during the summer months when discrimination is lower. Theoretically, this
20 could be achieved by explicitly including carbohydrate storage pools within CLM. Isotopic
21 tracer studies have shown assimilated carbon can exist for weeks to months within the
22 vegetation and soil before it is finally respired (Epron et al., 2012; Hogberg et al., 2008).
23 Although carbon storage pools are included in CLM, their allocation is almost always
24 instantaneous for evergreen systems and could not provide the isotopic effect described above.

25 The CO_2 fertilization effect tends to favor photosynthesis in plants and has been shown to
26 simultaneously increase WUE and decrease stomatal conductance as inferred from $\delta^{13}C$ in tree
27 rings (Frank et al., 2015; Flanagan et al., 2012; Wingate et al., 2010). In general a decrease in
28 stomatal conductance and increase in WUE is associated with a decrease in C_3 discrimination
29 (Farquhar et al., 1982), which opposes the disequilibrium trend imposed by the Suess effect.
30 The model simulation agrees with both these trends in WUE and stomatal conductance, yet
31 simulates an *increase* in discrimination (Figure 6; Figure 7), which reinforces the Suess effect
32 pattern upon disequilibrium. Although this appears to be a mismatch between forest processes

Field Code Changed

Field Code Changed

Field Code Changed

1 and model performance the model is operating within the limits of the discrimination
2 parameterization (Eq. 17) in which the magnitude of photosynthetic discrimination is inversely
3 proportional to the iWUE, but is also proportional to atmospheric CO₂ (see section 3.2.1).

4 A multi-decadal decrease in photosynthetic discrimination may also result from change in
5 climate. Meteorological measurements at Niwot Ridge during the last several decades
6 generally support conditions of higher VPD based upon a warming trend from an average
7 annual temperature of 1.1 °C in the 1980's to 2.7 °C in the 2000's (Mitton and Ferrenberg,
8 2012) and no overall trend in precipitation. It is possible that a multi-decadal trend in increasing
9 VPD contributed to multi-decadal weakening in photosynthetic discrimination given the
10 observed (Bowling et al., 2014) and modelled (Figure 10) correlation between Δ_{canopy} and VPD.
11 The model meteorology only included the years 1998-2013 and did not include the rapid
12 warming after the 1980's. It is unclear whether, if the full period of warming were to be
13 included in the simulation, the simulated discrimination response to VPD would be enough to
14 counter the Suess effect and lead to negative disequilibrium. Still, there is evidence that the
15 model is overestimating contemporary discrimination (Section 4.2.3-4) and the exclusion of the
16 full multi-decadal shift in VPD could be a significant reason why.

17 Finally, post-photosynthetic discrimination processes are likely to impact the magnitude
18 and sign of the isotopic disequilibrium (Bowling et al., 2008; Brüggemann et al., 2011) at
19 multiple temporal scales. None of these isotopic processes are currently modelled within CLM
20 4.5, so at present the model cannot be used to examine them.

21 4.5 Conclusions

22 This study provides a rigorous test of the representation of C isotope discrimination within
23 the highly mechanistic terrestrial carbon model CLM. CLM was able to accurately simulate
24 $\delta^{13}\text{C}$ in leaf and stem biomass and the seasonal cycle in Δ_{canopy} , but only when V_{max} was
25 calibrated to mimic the functionality of a foliar nitrogen model by accounting to account for
26 nitrogen limitation prior to photosynthesis (unlimited nitrogen formulation).

27 Although the unlimited nitrogen formulation (fully-coupled carbon -water cycle) was able
28 to match observed $\delta^{13}\text{C}$ of biomass and seasonal patterns in discrimination, it still overestimated
29 the contemporary magnitude of discrimination (2006-2012). Future work should identify
30 whether this overestimation was a result of parameterization (stomatal slope), exclusion of
31 multi-decadal shifts in VPD, limitations in the representation of stomatal conductance (Ball-
32 Berry model) or absence of the representation of mesophyll conductance.

Field Code Changed

Field Code Changed

Formatted: Font: Italic

1 The model attributed most of the range in seasonal discrimination to variation in net
2 assimilation rate (A_n) followed by variation in VPD, with little to no impact from soil moisture.
3 The model suggested that A_n drove the seasonal range in discrimination (across-month
4 variation) whereas VPD drove the inter-annual variation during the summer months. This
5 finding suggests that to simulate multi-decadal trends in photosynthetic discrimination,
6 response to assimilation rate and VPD must be well represented within the model.

7 The model simulated a positive disequilibrium that was driven by both the Suess effect,
8 and increased photosynthetic discrimination from CO_2 fertilization. It is possible that the
9 negative disequilibrium that was inferred from observations (Bowling et al., 2014) was driven
10 from the impacts of climate change and/or post-photosynthetic discrimination – not considered
11 in this version of the model.

12 The model simulated a consistent increase in water-use efficiency as a response to CO_2
13 fertilization and decrease in stomatal conductance. The model simulated an increase in WUE
14 despite an increase in discrimination, however C3 plants typically express the opposite trends
15 (increase in WUE, decrease in discrimination). Although CLM includes parameterization that
16 promotes an increase in WUE with a decrease in discrimination, this trend was likely moderated
17 by an increase in c_a .

18 Initial indications are that $\delta^{13}\text{C}$ isotope data can bring additional constraint to model
19 parameterization beyond what traditional flux tower measurements of carbon, water exchange,
20 and biomass measurements. The isotope measurements suggested a stomatal conductance
21 value generally lower than what was consistent with the flux tower measurements.
22 Unexpectedly, the isotopes also provided guidance upon model formulation related to nitrogen
23 limitation. The success of our empirical approach to account for nutrient limitation within the
24 V_{cmax} parameterization, suggests that additional testing of foliar nitrogen models are
25 worthwhile.

26 27 28 **Acknowledgements**

29 This research was supported by the U.S. Department of Energy, Office of Science, Office of
30 Biological and Environmental Research, Terrestrial Ecosystem Science Program under Award
31 Number DE-SC0010625. Thank you to Sean Burns and Peter Blanken for sharing flux tower

1 and meteorological data from Niwot Ridge. Thank you to those at NOAA who provided the
2 atmospheric flask data from Niwot Ridge including Bruce Vaughn, Ed Dlugokencky, the
3 INSTAAR Stable Isotope Lab and NOAA GMD. A special thanks to Keith Lindsay at NCAR
4 for providing global CESM output to help improve the discussion of model behavior. We are
5 grateful to Ralph Keeling and two anonymous reviewers who provided helpful comments. The
6 support and resources from the Center for High Performance Computing at the University of
7 Utah are gratefully acknowledged.

8

References

- Ainsworth, E. A. and Long, S. P.: What have we learned from 15 years of free-air CO₂ enrichment (FACE)? A meta-analytic review of the responses of photosynthesis, canopy properties and plant production to rising CO₂, *New Phytol.*, 165(2), 351–372, doi:10.1111/j.1469-8137.2004.01224.x, 2005.
- Andrews, S. F., Flanagan, L. B., Sharp, E. J. and Cai, T.: Variation in water potential, hydraulic characteristics and water source use in montane Douglas-fir and lodgepole pine trees in southwestern Alberta and consequences for seasonal changes in photosynthetic capacity, *Tree Physiol.*, 32, 146–160, doi:10.1093/treephys/tpr136, 2012.
- Aranibar, J. N., Berry, J. A., Riley, W. J., Pataki, D. E., Law, B. E. and Ehleringer, J. R.: Combining meteorology, eddy fluxes, isotope measurements, and modeling to understand environmental controls of carbon isotope discrimination at the canopy scale, *Glob. Change Biol.*, 12(4), 710–730, 2006.
- Arora, V. K., Boer, G. J., Friedlingstein, P., Eby, M., Jones, C. D., Christian, J. R., Bonan, G., Bopp, L., Brovkin, V., Cadule, P., Hajima, T., Ilyina, T., Lindsay, K., Tjiputra, J. F. and Wu, T.: Carbon-Concentration and Carbon-Climate Feedbacks in CMIP5 Earth System Models, *J. Clim.*, 26(15), 5289–5314, doi:10.1175/jcli-d-12-00494.1, 2013.
- Ballantyne, A. P., Miller, J. B. and Tans, P. P.: Apparent seasonal cycle in isotopic discrimination of carbon in the atmosphere and biosphere due to vapor pressure deficit, *Glob. Biogeochem. Cycles*, 24, GB3018, doi:10.1029/2009GB003623, 2010.
- Ballantyne, A. P., Miller, J. B., Baker, I. T., Tans, P. P. and White, J. W. C.: Novel applications of carbon isotopes in atmospheric CO₂: What can atmospheric measurements teach us about processes in the biosphere?, *Biogeosciences*, 8(10), 3093–3106, 2011.
- Belmecheri, S., Maxwell, R. S., Taylor, A. H., Davis, K. J., Freeman, K. H. and Munger, W. J.: Tree-ring $\delta^{13}\text{C}$ tracks flux tower ecosystem productivity estimates in a NE temperate forest, *Environ. Res. Lett.*, 9(7), 74011, doi:10.1088/1748-9326/9/7/074011, 2014.
- Boisvenue, C. and Running, S. W.: Simulations show decreasing carbon stocks and potential for carbon emissions in Rocky Mountain forests over the next century, *Ecol. Appl.*, 20(5), 1302–1319, 2010.
- Bowling, D. R., Pataki, D. E. and Randerson, J. T.: Carbon isotopes in terrestrial ecosystem pools and CO₂ fluxes, *New Phytol.*, 178, 24–40, doi: 10.1111/j.1469-8137.2007.02342.x, 2008.
- Bowling, D. R., Ballantyne, A. P., Miller, J. B., Burns, S. P., Conway, T. J., Menzer, O., Stephens, B. B. and Vaughn, B. H.: Ecological processes dominate the $\delta^{13}\text{C}$ land disequilibrium in a Rocky Mountain subalpine forest, *Glob. Biogeochem. Cycles*, 28(4), 2013GB004686, doi:10.1002/2013GB004686, 2014a.
- Bowling, D. R., Ballantyne, A. P., Miller, J. B., Burns, S. P., Conway, T. J., Menzer, O., Stephens, B. B. and Vaughn, B. H.: Ecological processes dominate the $\delta^{13}\text{C}$ land disequilibrium in a Rocky Mountain subalpine forest, *Glob. Biogeochem. Cycles*, 28(4), 2013GB004686, doi:10.1002/2013GB004686, 2014b.

Formatted: Bibliography, Widow/Orphan control, Adjust space between Latin and Asian text, Adjust space between Asian text and numbers

Field Code Changed

1 [Bradford, M. A., Fierer, N. and Reynolds, J. F.: Soil carbon stocks in experimental mesocosms](#)
2 [are dependent on the rate of labile carbon, nitrogen and phosphorus inputs to soils, *Funct. Ecol.*,](#)
3 [22\(6\), 964–974, doi:10.1111/j.1365-2435.2008.01404.x, 2008.](#)

4 [Braswell, B. H., Sacks, W. J., Linder, E. and Schimel, D. S.: Estimating diurnal to annual](#)
5 [ecosystem parameters by synthesis of a carbon flux model with eddy covariance net ecosystem](#)
6 [exchange observations, *Glob. Change Biol.*, 11, 335–355, doi:10.1111/j.1365-](#)
7 [2486.2005.00897.x, 2005.](#)

8 [Brüggemann, N., Gessler, A., Kayler, Z., Keel, S. G., Badeck, F., Barthel, M., Boeckx, P.,](#)
9 [Buchmann, N., Brugnoli, E., Esperschütz, J., Gavrichkova, O., Ghashghaie, J., Gomez-](#)
10 [Casanovas, N., Keitel, C., Knohl, A., Kuptz, D., Palacio, S., Salmon, Y., Uchida, Y. and Bahn,](#)
11 [M.: Carbon allocation and carbon isotope fluxes in the plant-soil-atmosphere continuum: a](#)
12 [review, *Biogeosciences*, 8\(11\), 3457–3489, doi:10.5194/bg-8-3457-2011, 2011a.](#)

13 [Brüggemann, N., Gessler, A., Kayler, Z., Keel, S. G., Badeck, F., Barthel, M., Boeckx, P.,](#)
14 [Buchmann, N., Brugnoli, E., Esperschütz, J., Gavrichkova, O., Ghashghaie, J., Gomez-](#)
15 [Casanovas, N., Keitel, C., Knohl, A., Kuptz, D., Palacio, S., Salmon, Y., Uchida, Y. and Bahn,](#)
16 [M.: Carbon allocation and carbon isotope fluxes in the plant-soil-atmosphere continuum: A](#)
17 [review, *Biogeosciences*, 8\(11\), 3457–3489, 2011b.](#)

18 [Cernusak, L. A., Ubierna, N., Winter, K., Holtum, J. A. M., Marshall, J. D. and Farquhar, G.](#)
19 [D.: Environmental and physiological determinants of carbon isotope discrimination in](#)
20 [terrestrial plants, *New Phytol.*, 200\(4\), 950–965, //.](#)

21 [Collatz, G. J., Ball, J. T., Grivet, C. and Berry, J. A.: Regulation of stomatal conductances and](#)
22 [transpiration a physiological model of canopy processes, *Agric. For. Meteorol.*, 54, 107–136,](#)
23 [1991.](#)

24 [De Kauwe, M. G., Medlyn, B. E., Zaehle, S., Walker, A. P., Dietze, M. C., Hickler, T., Jain, A.](#)
25 [K., Luo, Y., Parton, W. J., Prentice, I. C., Smith, B., Thornton, P. E., Wang, S., Wang, Y.-P.,](#)
26 [Wärnlind, D., Weng, E., Crous, K. Y., Ellsworth, D. S., Hanson, P. J., Seok Kim, H., Warren, J.](#)
27 [M., Oren, R. and Norby, R. J.: Forest water use and water use efficiency at elevated CO₂: a](#)
28 [model-data intercomparison at two contrasting temperate forest FACE sites, *Glob. Change*](#)
29 [Biol., 19\(6\), 1759–1779, doi:10.1111/gcb.12164, 2013.](#)

30 [Desai, A. R., Moore, D. J. P., Ahue, W. K. M., Wilkes, P. T. V., De Wekker, S. F. J., Brooks,](#)
31 [B. G., Campos, T. L., Stephens, B. B., Monson, R. K., Burns, S. P., Quaife, T., Aulenbach, S.](#)
32 [M. and Schimel, D. S.: Seasonal pattern of regional carbon balance in the central Rocky](#)
33 [Mountains from surface and airborne measurements, *J. Geophys. Res.*, 116, G04009\(4\),](#)
34 [doi:10.1029/2011JG001655, 2011.](#)

35 [Di Marco, G., Manes, F., Tricoli, D. and Vitale, E.: Fluorescence Parameters Measured](#)
36 [Concurrently with Net Photosynthesis to Investigate Chloroplastic CO₂ Concentration in](#)
37 [Leaves of *Quercus ilex* L., *J. Plant Physiol.*, 136\(5\), 538–543, doi:10.1016/S0176-](#)
38 [1617\(11\)80210-5, 1990.](#)

39 [Dlugokencky, E. J., Lang, P. M., Masarie, K. A., Crotwell, A. M. and Crotwell, M. J.:](#)
40 [Atmospheric Carbon Dioxide Dry Air Mole Fractions from the NOAA ESRL Carbon Cycle](#)

1 [Cooperative Global Air Sampling network, 1968-2014, Version: 2015-08-03, Path:](#)
2 [ftp://aftp.cmdl.noaa.gov/data/trace_gases/co2/flask/surface/, 2015.](#)

3 [Ehleringer, J. R., Buchmann, N. and Flanagan, L. B.: Carbon isotope ratios in belowground](#)
4 [carbon cycle processes, *Ecol. Appl.*, 10\(2\), 412–422, 2000.](#)

5 [Epron, D., Bahn, M., Derrien, D., Lattanzi, F. A., Pumpanen, J., Gessler, A., Högberg, P.,](#)
6 [Maillard, P., Dannoura, M., Gérant, D. and Buchmann, N.: Pulse-labelling trees to study carbon](#)
7 [allocation dynamics: a review of methods, current knowledge and future prospects, *Tree*](#)
8 [Physiol., 32\(6\), 776–798, doi:10.1093/treephys/tps057, 2012.](#)

9 [Farquhar, G. D., von Caemmerer, S. and Berry, J. A.: A Biochemical Model of Photosynthetic](#)
10 [CO₂ Assimilation in Leaves of C₃ Species, *Planta*, 149, 78–90, 1980.](#)

11 [Farquhar, G. D., O’Leary, M. H. and Berry, J. A.: On the relationship between carbon isotope](#)
12 [discrimination and the intercellular carbon dioxide concentration in leaves, *Aust. J. Plant*](#)
13 [Physiol., 9\(2\), 121–137, 1982.](#)

14 [Farquhar, G. D., Ehleringer, J. R. and Hubick, K. T.: Carbon isotope discrimination and](#)
15 [photosynthesis, *Annu. Rev. Plant Physiol. Plant Mol. Biol.*, 40, 503–537, 1989.](#)

16 [Flanagan, L. B., Cai, T., Black, T. A., Barr, A. G., McCaughey, J. H. and Margolis, H. A.:](#)
17 [Measuring and modeling ecosystem photosynthesis and the carbon isotope composition of](#)
18 [ecosystem-respired CO₂ in three boreal coniferous forests, *Agric. For. Meteorol.*, 153, 165–](#)
19 [176, 2012.](#)

20 [Flexas, J., Ribas-Carbó, M., Hanson, D. T., Bota, J., Otto, B., Cifre, J., McDowell, N., Medrano,](#)
21 [H. and Kaldenhoff, R.: Tobacco aquaporin NtAQP1 is involved in mesophyll conductance to](#)
22 [CO₂ in vivo, *Plant J.*, 48\(3\), 427–439, doi:10.1111/j.1365-313X.2006.02879.x, 2006.](#)

23 [Flexas, J., Ribas-Carbo, M., Diaz-Espej, A., Galmes, J. and Medrano, H.: Mesophyll](#)
24 [conductance to CO₂: current knowledge and future prospects, *Plant Cell Environ.*, 31\(5\), 602–](#)
25 [621, 2008.](#)

26 [Francey, R. J., Allison, C. E., Etheridge, D. M., Trudinger, C. M., Enting, I. G., Leuenberger,](#)
27 [M., Langenfelds, R. L., Michel, E. and Steele, L. P.: A 1000-year high precision record of δ¹³C](#)
28 [in atmospheric CO₂, *Tellus*, 51B, 170–193, 1999.](#)

29 [Frank, D. C., Poulter, B., Saurer, M., Esper, J., Huntingford, C., Helle, G., Treydte, K.,](#)
30 [Zimmermann, N. E., Schleser, G. H., Ahlström, A., Ciais, P., Friedlingstein, P., Levis, S.,](#)
31 [Lomas, M., Sitch, S., Viovy, N., Andreu-Hayles, L., Bednarz, Z., Berninger, F., Boettger, T.,](#)
32 [D’Alessandro, C. M., Daux, V., Filot, M., Grabner, M., Gutierrez, E., Haupt, M., Hiltunen, J.,](#)
33 [Jungner, H., Kalela-Brundin, M., Krapiec, M., Leuenberger, M., Loader, N. J., Marah, H.,](#)
34 [Masson-Delmotte, V., Pazdur, A., Pawelczyk, S., Pierre, M., Planells, O., Pukienė, R.,](#)
35 [Reynolds-Henne, C. E., Rinne, K. T., Saracino, A., Sonninen, E., Stievenard, M., Switsur, V.,](#)
36 [R., Szczepanek, M., Szychowska-Krapiec, E., Todaro, L., Waterhouse, J. S. and Weigl, M.:](#)
37 [Water-use efficiency and transpiration across European forests during the Anthropocene, *Nat.*](#)
38 [Clim. Change, 5\(6\), 579–583, doi:10.1038/nclimate2614, 2015.](#)

39 [Franks, P. J., Adams, M. A., Amthor, J. S., Barbour, M. M., Berry, J. A., Ellsworth, D. S.,](#)
40 [Farquhar, G. D., Ghannoum, O., Lloyd, J., McDowell, N., Norby, R. J., Tissue, D. T. and von](#)

1 [Caemmerer, S.: Sensitivity of plants to changing atmospheric CO₂ concentration: From the](#)
2 [geological past to the next century, *New Phytol.*, 197\(4\), 1077–1094, 2013.](#)

3 [Friedlingstein, P., Cox, P. M., Betts, R. A., Bopp, L., von Bloh, W., Brovkin, V., Cadule, P.,](#)
4 [Doney, S. C., Eby, M., Fung, I. Y., Bala, G., John, J., Jones, C. D., Joos, F., Kato, T., Kawamiya,](#)
5 [M., Knorr, W., Lindsay, K., Matthews, H. D., Raddatz, T., Rayner, P., Reick, C., Roeckner, E.,](#)
6 [Schnitzler, K.-G., Schnur, R., Strassmann, K., Weaver, A. J., Yoshikawa, C. and Zeng, N.: Climate-carbon cycle feedback analysis: Results from the C4MIP model intercomparison, *J.*
7 \[Clim.\]\(#\), 19, 3337–3353, 2006.](#)

9 [Fung, I. Y., Field, C. B., Berry, J. A., Thompson, M. V., Randerson, J. T., Malmstrom, C. M.,](#)
10 [Vitousek, P. M., Collatz, G. J., Sellers, P. J., Randall, D. A., Denning, A. S., Badeck, F. and](#)
11 [John, J.: Carbon 13 exchanges between the atmosphere and biosphere, *Glob. Biogeochem.*
12 \[Cycles\]\(#\), 11\(4\), 507–533, 1997.](#)

13 [Ghimire, B., Riley, W. J., Koven, C. D., Mu, M. and Randerson, J. T.: Representing leaf and](#)
14 [root physiological traits in CLM improves global carbon and nitrogen cycling predictions, *J.*
15 \[Adv. Model. Earth Syst.\]\(#\), n/a-n/a, doi:10.1002/2015MS000538, 2016.](#)

16 [Greenland, D.: The Climate of Niwot Ridge, Front Range, Colorado, U.S.A., *Arct. Alp. Res.*,](#)
17 [21\(4\), 380–391, 1989.](#)

18 [Hogberg, P., Hogberg, M. N., Gottlicher, S. G., Betson, N. R., Keel, S. G., Metcalfe, D. B.,](#)
19 [Campbell, C., Schindlbacher, A., Hurry, V., Lundmark, T., Linder, S. and Nasholm, T.: High](#)
20 [temporal resolution tracing of photosynthate carbon from the tree canopy to forest soil](#)
21 [microorganisms, *New Phytol.*, 177\(1\), 220–228, 2008.](#)

22 [Hu, J., Moore, D. J. P., Burns, S. P. and Monson, R. K.: Longer growing seasons lead to less](#)
23 [carbon sequestration by a subalpine forest, *Glob. Change Biol.*, 16\(2\), 771–783,](#)
24 [doi:10.1111/j.1365-2486.2009.01967.x, 2010.](#)

25 [Katul, G. G., Ellsworth, D. S. and Lai, C.-T.: Modelling assimilation and intercellular CO₂](#)
26 [from measured conductance: a synthesis of approaches, *Plant Cell Environ.*, 23\(12\), 1313–](#)
27 [1328, doi:10.1046/j.1365-3040.2000.00641.x, 2000.](#)

28 [Keenan, T. F., Hollinger, D. Y., Bohrer, G., Dragoni, D., Munger, J. W., Schmid, H. P. and](#)
29 [Richardson, A. D.: Increase in forest water-use efficiency as atmospheric carbon dioxide](#)
30 [concentrations rise, *Nature*, 499\(7458\), 324–327, doi:10.1038/nature12291, 2013.](#)

31 [Kolari, P., Lappalainen, H. K., HäNninen, H. and Hari, P.: Relationship between temperature](#)
32 [and the seasonal course of photosynthesis in Scots pine at northern timberline and in southern](#)
33 [boreal zone, *Tellus B*, 59\(3\), 542–552, doi:10.1111/j.1600-0889.2007.00262.x, 2007.](#)

34 [Lasslop, G., Reichstein, M., Papale, D., Richardson, A., Arneth, A., Barr, A., Stoy, P. and](#)
35 [Wohlfahrt, G.: Separation of net ecosystem exchange into assimilation and respiration using a](#)
36 [light response curve approach: critical issues and global evaluation, *Glob. Change Biol.*, 16,](#)
37 [187–208, 2010.](#)

38 [Le Quéré, C., Moriarty, R., Andrew, R. M., Peters, G. P., Ciais, P., Friedlingstein, P., Jones, S.](#)
39 [D., Sitch, S., Tans, P., Arneth, A., Boden, T. A., Bopp, L., Bozec, Y., Canadell, J. G., Chini, L.](#)
40 [P., Chevallier, F., Cosca, C. E., Harris, I., Hoppema, M., Houghton, R. A., House, J. I., Jain, A.](#)

1 [K., Johannessen, T., Kato, E., Keeling, R. F., Kitidis, V., Klein Goldewijk, K., Koven, C.,](#)
2 [Landa, C. S., Landschützer, P., Lenton, A., Lima, I. D., Marland, G., Mathis, J. T., Metzl, N.,](#)
3 [Nojiri, Y., Olsen, A., Ono, T., Peng, S., Peters, W., Pfeil, B., Poulter, B., Raupach, M. R.,](#)
4 [Regnier, P., Rödenbeck, C., Saito, S., Salisbury, J. E., Schuster, U., Schwinger, J., Séférian, R.,](#)
5 [Segschneider, J., Steinhoff, T., Stocker, B. D., Sutton, A. J., Takahashi, T., Tilbrook, B., van](#)
6 [der Werf, G. R., Viovy, N., Wang, Y.-P., Wanninkhof, R., Wiltshire, A. and Zeng, N.: Global](#)
7 [carbon budget 2014, Earth Syst. Sci. Data, 7\(1\), 47–85, doi:10.5194/essd-7-47-2015, 2015.](#)

8 [Leuning, R.: A critical appraisal of a combined stomatal-photosynthesis model for C3 plants,](#)
9 [Plant Cell Environ., 18\(4\), 339–355, doi:10.1111/j.1365-3040.1995.tb00370.x, 1995.](#)

10 [Lin, Y.-S., Medlyn, B. E., Duursma, R. A., Prentice, I. C., Wang, H., Baig, S., Eamus, D., de](#)
11 [Dios, V. R., Mitchell, P., Ellsworth, D. S., de Beeck, M. O., Wallin, G., Uddling, J., Tarvainen,](#)
12 [L., Linderson, M.-L., Cernusak, L. A., Nippert, J. B., Ocheltree, T. W., Tissue, D. T., Martin-](#)
13 [StPaul, N. K., Rogers, A., Warren, J. M., De Angelis, P., Hikosaka, K., Han, Q., Onoda, Y.,](#)
14 [Gimeno, T. E., Barton, C. V. M., Bennie, J., Bonal, D., Bosc, A., Löw, M., Macinins-Ng, C.,](#)
15 [Rey, A., Rowland, L., Setterfield, S. A., Tausz-Posch, S., Zaragoza-Castells, J., Broadmeadow,](#)
16 [M. S. J., Drake, J. E., Freeman, M., Ghannoum, O., Hutley, L. B., Kelly, J. W., Kikuzawa, K.,](#)
17 [Kolari, P., Koyama, K., Limousin, J.-M., Meir, P., Lola da Costa, A. C., Mikkelsen, T. N.,](#)
18 [Salinas, N., Sun, W. and Wingate, L.: Optimal stomatal behaviour around the world, Nat. Clim.](#)
19 [Change, 5\(5\), 459–464, doi:10.1038/nclimate2550, 2015.](#)

20 [Mao, J., Ricciuto, D. M., Thornton, P. E., Warren, J. M., King, A. W., Shi, X., Iversen, C. M.](#)
21 [and Norby, R. J.: Evaluating the Community Land Model in a pine stand with shading](#)
22 [manipulations and ¹³C and ¹⁸O labeling,](#)
23 [Biogeosciences, 13\(3\), 641–657, doi:10.5194/bg-13-641-2016, 2016.](#)

24 [Martinelli, L. A., Almeida, S., Brown, I. F., Moreira, M. Z., Victoria, R. L., Sternberg, L. S. L.,](#)
25 [Ferreira, C. A. C. and Thomas, W. W.: Stable carbon isotope ratio of tree leaves, boles and fine](#)
26 [litter in a tropical forest in Rondonia, Brazil, Oecologia, 114\(2\), 170–179, 1998.](#)

27 [McDowell, N. G., Allen, C. D. and Marshall, L.: Growth, carbon-isotope discrimination, and](#)
28 [drought-associated mortality across a Pinus ponderosa elevational transect, Glob. Change Biol.,](#)
29 [16\(1\), 399–415, 2010.](#)

30 [Medvigy, D., Wofsy, S. C., Munger, J. W., Hollinger, D. Y. and Moorcroft, P. R.: Mechanistic](#)
31 [scaling of ecosystem function and dynamics in space and time: Ecosystem Demography model](#)
32 [version 2, J. Geophys. Res.-Biogeosciences, 114, G01002, doi:10.1029/2008JG000812, 2009.](#)

33 [Mitton, J. . and Ferrenberg, S. M.: Mountain pine beetle develops an unprecedented summer](#)
34 [generation in response to climate warming, Am. Nat., 179\(5\), 1–9, 2012.](#)

35 [Monson, R. K., Turnipseed, A. A., Sparks, J. P., Harley, P. C., Scott-Denton, L. E., Sparks, K.](#)
36 [and Huxman, T. E.: Carbon sequestration in a high-elevation, subalpine forest, Glob. Change](#)
37 [Biol., 8, 459–478, 2002.](#)

38 [Monson, R. K., Sparks, J. P., Rosentiel, T. N., Scott-Denton, L. E., Huxman, T. E., Harley, P.](#)
39 [C., Turnipseed, A. A., Burns, S. P., Backlund, B. and Hu, J.: Climatic influences on net](#)
40 [ecosystem CO₂ exchange during the transition from wintertime carbon source to springtime](#)
41 [carbon sink in a high-elevation, subalpine forest, Oecologia, 146, 130-147-5-169–2, 2005.](#)

1 [Oleson et al.: Technical Description of version 4.5 of the Community Land Model \(CLM\),](#)
2 [\[online\]](#) Available from:
3 http://www.cesm.ucar.edu/models/cesm1.2/clm/CLM45_Tech_Note.pdf, 2013.

4 [Parton, W. J., Hanson, P. J., Swanston, C., Torn, M., Trumbore, S. E., Riley, W. and Kelly, R.: ForCent model development and testing using the Enriched Background Isotope Study experiment, J. Geophys. Res. Biogeosciences, 115\(G4\), G04001, doi:10.1029/2009JG001193, 2010.](#)

8 [Peñuelas, J., Canadell, J. G. and Ogaya, R.: Increased water-use efficiency during the 20th century did not translate into enhanced tree growth, Glob. Ecol. Biogeogr., 20\(4\), 597–608, doi:10.1111/j.1466-8238.2010.00608.x, 2011.](#)

11 [Reichstein, M., Falge, E., Baldocchi, D., Papale, D., Aubinet, M., Berbigier, P., Bernhofer, C., Buchmann, N., Gilmanov, T., Granier, A., Grunwald, T., Havrankova, K., Ilvesniemi, H., Janous, D., Knohl, A., Laurila, T., Lohila, A., Loustau, D., Matteucci, G., Meyers, T., Miglietta, F., Ourcival, J. M., Pumpanen, J., Rambal, S., Rotenberg, E., Sanz, M., Tenhunen, J., Seufert, G., Vaccari, F., Vesala, T., Yakir, D. and Valentini, R.: On the separation of net ecosystem exchange into assimilation and ecosystem respiration: review and improved algorithm, Glob. Change Biol., 11\(9\), 1424–1439, 2005.](#)

18 [Ricciuto, D. M., Davis, K. J. and Keller, K.: A Bayesian calibration of a simple carbon cycle model: The role of observations in estimating and reducing uncertainty, Glob. Biogeochem. Cycles, 22, GB2030, doi:10.1029/2006GB002908, 2008.](#)

21 [Ricciuto, D. M., King, A. W., Dragoni, D. and Post, W. M.: Parameter and prediction uncertainty in an optimized terrestrial carbon cycle model: Effects of constraining variables and data record length, J. Geophys. Res. Biogeosciences, 116\(G1\), G01033, doi:10.1029/2010JG001400, 2011.](#)

25 [Richardson, A. D., Williams, M., Hollinger, D. Y., Moore, D. J. P., Dail, D. B., Davidson, E. A., Scott, N. A., Evans, R. S., Hughes, H., Lee, J. T., Rodrigues, C. and Savage, K.: Estimating parameters of a forest ecosystem C model with measurements of stocks and fluxes as joint constraints, Oecologia, 164\(1\), 25–40, 2010.](#)

29 [Roden, J. S. and Ehleringer, J. R.: Summer precipitation influences the stable oxygen and carbon isotopic composition of tree-ring cellulose in *Pinus ponderosa*, Tree Physiol., 27\(4\), 491–501, 2007.](#)

32 [Rubino, M., Etheridge, D. M., Trudinger, C. M., Allison, C. E., Battle, M. O., Langenfelds, R. L., Steele, L. P., Curran, M., Bender, M., White, J. W. C., Jenk, T. M., Blunier, T. and Francey, R. J.: A revised 1000 year atmospheric \$\delta^{13}\text{C}\$ -CO₂ record from Law Dome and South Pole, Antarctica, J. Geophys. Res. Atmospheres, 118\(15\), 8482–8499, doi:10.1002/jgrd.50668, 2013.](#)

36 [Sánchez-Rodríguez, J., Pérez, P. and Martínez-Carrasco, R.: Photosynthesis, carbohydrate levels and chlorophyll fluorescence-estimated intercellular CO₂ in water-stressed *Casuarina equisetifolia* Forst. & Forst., Plant Cell Environ., 22\(7\), 867–873, doi:10.1046/j.1365-3040.1999.00447.x, 1999.](#)

1 [Saurer, M., Siegwolf, R. T. W. and Schweingruber, F. H.: Carbon isotope discrimination](#)
2 [indicates improving water-use efficiency of trees in northern Eurasia over the last 100 years,](#)
3 [Glob. Change Biol., 10\(12\), 2109–2120, doi:10.1111/j.1365-2486.2004.00869.x, 2004.](#)

4 [Saurer, M., Spahni, R., Frank, D. C., Joos, F., Leuenberger, M., Loader, N. J., McCarroll, D.,](#)
5 [Gagen, M., Poulter, B., Siegwolf, R. T. W., Andreu-Hayles, L., Boettger, T., Dorado Liñán, I.,](#)
6 [Fairchild, I. J., Friedrich, M., Gutierrez, E., Haupt, M., Hiltunen, E., Heinrich, I., Helle, G.,](#)
7 [Grubb, H., Jalkanen, R., Levanič, T., Linderholm, H. W., Robertson, I., Sonninen, E., Treydte,](#)
8 [K., Waterhouse, J. S., Woodley, E. J., Wynn, P. M. and Young, G. H. F.: Spatial variability and](#)
9 [temporal trends in water-use efficiency of European forests, Glob. Change Biol., 20\(12\), 3700–](#)
10 [3712, doi:10.1111/gcb.12717, 2014.](#)

11 [Schaeffer, S. M., Miller, J. B., Vaughn, B. H., White, J. W. C. and Bowling, D. R.: Long-term](#)
12 [field performance of a tunable diode laser absorption spectrometer for analysis of carbon](#)
13 [isotopes of CO₂ in forest air, Atmospheric Chem. Phys., 8, 5263–5277, 2008.](#)

14 [Schimel, D. T., Kittel, G. F., Running, S., Monson, R., Turnispeed, A. and Anderson, D.:](#)
15 [Carbon sequestration studied in western U.S. mountains, Eos Trans AGU, 83\(40\), 445–449,](#)
16 [2002.](#)

17 [Scott-Denton, L. E., Sparks, K. L. and Monson, R. K.: Spatial and temporal controls of soil](#)
18 [respiration rate in a high-elevation, subalpine forest, Soil Biol. Biochem., 35, 525–534, 2003.](#)

19 [Sellers, P. J., Randall, D. A., Collatz, G. J., Berry, J. A., Field, C. B., Dazlich, D. A., Zhang, C.,](#)
20 [Collelo, G. D. and Bounoua, L.: A revised land surface parameterization \(SiB2\) for atmospheric](#)
21 [GCMs. Part I: Model formulation, J. Clim., 9\(4\), 676–705, 1996.](#)

22 [Thornton, P. E. and Rosenbloom, N. A.: Ecosystem model spin-up: Estimating steady state](#)
23 [conditions in a coupled terrestrial carbon and nitrogen cycle model, Ecol. Model., 189\(1–2\),](#)
24 [25–48, doi:10.1016/j.ecolmodel.2005.04.008, 2005.](#)

25 [Thornton, P. E., Law, B. E., Gholz, H. L., Clark, K. L., Falge, E., Ellsworth, D. S., Golstein, A.](#)
26 [H., Monson, R. K., Hollinger, D., Falk, M., Chen, J. and Sparks, J. P.: Modeling and measuring](#)
27 [the effects of disturbance history and climate on carbon and water budgets in evergreen](#)
28 [needleleaf forests, Agric. For. Meteorol., 113\(1–4\), 185–222, 2002.](#)

29 [Thornton, P. E., Lamarque, J.-F., Rosenbloom, N. A. and Mahowald, N. M.: Influence of](#)
30 [carbon-nitrogen cycle coupling on land model response to CO₂ fertilization and climate](#)
31 [variability, Glob. Biogeochem. Cycles, 21, GB4018, doi:10.1029/2006GB002868, 2007.](#)

32 [Trolier, M., White, J. W. C., Tans, P. P., Masarie, K. A. and Gemery, P. A.: Monitoring the](#)
33 [isotopic composition of atmospheric CO₂: Measurements from the NOAA Global Air](#)
34 [Sampling Network, J. Geophys. Res.-Atmospheres, 101\(D20\), 25,897–25,916, 1996.](#)

35 [van der Velde, I. R., Miller, J. B., Schaefer, K., Masarie, K. A., Denning, S., White, J. W. C.,](#)
36 [Tans, P. P., Krol, M. C. and Peters, W.: Biosphere model simulations of interannual variability](#)
37 [in terrestrial 13C/12C exchange, Glob. Biogeochem. Cycles, 27\(3\), 637–649,](#)
38 [doi:10.1002/gbc.20048, 2013.](#)

39 [Ward, E. J., Oren, R., Bell, D. M., Clark, J. S., McCarthy, H. R., Kim, H.-S. and Domec, J.-C.:](#)
40 [The effects of elevated CO₂ and nitrogen fertilization on stomatal conductance estimated from](#)

1 [11 years of scaled sap flux measurements at Duke FACE, Tree Physiol.,](#)
2 [doi:10.1093/treephys/tps118, 2012.](#)

3 [Wehr, R. and Saleska, S. R.: An improved isotopic method for partitioning net ecosystem–](#)
4 [atmosphere CO₂ exchange, Agric. For. Meteorol., 214–215, 515–531,](#)
5 [doi:10.1016/j.agrformet.2015.09.009, 2015.](#)

6 [White et al.: Parameterization and Sensitivity Analysis of the Biome-BGC Terrestrial](#)
7 [Ecosystem Model: Net Primary Production Controls, \[online\] Available from:](#)
8 [http://secure.nts.umd.edu/publications/2000/WTRN00/White_2000.pdf, 2000.](#)

9 [White, J. W. C., Vaughn, B. H., Michel, S. E., University of Colorado and Institute of Arctic](#)
10 [and Alpine Research \(INSTAAR\): Stable Isotopic Composition of Atmospheric Carbon](#)
11 [Dioxide \(13C and 18O\) from the NOAA ESRL Carbon Cycle Cooperative Global Air Sampling](#)
12 [Network, 1990–2014, Version: 2015–10–26, Path:](#)
13 [ftp://aftp.cmdl.noaa.gov/data/trace_gases/co2c13/flask/, 2015.](#)

14 [Wingate, L., Ogee, J., Burlett, R., Bosc, A., Devaux, M., Grace, J., Loustau, D. and Gessler,](#)
15 [A.: Photosynthetic carbon isotope discrimination and its relationship to the carbon isotope](#)
16 [signals of stem, soil and ecosystem respiration, New Phytol., 188\(2\), 576–589, 2010.](#)

17 [Zachle, S., Medlyn, B. E., De Kauwe, M. G., Walker, A. P., Dietze, M. C., Hickler, T., Luo,](#)
18 [Y., Wang, Y.-P., El-Masri, B., Thornton, P., Jain, A., Wang, S., Warlind, D., Weng, E., Parton,](#)
19 [W., Iversen, C. M., Gallet-Budynek, A., McCarthy, H., Finzi, A., Hanson, P. J., Prentice, I. C.,](#)
20 [Oren, R. and Norby, R. J.: Evaluation of 11 terrestrial carbon–nitrogen cycle models against](#)
21 [observations from two temperate Free-Air CO₂ Enrichment studies, New Phytol., 202\(3\), 803–](#)
22 [822, doi:10.1111/nph.12697, 2014.](#)

23 [Zarter, C. R., Demmig-Adams, B., Ebbert, V., Adamska, I. and Adams, W. W.: Photosynthetic](#)
24 [capacity and light harvesting efficiency during the winter-to-spring transition in subalpine](#)
25 [conifers, New Phytol., 172\(2\), 283–292, doi:10.1111/j.1469-8137.2006.01816.x, 2006.](#)

26 [Zeng, X.: Global Vegetation Root Distribution for Land Modeling, J. Hydrometeorol., 2\(5\),](#)
27 [525–530, doi:10.1175/1525-7541\(2001\)002<0525:GVRDFL>2.0.CO;2, 2001.](#)

28 [Zeng, X. and Decker, M.: Improving the Numerical Solution of Soil Moisture–Based Richards](#)
29 [Equation for Land Models with a Deep or Shallow Water Table, J. Hydrometeorol., 10\(1\), 308–](#)
30 [319, doi:10.1175/2008JHM1011.1, 2009.](#)

31 [Ainsworth, E. A. and Long, S. P.: What have we learned from 15 years of free air CO₂](#)
32 [enrichment \(FACE\)? A meta analytic review of the responses of photosynthesis, canopy](#)
33 [properties and plant production to rising CO₂, New Phytol., 165\(2\), 351–372,](#)
34 [doi:10.1111/j.1469-8137.2004.01224.x, 2005.](#)

35 [Andrews, S. F., Flanagan, L. B., Sharp, E. J. and Cai, T.: Variation in water potential, hydraulic](#)
36 [characteristics and water source use in montane Douglas fir and lodgepole pine trees in](#)
37 [southwestern Alberta and consequences for seasonal changes in photosynthetic capacity, Tree](#)
38 [Physiol., 32, 146–160, doi:10.1093/treephys/tpr136, 2012.](#)

39 [Aranibar, J. N., Berry, J. A., Riley, W. J., Pataki, D. E., Law, B. E. and Ehleringer, J. R.:](#)
40 [Combining meteorology, eddy fluxes, isotope measurements, and modeling to understand](#)

Formatted: Bibliography, Widow/Orphan control,
Adjust space between Latin and Asian text, Adjust space
between Asian text and numbers

environmental controls of carbon isotope discrimination at the canopy scale, *Glob. Change Biol.*, 12(4), 710–730, 2006.

Arora, V. K., Boer, G. J., Friedlingstein, P., Eby, M., Jones, C. D., Christian, J. R., Bonan, G., Bopp, L., Brovkin, V., Cadule, P., Hajima, T., Ilyina, T., Lindsay, K., Tziputra, J. F. and Wu, T.: Carbon Concentration and Carbon Climate Feedbacks in CMIP5 Earth System Models, *J. Clim.*, 26(15), 5289–5314, doi:10.1175/jcli-d-12-00494.1, 2013.

Ballantyne, A. P., Miller, J. B. and Tans, P. P.: Apparent seasonal cycle in isotopic discrimination of carbon in the atmosphere and biosphere due to vapor pressure deficit, *Glob. Biogeochem. Cycles*, 24, GB3018, doi:10.1029/2009GB003623, 2010.

Ballantyne, A. P., Miller, J. B., Baker, I. T., Tans, P. P. and White, J. W. C.: Novel applications of carbon isotopes in atmospheric CO₂: What can atmospheric measurements teach us about processes in the biosphere?, *Biogeosciences*, 8(10), 3093–3106, 2011.

Belmecheri, S., Maxwell, R. S., Taylor, A. H., Davis, K. J., Freeman, K. H. and Munger, W. J.: Tree-ring $\delta^{13}\text{C}$ tracks flux tower ecosystem productivity estimates in a NE temperate forest, *Environ. Res. Lett.*, 9(7), 74011, doi:10.1088/1748-9326/9/7/074011, 2014.

Boisvenue, C. and Running, S. W.: Simulations show decreasing carbon stocks and potential for carbon emissions in Rocky Mountain forests over the next century, *Ecol. Appl.*, 20(5), 1302–1319, 2010.

Bowling, D. R., Pataki, D. E. and Randerson, J. T.: Carbon isotopes in terrestrial ecosystem pools and CO₂ fluxes, *New Phytol.*, 178, 24–40, doi: 10.1111/j.1469-8137.2007.02342.x, 2008.

Bowling, D. R., Ballantyne, A. P., Miller, J. B., Burns, S. P., Conway, T. J., Menzer, O., Stephens, B. B. and Vaughn, B. H.: Ecological processes dominate the $\delta^{13}\text{C}$ land disequilibrium in a Rocky Mountain subalpine forest, *Glob. Biogeochem. Cycles*, 28(4), 2013GB004686, doi:10.1002/2013GB004686, 2014a.

Bowling, D. R., Ballantyne, A. P., Miller, J. B., Burns, S. P., Conway, T. J., Menzer, O., Stephens, B. B. and Vaughn, B. H.: Ecological processes dominate the $\delta^{13}\text{C}$ land disequilibrium in a Rocky Mountain subalpine forest, *Glob. Biogeochem. Cycles*, 28(4), 2013GB004686, doi:10.1002/2013GB004686, 2014b.

Bradford, M. A., Fierer, N. and Reynolds, J. F.: Soil carbon stocks in experimental mesocosms are dependent on the rate of labile carbon, nitrogen and phosphorus inputs to soils, *Funct. Ecol.*, 22(6), 964–974, doi:10.1111/j.1365-2435.2008.01404.x, 2008.

Braswell, B. H., Sacks, W. J., Linder, E. and Schimel, D. S.: Estimating diurnal to annual ecosystem parameters by synthesis of a carbon flux model with eddy covariance net ecosystem exchange observations, *Glob. Change Biol.*, 11, 335–355, doi:10.1111/j.1365-2486.2005.00897.x, 2005.

Brüggemann, N., Gessler, A., Kayler, Z., Keel, S. G., Badeck, F., Barthel, M., Boeckx, P., Buchmann, N., Brugnoli, E., Esperschütz, J., Gavrichkova, O., Ghashghaie, J., Gomez-Casanovas, N., Keitel, C., Knohl, A., Kuptz, D., Palacio, S., Salmon, Y., Uchida, Y. and Bahn

1 [M.: Carbon allocation and carbon isotope fluxes in the plant-soil-atmosphere continuum: a](#)
2 [review, Biogeosciences, 8\(11\), 3457–3489, doi:10.5194/bg-8-3457-2011, 2011a.](#)

3 [Brüggemann, N., Gessler, A., Kayler, Z., Keel, S. G., Badeck, F., Barthel, M., Boeckx, P.,](#)
4 [Buchmann, N., Brugnoli, E., Esperschütz, J., Gavrichkova, O., Ghashghaie, J., Gomez-](#)
5 [Casanovas, N., Keitel, C., Knohl, A., Kuptz, D., Palacio, S., Salmon, Y., Uchida, Y. and Bahn-](#)
6 [M.: Carbon allocation and carbon isotope fluxes in the plant-soil-atmosphere continuum: A](#)
7 [review, Biogeosciences, 8\(11\), 3457–3489, 2011b.](#)

8 [Cernusak, L. A., Ubierna, N., Winter, K., Holtum, J. A. M., Marshall, J. D. and Farquhar, G.](#)
9 [D.: Environmental and physiological determinants of carbon isotope discrimination in](#)
10 [terrestrial plants, New Phytol., 2013, 950–965, //.](#)

11 [Collatz, G. J., Ball, J. T., Griwet, C. and Berry, J. A.: Regulation of stomatal conductances and](#)
12 [transpiration a physiological model of canopy processes, Agric. For. Meteorol., 54, 107–136.](#)
13 [1991.](#)

14 [De Kauwe, M. G., Medlyn, B. E., Zaehle, S., Walker, A. P., Dietze, M. C., Hickler, T., Jain, A.](#)
15 [K., Luo, Y., Parton, W. J., Prentice, I. C., Smith, B., Thornton, P. E., Wang, S., Wang, Y. P.,](#)
16 [Wärnlind, D., Weng, E., Crous, K. Y., Ellsworth, D. S., Hanson, P. J., Seok Kim, H., Warren, J.](#)
17 [M., Oren, R. and Norby, R. J.: Forest water use and water use efficiency at elevated CO₂: a](#)
18 [model-data intercomparison at two contrasting temperate forest FACE sites, Glob. Change](#)
19 [Biol., 19\(6\), 1759–1779, doi:10.1111/gcb.12164, 2013.](#)

20 [Desai, A. R., Moore, D. J. P., Ahue, W. K. M., Wilkes, P. T. V., De Wekker, S. F. J., Brooks-](#)
21 [B. G., Campos, T. L., Stephens, B. B., Monson, R. K., Burns, S. P., Quaife, T., Aulenbach, S.](#)
22 [M. and Schimel, D. S.: Seasonal pattern of regional carbon balance in the central Rocky](#)
23 [Mountains from surface and airborne measurements, J. Geophys. Res., 116, G04009\(4\).](#)
24 [doi:10.1029/2011JG001655, 2011.](#)

25 [Di Marco, G., Manes, F., Tricoli, D. and Vitale, E.: Fluorescence Parameters Measured](#)
26 [Concurrently with Net Photosynthesis to Investigate Chloroplastic CO₂ Concentration in](#)
27 [Leaves of Quercus ilex L., J. Plant Physiol., 136\(5\), 538–543, doi:10.1016/S0176-](#)
28 [4617\(11\)80210-5, 1990.](#)

29 [Dlugokencky, E. J., Lang, P. M., Masarie, K. A., Crotwell, A. M. and Crotwell, M. J.:](#)
30 [Atmospheric Carbon Dioxide Dry Air Mole Fractions from the NOAA ESRL Carbon Cycle](#)
31 [Cooperative Global Air Sampling network, 1968–2014, Version: 2015-08-03, Path:](#)
32 [ftp://afsp.cmdl.noaa.gov/data/trace_gases/co2/flask/surface/, 2015.](#)

33 [Ehleringer, J. R., Buchmann, N. and Flanagan, L. B.: Carbon isotope ratios in belowground](#)
34 [carbon cycle processes, Ecol. Appl., 10\(2\), 412–422, 2000.](#)

35 [Epron, D., Bahn, M., Derrien, D., Lattanzi, F. A., Pumpanen, J., Gessler, A., Höglberg, P.,](#)
36 [Maillard, P., Dannoura, M., Gérant, D. and Buchmann, N.: Pulse-labelling trees to study carbon](#)
37 [allocation dynamics: a review of methods, current knowledge and future prospects, Tree](#)
38 [Physiol., 32\(6\), 776–798, doi:10.1093/treephys/tps057, 2012.](#)

39 [Farquhar, G. D., von Caemmerer, S. and Berry, J. A.: A Biochemical Model of Photosynthetic](#)
40 [CO₂ Assimilation in Leaves of C₃ Species, Planta, 149, 78–90, 1980.](#)

- 1 [Farquhar, G. D., O'Leary, M. H. and Berry, J. A.: On the relationship between carbon isotope](#)
- 2 [discrimination and the intercellular carbon dioxide concentration in leaves, Aust. J. Plant](#)
- 3 [Physiol., 9\(2\), 121–137, 1982.](#)
- 4 [Farquhar, G. D., Ehleringer, J. R. and Hubick, K. T.: Carbon isotope discrimination and](#)
- 5 [photosynthesis, Annu. Rev. Plant Physiol. Plant Mol. Biol., 40, 503–537, 1989.](#)
- 6 [Flanagan, L. B., Cai, T., Black, T. A., Barr, A. G., McCaughey, J. H. and Margolis, H. A.:](#)
- 7 [Measuring and modeling ecosystem photosynthesis and the carbon isotope composition of](#)
- 8 [ecosystem-respired CO₂ in three boreal coniferous forests, Agric. For. Meteorol., 153, 165–](#)
- 9 [176, 2012.](#)
- 10 [Flexas, J., Ribas Carbó, M., Hanson, D. T., Bota, J., Otto, B., Cifre, J., McDowell, N., Medrano,](#)
- 11 [H. and Kaldenhoff, R.: Tobacco aquaporin NtAQP1 is involved in mesophyll conductance to](#)
- 12 [CO₂ in vivo, Plant J., 48\(3\), 427–439, doi:10.1111/j.1365-3113X.2006.02879.x, 2006.](#)
- 13 [Flexas, J., Ribas Carbo, M., Diaz Espej, A., Galmes, J. and Medrano, H.: Mesophyll](#)
- 14 [conductance to CO₂: current knowledge and future prospects, Plant Cell Environ., 31\(5\), 602–](#)
- 15 [621, 2008.](#)
- 16 [Francey, R. J., Allison, C. E., Etheridge, D. M., Trudinger, C. M., Enting, I. G., Leuenberger,](#)
- 17 [M., Langenfelds, R. L., Michel, E. and Steele, L. P.: A 1000 year high precision record of δ¹³C](#)
- 18 [in atmospheric CO₂, Tellus, 51B, 170–193, 1999.](#)
- 19 [Frank, D. C., Poulter, B., Saurer, M., Esper, J., Huntingford, C., Helle, G., Treydte, K.,](#)
- 20 [Zimmermann, N. E., Schleser, G. H., Ahlström, A., Ciais, P., Friedlingstein, P., Levis, S.,](#)
- 21 [Lomas, M., Sitch, S., Viovy, N., Andreu Hayles, L., Bednarz, Z., Berninger, F., Boettger, T.,](#)
- 22 [D'Alessandro, C. M., Daux, V., Filot, M., Grabner, M., Gutierrez, E., Haupt, M., Hidasvuori,](#)
- 23 [E., Jungner, H., Kalela-Brundin, M., Krapiec, M., Leuenberger, M., Loader, N. J., Marah, H.,](#)
- 24 [Masson Delmotte, V., Pazdur, A., Pawelczyk, S., Pierre, M., Planells, O., Pukiene, R.,](#)
- 25 [Reynolds Henne, C. E., Rinne, K. T., Saracino, A., Sonninen, E., Stievenard, M., Switsur, V.,](#)
- 26 [Szezepanek, M., Szychowska Krapiec, E., Todaro, L., Waterhouse, J. S. and Weigl, M.:](#)
- 27 [Water use efficiency and transpiration across European forests during the Anthropocene, Nat.](#)
- 28 [Clim. Change, 5\(6\), 579–583, doi:10.1038/nclimate2614, 2015.](#)
- 29 [Franks, P. J., Adams, M. A., Amthor, J. S., Barbour, M. M., Berry, J. A., Ellsworth, D. S.,](#)
- 30 [Farquhar, G. D., Ghannoum, O., Lloyd, J., McDowell, N., Norby, R. J., Tissue, D. T. and von](#)
- 31 [Caemmerer, S.: Sensitivity of plants to changing atmospheric CO₂ concentration: From the](#)
- 32 [geological past to the next century, New Phytol., 197\(4\), 1077–1094, 2013.](#)
- 33 [Friedlingstein, P., Cox, P. M., Betts, R. A., Bopp, L., von Bloh, W., Brovkin, V., Cadule, P.,](#)
- 34 [Doney, S. C., Eby, M., Fung, I. Y., Bala, G., John, J., Jones, C. D., Joos, F., Kato, T., Kawamiya,](#)
- 35 [M., Knorr, W., Lindsay, K., Matthews, H. D., Raddatz, T., Rayner, P., Reick, C., Roeckner, E.,](#)
- 36 [Schnitzler, K. G., Schnur, R., Strassmann, K., Weaver, A. J., Yoshikawa, C. and Zeng, N.:](#)
- 37 [Climate carbon cycle feedback analysis: Results from the C4MIP model intercomparison, J.](#)
- 38 [Clim., 19, 3337–3353, 2006.](#)
- 39 [Fung, I. Y., Field, C. B., Berry, J. A., Thompson, M. V., Randerson, J. T., Malmstrom, C. M.,](#)
- 40 [Vitousek, P. M., Collatz, G. J., Sellers, P. J., Randall, D. A., Denning, A. S., Badeck, F. and](#)

John, J.: Carbon 13 exchanges between the atmosphere and biosphere, *Glob. Biogeochem. Cycles*, 11(4), 507–533, 1997.

Ghimire, B., Riley, W. J., Koven, C. D., Mu, M. and Randerson, J. T.: Representing leaf and root physiological traits in CLM improves global carbon and nitrogen cycling predictions, *J. Adv. Model. Earth Syst.*, n/a n/a, doi:10.1002/2015MS000538, 2016.

Greenland, D.: The Climate of Niwot Ridge, Front Range, Colorado, U.S.A., *Arct. Alp. Res.*, 21(4), 380–391, 1989.

Hogberg, P., Hogberg, M. N., Gottlicher, S. G., Betson, N. R., Keel, S. G., Metcalfe, D. B., Campbell, C., Schindlbacher, A., Hurry, V., Lundmark, T., Linder, S. and Nasholm, T.: High temporal resolution tracing of photosynthate carbon from the tree canopy to forest soil microorganisms, *New Phytol.*, 177(1), 220–228, 2008.

Hu, J., Moore, D. J. P., Burns, S. P. and Monson, R. K.: Longer growing seasons lead to less carbon sequestration by a subalpine forest, *Glob. Change Biol.*, 16(2), 771–783, doi:10.1111/j.1365-2486.2009.01967.x, 2010.

Katul, G. G., Ellsworth, D. S. and Lai, C. T.: Modelling assimilation and intercellular CO₂ from measured conductance: a synthesis of approaches, *Plant Cell Environ.*, 23(12), 1313–1328, doi:10.1046/j.1365-3040.2000.00641.x, 2000.

Keenan, T. F., Hollinger, D. Y., Bohrer, G., Dragoni, D., Munger, J. W., Schmid, H. P. and Richardson, A. D.: Increase in forest water use efficiency as atmospheric carbon dioxide concentrations rise, *Nature*, 499(7458), 324–327, doi:10.1038/nature12291, 2013.

Kolari, P., Lappalainen, H. K., HäNninen, H. and Hari, P.: Relationship between temperature and the seasonal course of photosynthesis in Scots pine at northern timberline and in southern boreal zone, *Tellus B*, 59(3), 542–552, doi:10.1111/j.1600-0889.2007.00262.x, 2007.

Lasslop, G., Reichstein, M., Papale, D., Richardson, A., Arneth, A., Barr, A., Stoy, P. and Wohlfahrt, G.: Separation of net ecosystem exchange into assimilation and respiration using a light response curve approach: critical issues and global evaluation, *Glob. Change Biol.*, 16, 187–208, 2010.

Le Quéré, C., Moriarty, R., Andrew, R. M., Peters, G. P., Ciais, P., Friedlingstein, P., Jones, S. D., Sitch, S., Tans, P., Arneth, A., Boden, T. A., Bopp, L., Bozec, Y., Canadell, J. G., Chini, L. P., Chevallier, F., Cosea, C. E., Harris, I., Hoppema, M., Houghton, R. A., House, J. I., Jain, A. K., Johannessen, T., Kato, E., Keeling, R. F., Kitidis, V., Klein Goldewijk, K., Koven, C., Landa, C. S., Landschützer, P., Lenton, A., Lima, I. D., Marland, G., Mathis, J. T., Metzl, N., Nojiri, Y., Olsen, A., Ono, T., Peng, S., Peters, W., Pfeil, B., Poulter, B., Raupach, M. R., Regnier, P., Rödenbeck, C., Saito, S., Salisbury, J. E., Schuster, U., Schwinger, J., Séférian, R., Segschneider, J., Steinhoff, T., Stocker, B. D., Sutton, A. J., Takahashi, T., Tilbrook, B., van der Werf, G. R., Viovy, N., Wang, Y. P., Wanninkhof, R., Wiltshire, A. and Zeng, N.: Global carbon budget 2014, *Earth Syst. Sci. Data*, 7(1), 47–85, doi:10.5194/essd-7-47-2015, 2015.

Leuning, R.: A critical appraisal of a combined stomatal-photosynthesis model for C₃ plants, *Plant Cell Environ.*, 18(4), 339–355, doi:10.1111/j.1365-3040.1995.tb00370.x, 1995.

[Lin, Y. S., Medlyn, B. E., Duursma, R. A., Prentice, I. C., Wang, H., Baig, S., Eamus, D., de
 Dios, V. R., Mitchell, P., Ellsworth, D. S., de Beeck, M. O., Wallin, G., Uddling, J., Tarvainen,
 L., Linderson, M. L., Cernusak, L. A., Nippert, J. B., Oecheltree, T. W., Tissue, D. T., Martin-
 StPaul, N. K., Rogers, A., Warren, J. M., De Angelis, P., Hikosaka, K., Han, Q., Onoda, Y.,
 Gimeno, T. E., Barton, C. V. M., Bennie, J., Bonal, D., Bose, A., Löw, M., Macinins Ng, C.,
 Rey, A., Rowland, L., Setterfield, S. A., Tausz Posch, S., Zaragoza Castells, J., Broadmeadow,
 M. S. J., Drake, J. E., Freeman, M., Ghannoum, O., Hutley, L. B., Kelly, J. W., Kikuzawa, K.,
 Kolari, P., Koyama, K., Limousin, J. M., Meir, P., Lola da Costa, A. C., Mikkelsen, T. N.,
 Salinas, N., Sun, W. and Wingate, L.: Optimal stomatal behaviour around the world, *Nat. Clim.
 Change*, 5\(5\), 459–464, doi:10.1038/nclimate2550, 2015.](#)

[Mao, J., Ricciuto, D. M., Thornton, P. E., Warren, J. M., King, A. W., Shi, X., Iversen, C. M.
 and Norby, R. J.: Evaluating the Community Land Model in a pine stand with shading
 manipulations — and — <sup>13</sup></sup>CO<sub>2</sub></sub> — labeling,
Biogeosciences, 13\(3\), 641–657, doi:10.5194/bg-13-641-2016, 2016.](#)

[Martinelli, L. A., Almeida, S., Brown, I. F., Moreira, M. Z., Victoria, R. L., Sternberg, L. S. L.,
 Ferreira, C. A. C. and Thomas, W. W.: Stable carbon isotope ratio of tree leaves, boles and fine
 litter in a tropical forest in Rondonia, Brazil, *Oecologia*, 114\(2\), 170–179, 1998.](#)

[McDowell, N. G., Allen, C. D. and Marshall, L.: Growth, carbon isotope discrimination, and
 drought-associated mortality across a *Pinus ponderosa* elevational transect, *Glob. Change Biol.*,
 16\(1\), 399–415, 2010.](#)

[Medvigy, D., Wofsy, S. C., Munger, J. W., Hollinger, D. Y. and Moorcroft, P., R.: Mechanistic
 scaling of ecosystem function and dynamics in space and time: Ecosystem Demography model
 version 2, *J. Geophys. Res. Biogeosciences*, 114, G01002, doi:10.1029/2008JG000812, 2009.](#)

[Mitton, J. . and Ferrenberg, S. M.: Mountain pine beetle develops an unprecedented summer
 generation in response to climate warming, *Am. Nat.*, 179\(5\), 1–9, 2012.](#)

[Monson, R. K., Turnipseed, A. A., Sparks, J. P., Harley, P. C., Scott Denton, L. E., Sparks, K.
 and Huxman, T. E.: Carbon sequestration in a high elevation, subalpine forest, *Glob. Change
 Biol.*, 8, 459–478, 2002.](#)

[Monson, R. K., Sparks, J. P., Rosentiel, T. N., Scott Denton, L. E., Huxman, T. E., Harley, P.
 C., Turnipseed, A. A., Burns, S. P., Backlund, B. and Hu, J.: Climatic influences on net
 ecosystem CO₂ exchange during the transition from wintertime carbon source to springtime
 carbon sink in a high elevation, subalpine forest, *Oecologia*, 146, 130–147–5–169–2, 2005.](#)

[Oleson et al.: Technical Description of version 4.5 of the Community Land Model \(CLM\).
 \[online\] Available from:
\[http://www.cesm.ucar.edu/models/cesm1.2/clm/CLM45_Tech_Note.pdf\]\(http://www.cesm.ucar.edu/models/cesm1.2/clm/CLM45_Tech_Note.pdf\), 2013.](#)

[Parton, W. J., Hanson, P. J., Swanston, C., Torn, M., Trumbore, S. E., Riley, W. and Kelly, R.:
 ForCent model development and testing using the Enriched Background Isotope Study
 experiment, *J. Geophys. Res. Biogeosciences*, 115\(G4\), G04001, doi:10.1029/2009JG001193,
 2010.](#)

Peñuelas, J., Canadell, J. G. and Ogaya, R.: Increased water use efficiency during the 20th century did not translate into enhanced tree growth, *Glob. Ecol. Biogeogr.*, 20(4), 597–608, doi:10.1111/j.1466-8238.2010.00608.x, 2011.

Reichstein, M., Falge, E., Baldocchi, D., Papale, D., Aubinet, M., Berbigier, P., Bernhofer, C., Buchmann, N., Gilmanov, T., Granier, A., Grunwald, T., Havrankova, K., Ilvesniemi, H., Janous, D., Knohl, A., Laurila, T., Lohila, A., Loustau, D., Matteucci, G., Meyers, T., Miglietta, F., Ourival, J. M., Pumpanen, J., Rambal, S., Rotenberg, E., Sanz, M., Tenhunen, J., Seufert, G., Vaceari, F., Vesala, T., Yakir, D. and Valentini, R.: On the separation of net ecosystem exchange into assimilation and ecosystem respiration: review and improved algorithm, *Glob. Change Biol.*, 11(9), 1424–1439, 2005.

Riccio, D. M., Davis, K. J. and Keller, K.: A Bayesian calibration of a simple carbon cycle model: The role of observations in estimating and reducing uncertainty, *Glob. Biogeochem. Cycles*, 22, GB2030, doi:10.1029/2006GB002908, 2008.

Riccio, D. M., King, A. W., Dragoni, D. and Post, W. M.: Parameter and prediction uncertainty in an optimized terrestrial carbon cycle model: Effects of constraining variables and data record length, *J. Geophys. Res. Biogeosciences*, 116(G1), G01033, doi:10.1029/2010JG001400, 2011.

Richardson, A. D., Williams, M., Hollinger, D. Y., Moore, D. J. P., Dail, D. B., Davidson, E. A., Scott, N. A., Evans, R. S., Hughes, H., Lee, J. T., Rodrigues, C. and Savage, K.: Estimating parameters of a forest ecosystem C model with measurements of stocks and fluxes as joint constraints, *Oecologia*, 164(1), 25–40, 2010.

Roden, J. S. and Ehleringer, J. R.: Summer precipitation influences the stable oxygen and carbon isotopic composition of tree-ring cellulose in *Pinus ponderosa*, *Tree Physiol.*, 27(4), 491–501, 2007.

Rubino, M., Etheridge, D. M., Trudinger, C. M., Allison, C. E., Battle, M. O., Langenfelds, R. L., Steele, L. P., Curran, M., Bender, M., White, J. W. C., Jenk, T. M., Blunier, T. and Francey, R. J.: A revised 1000-year atmospheric $\delta^{13}\text{C}$ CO₂ record from Law Dome and South Pole, *Antarctica, J. Geophys. Res. Atmospheres*, 118(15), 8482–8499, doi:10.1002/jgrd.50668, 2013.

Sánchez-Rodríguez, J., Pérez, P. and Martínez-Carrasco, R.: Photosynthesis, carbohydrate levels and chlorophyll fluorescence estimated intercellular CO₂ in water stressed *Casuarina equisetifolia* Forst. & Forst., *Plant Cell Environ.*, 22(7), 867–873, doi:10.1046/j.1365-3040.1999.00447.x, 1999.

Saurer, M., Siegwolf, R. T. W. and Schweingruber, F. H.: Carbon isotope discrimination indicates improving water use efficiency of trees in northern Eurasia over the last 100 years, *Glob. Change Biol.*, 10(12), 2109–2120, doi:10.1111/j.1365-2486.2004.00869.x, 2004.

Saurer, M., Spahni, R., Frank, D. C., Joos, F., Leuenberger, M., Loader, N. J., McCarroll, D., Gagen, M., Poulter, B., Siegwolf, R. T. W., Andreu-Hayles, L., Boettger, T., Dorado Liñán, I., Fairchild, I. J., Friedrich, M., Gutierrez, E., Haupt, M., Hiltunen, E., Heinrich, I., Helle, G., Grudd, H., Jalkanen, R., Levanič, T., Linderholm, H. W., Robertson, I., Sonninen, E., Treydte, K., Waterhouse, J. S., Woodley, E. J., Wynn, P. M. and Young, G. H. F.: Spatial variability and

temporal trends in water use efficiency of European forests, *Glob. Change Biol.*, 20(12), 3700–3712, doi:10.1111/gcb.12717, 2014.

Schaeffer, S. M., Miller, J. B., Vaughn, B. H., White, J. W. C. and Bowling, D. R.: Long term field performance of a tunable diode laser absorption spectrometer for analysis of carbon isotopes of CO₂ in forest air, *Atmospheric Chem. Phys.*, 8, 5263–5277, 2008.

Schimel, D. T., Kittel, G. F., Running, S., Monson, R., Turnispeed, A. and Anderson, D.: Carbon sequestration studied in western U.S. mountains, *Eos Trans AGU*, 83(40), 445–449, 2002.

Scott-Denton, L. E., Sparks, K. L. and Monson, R. K.: Spatial and temporal controls of soil respiration rate in a high elevation, subalpine forest, *Soil Biol. Biochem.*, 35, 525–534, 2003.

Sellers, P. J., Randall, D. A., Collatz, G. J., Berry, J. A., Field, C. B., Dazlich, D. A., Zhang, C., Collelo, G. D. and Bounoua, L.: A revised land surface parameterization (SiB2) for atmospheric GCMs. Part I: Model formulation, *J. Clim.*, 9(4), 676–705, 1996.

Thornton, P. E. and Rosenbloom, N. A.: Ecosystem model spin-up: Estimating steady state conditions in a coupled terrestrial carbon and nitrogen cycle model, *Ecol. Model.*, 189(1–2), 25–48, doi:10.1016/j.ecolmodel.2005.04.008, 2005.

Thornton, P. E., Law, B. E., Gholz, H. L., Clark, K. L., Falge, E., Ellsworth, D. S., Golstein, A. H., Monson, R. K., Hollinger, D., Falk, M., Chen, J. and Sparks, J. P.: Modeling and measuring the effects of disturbance history and climate on carbon and water budgets in evergreen needleleaf forests, *Agric. For. Meteorol.*, 113(1–4), 185–222, 2002.

Thornton, P. E., Lamarque, J. F., Rosenbloom, N. A. and Mahowald, N. M.: Influence of carbon-nitrogen cycle coupling on land model response to CO₂ fertilization and climate variability, *Glob. Biogeochem. Cycles*, 21, GB4018, doi:10.1029/2006GB002868, 2007.

Trolier, M., White, J. W. C., Tans, P. P., Masarie, K. A. and Gemery, P. A.: Monitoring the isotopic composition of atmospheric CO₂: Measurements from the NOAA Global Air Sampling Network, *J. Geophys. Res. Atmospheres*, 101(D20), 25,897–25,916, 1996.

van der Velde, I. R., Miller, J. B., Schaefer, K., Masarie, K. A., Denning, S., White, J. W. C., Tans, P. P., Krol, M. C. and Peters, W.: Biosphere model simulations of interannual variability in terrestrial ¹³C/¹²C exchange, *Glob. Biogeochem. Cycles*, 27(3), 637–649, doi:10.1002/gbc.20048, 2013.

Wehr, R. and Saleska, S. R.: An improved isotopic method for partitioning net ecosystem atmosphere CO₂ exchange, *Agric. For. Meteorol.*, 214–215, 515–531, doi:10.1016/j.agrformet.2015.09.009, 2015.

White, J. W. C., Vaughn, B. H., Michel, S. E., University of Colorado and Institute of Arctic and Alpine Research (INSTAAR): Stable Isotopic Composition of Atmospheric Carbon Dioxide (¹³C and ¹⁸O) from the NOAA ESRL Carbon Cycle Cooperative Global Air Sampling Network, 1990–2014, Version: 2015-10-26, Path: ftp://ftp.cmdl.noaa.gov/data/trace_gases/co2c13/flask/, 2015.

White et al.: Parameterization and Sensitivity Analysis of the Biome-BGC Terrestrial Ecosystem Model: Net Primary Production Controls, [online] Available from: http://secure.ntsg.unt.edu/publications/2000/WTRN00/White_2000.pdf, 2000.

Wingate, L., Ogee, J., Burlett, R., Bose, A., Devaux, M., Grace, J., Loustau, D. and Gessler, A.: Photosynthetic carbon isotope discrimination and its relationship to the carbon isotope signals of stem, soil and ecosystem respiration, *New Phytol.*, 188(2), 576–589, 2010.

Zachle, S., Medlyn, B. E., De Kauwe, M. G., Walker, A. P., Dietze, M. C., Hickler, T., Luo, Y., Wang, Y. P., El Masri, B., Thornton, P., Jain, A., Wang, S., Warland, D., Weng, E., Parton, W., Iversen, C. M., Gallet-Budynck, A., McCarthy, H., Finzi, A., Hanson, P. J., Prentice, I. C., Oren, R. and Norby, R. J.: Evaluation of 11 terrestrial carbon–nitrogen cycle models against observations from two temperate Free-Air CO₂ Enrichment studies, *New Phytol.*, 202(3), 803–822, doi:10.1111/nph.12697, 2014.

Zarter, C. R., Demmig-Adams, B., Ebbert, V., Adamska, I. and Adams, W. W.: Photosynthetic capacity and light harvesting efficiency during the winter to spring transition in subalpine conifers, *New Phytol.*, 172(2), 283–292, doi:10.1111/j.1469-8137.2006.01816.x, 2006.

Zeng, X.: Global Vegetation Root Distribution for Land Modeling, *J. Hydrometeorol.*, 2(5), 525–530, doi:10.1175/1525-7541(2001)002<0525:GVRDFL>2.0.CO;2, 2001.

Zeng, X. and Decker, M.: Improving the Numerical Solution of Soil Moisture Based Richards Equation for Land Models with a Deep or Shallow Water Table, *J. Hydrometeorol.*, 10(1), 308–319, doi:10.1175/2008JHM1011.1, 2009.

Ainsworth, E. A. and Long, S. P.: What have we learned from 15 years of free-air CO₂ enrichment (FACE)? A meta-analytic review of the responses of photosynthesis, canopy properties and plant production to rising CO₂, *New Phytol.*, 165(2), 351–372, doi:10.1111/j.1469-8137.2004.01224.x, 2005.

Andrews, S. F., Flanagan, L. B., Sharp, E. J. and Cai, T.: Variation in water potential, hydraulic characteristics and water source use in montane Douglas fir and lodgepole pine trees in southwestern Alberta and consequences for seasonal changes in photosynthetic capacity, *Tree Physiol.*, 32, 146–160, doi:10.1093/treephys/tpr136, 2012.

Aranibar, J. N., Berry, J. A., Riley, W. J., Pataki, D. E., Law, B. E. and Ehleringer, J. R.: Combining meteorology, eddy fluxes, isotope measurements, and modeling to understand environmental controls of carbon isotope discrimination at the canopy scale, *Glob. Change Biol.*, 12(4), 710–730, 2006.

Arora, V. K., Boer, G. J., Friedlingstein, P., Eby, M., Jones, C. D., Christian, J. R., Bonan, G., Bopp, L., Brovkin, V., Cadule, P., Hajima, T., Ilyina, T., Lindsay, K., Tziputra, J. F. and Wu, T.: Carbon Concentration and Carbon Climate Feedbacks in CMIP5 Earth System Models, *J. Clim.*, 26(15), 5289–5314, doi:10.1175/jcli-d-12-00494.1, 2013.

Ballantyne, A. P., Miller, J. B. and Tans, P. P.: Apparent seasonal cycle in isotopic discrimination of carbon in the atmosphere and biosphere due to vapor pressure deficit, *Glob. Biogeochem. Cycles*, 24, GB3018, doi:10.1029/2009GB003623, 2010.

- 1 Ballantyne, A. P., Miller, J. B., Baker, I. T., Tans, P. P. and White, J. W. C.: Novel applications
2 of carbon isotopes in atmospheric CO₂: What can atmospheric measurements teach us about
3 processes in the biosphere?, *Biogeosciences*, 8(10), 3093–3106, 2011.
- 4 Ball, J. T., Woodrow, I. E. & Berry, J. A. *Progress in Photosynthesis Research*, Martinus Nijhoff
5 Publishers, 1987.
- 6 Bauerle, W. L., Oren, R., Way, D. A., Qian, S. S., Stoy, P. C., Thornton, P. E., Bowden, J. D.,
7 Hoffman, F. M. and Reynolds, R. F.: Photoperiodic regulation of the seasonal pattern of
8 photosynthetic capacity and the implications for carbon cycling, *Proc. Natl. Acad. Sci. U. S.*
9 *A.*, 109(22), 8612–8617, 2012.
- 10 Belmecheri, S., Maxwell, R. S., Taylor, A. H., Davis, K. J., Freeman, K. H. and Munger, W. J.:
11 Tree ring $\delta^{13}\text{C}$ tracks flux tower ecosystem productivity estimates in a NE temperate forest,
12 *Environ. Res. Lett.*, 9(7), 74011, doi:10.1088/1748-9326/9/7/074011, 2014.
- 13 Boisvenue, C. and Running, S. W.: Simulations show decreasing carbon stocks and potential
14 for carbon emissions in Rocky Mountain forests over the next century, *Ecol. Appl.*, 20(5),
15 1302–1319, 2010.
- 16 Bowling, D. R., Pataki, D. E. and Randerson, J. T.: Carbon isotopes in terrestrial ecosystem
17 pools and CO₂ fluxes, *New Phytol.*, 178, 24–40, doi: 10.1111/j.1469-8137.2007.02342.x,
18 2008.
- 19 Bowling, D. R., Ballantyne, A. P., Miller, J. B., Burns, S. P., Conway, T. J., Menzer, O.,
20 Stephens, B. B. and Vaughn, B. H.: Ecological processes dominate the $\delta^{13}\text{C}$ land disequilibrium
21 in a Rocky Mountain subalpine forest, *Glob. Biogeochem. Cycles*, 28(4), 2013GB004686,
22 doi:10.1002/2013GB004686, 2014a.
- 23 Bowling, D. R., Ballantyne, A. P., Miller, J. B., Burns, S. P., Conway, T. J., Menzer, O.,
24 Stephens, B. B. and Vaughn, B. H.: Ecological processes dominate the $\delta^{13}\text{C}$ land disequilibrium
25 in a Rocky Mountain subalpine forest, *Glob. Biogeochem. Cycles*, 28(4), 2013GB004686,
26 doi:10.1002/2013GB004686, 2014b.
- 27 Bradford, M. A., Fierer, N. and Reynolds, J. F.: Soil carbon stocks in experimental mesocosms
28 are dependent on the rate of labile carbon, nitrogen and phosphorus inputs to soils, *Funct. Ecol.*,
29 22(6), 964–974, doi:10.1111/j.1365-2435.2008.01404.x, 2008.
- 30 Braswell, B. H., Sacks, W. J., Linder, E. and Schimel, D. S.: Estimating diurnal to annual
31 ecosystem parameters by synthesis of a carbon flux model with eddy covariance net ecosystem
32 exchange observations, *Glob. Change Biol.*, 11, 335–355, doi:10.1111/j.1365-
33 2486.2005.00897.x, 2005.
- 34 Brüggemann, N., Gessler, A., Kayler, Z., Keel, S. G., Badeck, F., Barthel, M., Boeckx, P.,
35 Buchmann, N., Brugnoli, E., Esperschütz, J., Gavrichkova, O., Ghashghaie, J., Gomez-
36 Casanovas, N., Keitel, C., Knohl, A., Kuptz, D., Palacio, S., Salmon, Y., Uchida, Y. and Bahn, M.:
37 Carbon allocation and carbon isotope fluxes in the plant soil atmosphere continuum: a
38 review, *Biogeosciences*, 8(11), 3457–3489, doi:10.5194/bg-8-3457-2011, 2011.

Collatz, G. J., Ball, J. T., Grivet, C. and Berry, J. A.: Regulation of stomatal conductances and transpiration a physiological model of canopy processes, *Agric. For. Meteorol.*, 54, 107–136, 1991.

De Kauwe, M. G., Medlyn, B. E., Zachle, S., Walker, A. P., Dietze, M. C., Hickler, T., Jain, A. K., Luo, Y., Parton, W. J., Prentice, I. C., Smith, B., Thornton, P. E., Wang, S., Wang, Y. P., Wärlind, D., Weng, E., Crous, K. Y., Ellsworth, D. S., Hanson, P. J., Seok Kim, H., Warren, J. M., Oren, R. and Norby, R. J.: Forest water use and water use efficiency at elevated CO₂: a model-data intercomparison at two contrasting temperate forest FACE sites, *Glob. Change Biol.*, 19(6), 1759–1779, doi:10.1111/gcb.12164, 2013.

Desai, A. R., Moore, D. J. P., Ahue, W. K. M., Wilkes, P. T. V., De Wekker, S. F. J., Brooks, B. G., Campos, T. L., Stephens, B. B., Monson, R. K., Burns, S. P., Quaife, T., Aulenbach, S. M. and Schimel, D. S.: Seasonal pattern of regional carbon balance in the central Rocky Mountains from surface and airborne measurements, *J. Geophys. Res.*, 116, G04009(4), doi:10.1029/2011JG001655, 2011.

Di Mareo, G., Manes, F., Tricoli, D. and Vitale, E.: Fluorescence Parameters Measured Concurrently with Net Photosynthesis to Investigate Chloroplastic CO₂ Concentration in Leaves of *Quercus ilex* L., *J. Plant Physiol.*, 136(5), 538–543, doi:10.1016/S0176-1617(11)80210-5, 1990.

Dlugokencky, E. J., Lang, P. M., Masarie, K. A., Crotwell, A. M. and Crotwell, M. J.: Atmospheric Carbon Dioxide Dry Air Mole Fractions from the NOAA ESRL Carbon Cycle Cooperative Global Air Sampling network, 1968–2014, Version: 2015-08-03, Path: ftp://ftp.emdl.noaa.gov/data/trace_gases/co2/flask/surface/, 2015.

Ehleringer, J. R., Buchmann, N. and Flanagan, L. B.: Carbon isotope ratios in belowground carbon cycle processes, *Ecol. Appl.*, 10(2), 412–422, 2000.

Epron, D., Bahn, M., Derrien, D., Lattanzi, F. A., Pumpanen, J., Gessler, A., Höglberg, P., Maillard, P., Dannoura, M., Gérant, D. and Buchmann, N.: Pulse labelling trees to study carbon allocation dynamics: a review of methods, current knowledge and future prospects, *Tree Physiol.*, 32(6), 776–798, doi:10.1093/treephys/tps057, 2012.

Farquhar, G. D., von Caemmerer, S. and Berry, J. A.: A Biochemical Model of Photosynthetic CO₂ Assimilation in Leaves of C₃ Species, *Planta*, 149, 78–90, 1980.

Farquhar, G. D., O’Leary, M. H. and Berry, J. A.: On the relationship between carbon isotope discrimination and the intercellular carbon dioxide concentration in leaves, *Aust. J. Plant Physiol.*, 9(2), 121–137, 1982.

Farquhar, G. D., Ehleringer, J. R. and Hubick, K. T.: Carbon isotope discrimination and photosynthesis, *Annu. Rev. Plant Physiol. Plant Mol. Biol.*, 40, 503–537, 1989.

Flanagan, L. B., Cai, T., Black, T. A., Barr, A. G., McCaughey, J. H. and Margolis, H. A.: Measuring and modeling ecosystem photosynthesis and the carbon isotope composition of ecosystem-respired CO₂ in three boreal coniferous forests, *Agric. For. Meteorol.*, 153, 165–176, 2012.

- 1 Flexas, J., Ribas Carbó, M., Hanson, D. T., Bota, J., Otto, B., Cifre, J., McDowell, N., Medrano,
2 H. and Kaldenhoff, R.: Tobacco aquaporin NtAQP1 is involved in mesophyll conductance to
3 CO₂ in vivo, *Plant J.*, 48(3), 427–439, doi:10.1111/j.1365-3113X.2006.02879.x, 2006.
- 4 Flexas, J., Ribas Carbo, M., Diaz Espej, A., Galmes, J. and Medrano, H.: Mesophyll
5 conductance to CO₂: current knowledge and future prospects, *Plant Cell Environ.*, 31(5), 602–
6 621, 2008.
- 7 Francey, R. J., Allison, C. E., Etheridge, D. M., Trudinger, C. M., Enting, I. G., Leuenberger,
8 M., Langenfelds, R. L., Michel, E. and Steele, L. P.: A 1000-year high-precision record of δ¹³C
9 in atmospheric CO₂, *Tellus*, 51B, 170–193, 1999.
- 10 Frank, D. C., Poulter, B., Saurer, M., Esper, J., Huntingford, C., Helle, G., Treydte, K.,
11 Zimmermann, N. E., Schleser, G. H., Ahlström, A., Ciais, P., Friedlingstein, P., Levis, S.,
12 Lomas, M., Sitch, S., Viovy, N., Andreu-Hayles, L., Bednarz, Z., Berninger, F., Boettger, T.,
13 D'Alessandro, C. M., Daux, V., Filot, M., Grabner, M., Gutierrez, E., Haupt, M., Hidasvuori,
14 E., Jungner, H., Kalela-Brundin, M., Krapiec, M., Leuenberger, M., Loader, N. J., Marah, H.,
15 Masson-Delmotte, V., Pazdur, A., Paweleczyk, S., Pierre, M., Planells, O., Pukiene, R.,
16 Reynolds-Henne, C. E., Rinne, K. T., Saracino, A., Sonninen, E., Stievenard, M., Switsur, V.,
17 R., Szezepanek, M., Szychowska Krapiec, E., Todaro, L., Waterhouse, J. S. and Weigl, M.:
18 Water-use efficiency and transpiration across European forests during the Anthropocene, *Nat.*
19 *Clim. Change*, 5(6), 579–583, doi:10.1038/nclimate2614, 2015.
- 20 Franks, P. J., Adams, M. A., Amthor, J. S., Barbour, M. M., Berry, J. A., Ellsworth, D. S.,
21 Farquhar, G. D., Ghanoum, O., Lloyd, J., McDowell, N., Norby, R. J., Tissue, D. T. and von
22 Caemmerer, S.: Sensitivity of plants to changing atmospheric CO₂ concentration: From the
23 geological past to the next century, *New Phytol.*, 197(4), 1077–1094, 2013.
- 24 Friedlingstein, P., Cox, P. M., Betts, R. A., Bopp, L., von Bloh, W., Brovkin, V., Cadule, P.,
25 Doney, S. C., Eby, M., Fung, I. Y., Bala, G., John, J., Jones, C. D., Joos, F., Kato, T., Kawamiya,
26 M., Knorr, W., Lindsay, K., Matthews, H. D., Raddatz, T., Rayner, P., Reick, C., Roeckner, E.,
27 Schnitzler, K. G., Schnur, R., Strassmann, K., Weaver, A. J., Yoshikawa, C. and Zeng, N.:
28 Climate carbon cycle feedback analysis: Results from the C4MIP model intercomparison, *J.*
29 *Clim.*, 19, 3337–3353, 2006.
- 30 Fung, I. Y., Field, C. B., Berry, J. A., Thompson, M. V., Randerson, J. T., Malmstrom, C. M.,
31 Vitousek, P. M., Collatz, G. J., Sellers, P. J., Randall, D. A., Denning, A. S., Badeck, F. and
32 John, J.: Carbon-13 exchanges between the atmosphere and biosphere, *Glob. Biogeochem.*
33 *Cycles*, 11(4), 507–533, 1997.
- 34 Ghimire, B., Riley, W. J., Koven, C. D., Mu, M. and Randerson, J. T.: Representing leaf and
35 root physiological traits in CLM improves global carbon and nitrogen cycling predictions, *J.*
36 *Adv. Model. Earth Syst.*, n/a–n/a, doi:10.1002/2015MS000538, 2016.
- 37 Greenland, D.: The Climate of Niwot Ridge, Front Range, Colorado, U.S.A., *Arct. Alp. Res.*,
38 21(4), 380–391, 1989.
- 39 Hogberg, P., Hogberg, M. N., Gottlicher, S. G., Betson, N. R., Keel, S. G., Metcalfe, D. B.,
40 Campbell, C., Schindlbacher, A., Hurry, V., Lundmark, T., Linder, S. and Nasholm, T.: High

temporal resolution tracing of photosynthate carbon from the tree canopy to forest soil microorganisms, *New Phytol.*, 177(1), 220–228, 2008.

Hu, J., Moore, D. J. P., Burns, S. P. and Monson, R. K.: Longer growing seasons lead to less carbon sequestration by a subalpine forest, *Glob. Change Biol.*, 16(2), 771–783, doi:10.1111/j.1365-2486.2009.01967.x, 2010.

Katul, G. G., Ellsworth, D. S. and Lai, C. T.: Modelling assimilation and intercellular CO₂ from measured conductance: a synthesis of approaches, *Plant Cell Environ.*, 23(12), 1313–1328, doi:10.1046/j.1365-3040.2000.00641.x, 2000.

Keenan, T. F., Hollinger, D. Y., Bohrer, G., Dragoni, D., Munger, J. W., Schmid, H. P. and Richardson, A. D.: Increase in forest water use efficiency as atmospheric carbon dioxide concentrations rise, *Nature*, 499(7458), 324–327, doi:10.1038/nature12291, 2013.

Kolari, P., Lappalainen, H. K., HäNninen, H. and Hari, P.: Relationship between temperature and the seasonal course of photosynthesis in Scots pine at northern timberline and in southern boreal zone, *Tellus B*, 59(3), 542–552, doi:10.1111/j.1600-0889.2007.00262.x, 2007.

Lasslop, G., Reichstein, M., Papale, D., Richardson, A., Arneth, A., Barr, A., Stoy, P. and Wohlfahrt, G.: Separation of net ecosystem exchange into assimilation and respiration using a light response curve approach: critical issues and global evaluation, *Glob. Change Biol.*, 16, 187–208, 2010.

Le Quéré, C., Moriarty, R., Andrew, R. M., Peters, G. P., Ciais, P., Friedlingstein, P., Jones, S. D., Sitch, S., Tans, P., Arneth, A., Boden, T. A., Bopp, L., Bozec, Y., Canadell, J. G., Chini, L. P., Chevallier, F., Cosca, C. E., Harris, I., Hoppema, M., Houghton, R. A., House, J. I., Jain, A. K., Johannessen, T., Kato, E., Keeling, R. F., Kitidis, V., Klein Goldewijk, K., Koven, C., Landa, C. S., Landschützer, P., Lenton, A., Lima, I. D., Marland, G., Mathis, J. T., Metzl, N., Nojiri, Y., Olsen, A., Ono, T., Peng, S., Peters, W., Pfeil, B., Poulter, B., Raupach, M. R., Regnier, P., Rödenbeck, C., Saito, S., Salisbury, J. E., Schuster, U., Schwinger, J., Séférian, R., Segschneider, J., Steinhoff, T., Stocker, B. D., Sutton, A. J., Takahashi, T., Tilbrook, B., van der Werf, G. R., Viovy, N., Wang, Y. P., Wanninkhof, R., Wiltshire, A. and Zeng, N.: Global carbon budget 2014, *Earth Syst. Sci. Data*, 7(1), 47–85, doi:10.5194/essd-7-47-2015, 2015.

Leuning, R.: A critical appraisal of a combined stomatal-photosynthesis model for C₃ plants, *Plant Cell Environ.*, 18(4), 339–355, doi:10.1111/j.1365-3040.1995.tb00370.x, 1995.

Lin, Y. S., Medlyn, B. E., Duursma, R. A., Prentice, I. C., Wang, H., Baig, S., Eamus, D., de Dios, V. R., Mitchell, P., Ellsworth, D. S., de Beeck, M. O., Wallin, G., Uddling, J., Tarvainen, L., Linderson, M. L., Cernusak, L. A., Nippert, J. B., Oecheltree, T. W., Tissue, D. T., Martin-StPaul, N. K., Rogers, A., Warren, J. M., De Angelis, P., Hikosaka, K., Han, Q., Onoda, Y., Gimeno, T. E., Barton, C. V. M., Bennie, J., Bonal, D., Bosc, A., Löw, M., Macinins Ng, C., Rey, A., Rowland, L., Setterfield, S. A., Tausz Posch, S., Zaragoza Castells, J., Broadmeadow, M. S. J., Drake, J. E., Freeman, M., Ghannoum, O., Hutley, L. B., Kelly, J. W., Kikuzawa, K., Kolari, P., Koyama, K., Limousin, J. M., Meir, P., Lola da Costa, A. C., Mikkelsen, T. N., Salinas, N., Sun, W. and Wingate, L.: Optimal stomatal behaviour around the world, *Nat. Clim. Change*, 5(5), 459–464, doi:10.1038/nclimate2550, 2015.

Mao, J., Ricciuto, D. M., Thornton, P. E., Warren, J. M., King, A. W., Shi, X., Iversen, C. M. and Norby, R. J.: Evaluating the Community Land Model in a pine stand with shading manipulations and $\delta^{13}\text{C}$ labeling, *Biogeosciences*, 13(3), 641–657, doi:10.5194/bg-13-641-2016, 2016.

Martinelli, L. A., Almeida, S., Brown, I. F., Moreira, M. Z., Victoria, R. L., Sternberg, L. S. L., Ferreira, C. A. C. and Thomas, W. W.: Stable carbon isotope ratio of tree leaves, boles and fine litter in a tropical forest in Rondonia, Brazil, *Oecologia*, 114(2), 170–179, 1998.

McDowell, N. G., Allen, C. D. and Marshall, L.: Growth, carbon isotope discrimination, and drought-associated mortality across a *Pinus ponderosa* elevational transect, *Glob. Change Biol.*, 16(1), 399–415, 2010.

Medvigy, D., Wofsy, S. C., Munger, J. W., Hollinger, D. Y. and Moorcroft, P., R.: Mechanistic scaling of ecosystem function and dynamics in space and time: Ecosystem Demography model version 2, *J. Geophys. Res. Biogeosciences*, 114, G01002, doi:10.1029/2008JG000812, 2009.

Mitton, J. . and Ferrenberg, S. M.: Mountain pine beetle develops an unprecedented summer generation in response to climate warming, *Am. Nat.*, 179(5), 1–9, 2012.

Monson, R. K., Turnipseed, A. A., Sparks, J. P., Harley, P. C., Scott Denton, L. E., Sparks, K. and Huxman, T. E.: Carbon sequestration in a high elevation, subalpine forest, *Glob. Change Biol.*, 8, 459–478, 2002.

Monson, R. K., Sparks, J. P., Rosentiel, T. N., Scott Denton, L. E., Huxman, T. E., Harley, P. C., Turnipseed, A. A., Burns, S. P., Backlund, B. and Hu, J.: Climatic influences on net ecosystem CO_2 exchange during the transition from wintertime carbon source to springtime carbon sink in a high elevation, subalpine forest, *Oecologia*, 146, 130–147–5–169–2, 2005.

Oleson et al.: Technical Description of version 4.5 of the Community Land Model (CLM), [online] Available from: http://www.cesm.ucar.edu/models/cesm1.2/clm/CLM45_Tech_Note.pdf, 2013.

Parton, W. J., Hanson, P. J., Swanston, C., Torn, M., Trumbore, S. E., Riley, W. and Kelly, R.: ForCent model development and testing using the Enriched Background Isotope Study experiment, *J. Geophys. Res. Biogeosciences*, 115(G4), G04001, doi:10.1029/2009JG001193, 2010.

Parton, W.J., Schimel, D.S., Cole, C.V., Ojima, D.S., 1987. Analysis of factors controlling soil organic matter levels in great plains grasslands. *Soil Sci. Soc. Am. J.* 51 (5).

Peñuelas, J., Canadell, J. G. and Ogaya, R.: Increased water use efficiency during the 20th century did not translate into enhanced tree growth, *Glob. Ecol. Biogeogr.*, 20(4), 597–608, doi:10.1111/j.1466-8238.2010.00608.x, 2011.

Reichstein, M., Falge, E., Baldocchi, D., Papale, D., Aubinet, M., Berbigier, P., Bernhofer, C., Buchmann, N., Gilmanov, T., Granier, A., Grunwald, T., Havrankova, K., Ilvesniemi, H., Janous, D., Knohl, A., Laurila, T., Lohila, A., Loustau, D., Matteucci, G., Meyers, T., Miglietta, F., Ourival, J. M., Pumpanen, J., Rambal, S., Rotenberg, E., Sanz, M., Tenhunen, J., Seufert, G., Vaccari, F., Vesala, T., Yakir, D. and Valentini, R.: On the separation of net ecosystem

exchange into assimilation and ecosystem respiration: review and improved algorithm, *Glob. Change Biol.*, 11(9), 1424–1439, 2005.

Ricciuto, D. M., Davis, K. J. and Keller, K.: A Bayesian calibration of a simple carbon cycle model: The role of observations in estimating and reducing uncertainty, *Glob. Biogeochem. Cycles*, 22, GB2030, doi:10.1029/2006GB002908, 2008.

Ricciuto, D. M., King, A. W., Dragoni, D. and Post, W. M.: Parameter and prediction uncertainty in an optimized terrestrial carbon cycle model: Effects of constraining variables and data record length, *J. Geophys. Res. Biogeosciences*, 116(G1), G01033, doi:10.1029/2010JG001400, 2011.

Richardson, A. D., Williams, M., Hollinger, D. Y., Moore, D. J. P., Dail, D. B., Davidson, E. A., Scott, N. A., Evans, R. S., Hughes, H., Lee, J. T., Rodrigues, C. and Savage, K.: Estimating parameters of a forest ecosystem C model with measurements of stocks and fluxes as joint constraints, *Oecologia*, 164(1), 25–40, 2010.

Roden, J. S. and Ehleringer, J. R.: Summer precipitation influences the stable oxygen and carbon isotopic composition of tree ring cellulose in *Pinus ponderosa*, *Tree Physiol.*, 27(4), 491–501, 2007.

Rubino, M., Etheridge, D. M., Trudinger, C. M., Allison, C. E., Battle, M. O., Langenfelds, R. L., Steele, L. P., Curran, M., Bender, M., White, J. W. C., Jenk, T. M., Blunier, T. and Francey, R. J.: A revised 1000 year atmospheric $\delta^{13}\text{C}$ -CO₂ record from Law Dome and South Pole, Antarctica, *J. Geophys. Res. Atmospheres*, 118(15), 8482–8499, doi:10.1002/jgrd.50668, 2013.

Sanchez-Rodriguez, J., Perez, P. and Martinez-Carrasco, R.: Photosynthesis, carbohydrate levels and chlorophyll fluorescence estimated intercellular CO₂ in water stressed *Casuarina equisetifolia* Forst. & Forst., *Plant Cell Environ.*, 22(7), 867–873, doi:10.1046/j.1365-3040.1999.00447.x, 1999.

Saurer, M., Siegwolf, R. T. W. and Schweingruber, F. H.: Carbon isotope discrimination indicates improving water use efficiency of trees in northern Eurasia over the last 100 years, *Glob. Change Biol.*, 10(12), 2109–2120, doi:10.1111/j.1365-2486.2004.00869.x, 2004.

Saurer, M., Spahni, R., Frank, D. C., Joos, F., Leuenberger, M., Loader, N. J., McCarroll, D., Gagen, M., Poulter, B., Siegwolf, R. T. W., Andreu-Hayles, L., Boettger, T., Dorado-Liñán, I., Fairchild, I. J., Friedrich, M., Gutierrez, E., Haupt, M., Hiltavuori, E., Heinrich, I., Helle, G., Grudd, H., Jalkanen, R., Levanič, T., Linderholm, H. W., Robertson, I., Sonninen, E., Treydte, K., Waterhouse, J. S., Woodley, E. J., Wynn, P. M. and Young, G. H. F.: Spatial variability and temporal trends in water use efficiency of European forests, *Glob. Change Biol.*, 20(12), 3700–3712, doi:10.1111/geb.12717, 2014.

Schaeffer, S. M., Miller, J. B., Vaughn, B. H., White, J. W. C. and Bowling, D. R.: Long term field performance of a tunable diode laser absorption spectrometer for analysis of carbon isotopes of CO₂ in forest air, *Atmospheric Chem. Phys.*, 8, 5263–5277, 2008.

Schimel, D. T., Kittel, G. F., Running, S., Monson, R., Turnispeed, A. and Anderson, D.: Carbon sequestration studied in western U.S. mountains, *Eos Trans AGU*, 83(40), 445–449, 2002.

Scholze, M., Kaplan, J. O., Knorr, W. and Heimann, M.: Climate and interannual variability of the atmosphere-biosphere $^{13}\text{CO}_2$ flux, *Geophys. Res. Lett.*, 30(2), 1097, doi:10.1029/2002GL015631, 2003.

Scott-Denton, L. E., Sparks, K. L. and Monson, R. K.: Spatial and temporal controls of soil respiration rate in a high elevation, subalpine forest, *Soil Biol. Biochem.*, 35, 525–534, 2003.

Seibt, U., Rajabi, A., Griffiths, H. and Berry, J. A.: Carbon isotopes and water-use efficiency: sense and sensitivity, *Oecologia*, 155(3), 441–454, 2008.

Sellers, P. J., Randall, D. A., Collatz, G. J., Berry, J. A., Field, C. B., Dazlich, D. A., Zhang, C., Collelo, G. D. and Bounoua, L.: A revised land surface parameterization (SiB2) for atmospheric GCMs. Part I: Model formulation, *J. Clim.*, 9(4), 676–705, 1996.

Thornton, P. E. and Rosenbloom, N. A.: Ecosystem model spin-up: Estimating steady state conditions in a coupled terrestrial carbon and nitrogen cycle model, *Ecol. Model.*, 189(1–2), 25–48, doi:10.1016/j.ecolmodel.2005.04.008, 2005.

Thornton, P. E., Law, B. E., Gholz, H. L., Clark, K. L., Falge, E., Ellsworth, D. S., Golstein, A. H., Monson, R. K., Hollinger, D., Falk, M., Chen, J. and Sparks, J. P.: Modeling and measuring the effects of disturbance history and climate on carbon and water budgets in evergreen needleleaf forests, *Agric. For. Meteorol.*, 113(1–4), 185–222, 2002.

Thornton, P. E., Lamarque, J. F., Rosenbloom, N. A. and Mahowald, N. M.: Influence of carbon-nitrogen cycle coupling on land model response to CO_2 fertilization and climate variability, *Glob. Biogeochem. Cycles*, 21, GB4018, doi:10.1029/2006GB002868, 2007.

Tomaszewski, T. and Sievering, H.: Canopy uptake of atmospheric N deposition at a conifer forest: Part II—response of chlorophyll fluorescence and gas exchange parameters, *Tellus B*, 59(3) [online] Available from: <http://www.tellusb.net/index.php/tellusb/article/view/17021> (Accessed 28 May 2015), 2007.

Trolier, M., White, J. W. C., Tans, P. P., Masarie, K. A. and Gemery, P. A.: Monitoring the isotopic composition of atmospheric CO_2 : Measurements from the NOAA Global Air Sampling Network, *J. Geophys. Res. Atmospheres*, 101(D20), 25,897–25,916, 1996.

van der Velde, I. R., Miller, J. B., Schaefer, K., Masarie, K. A., Denning, S., White, J. W. C., Tans, P. P., Krol, M. C. and Peters, W.: Biosphere model simulations of interannual variability in terrestrial $^{13}\text{C}/^{12}\text{C}$ exchange, *Glob. Biogeochem. Cycles*, 27(3), 637–649, doi:10.1002/gbc.20048, 2013.

Wehr, R. and Saleska, S. R.: An improved isotopic method for partitioning net ecosystem-atmosphere CO_2 exchange, *Agric. For. Meteorol.*, 214–215, 515–531, doi:10.1016/j.agrformet.2015.09.009, 2015.

White, J. W. C., Vaughn, B. H., Michel, S. E., University of Colorado and Institute of Arctic and Alpine Research (INSTAAR): Stable Isotopic Composition of Atmospheric Carbon Dioxide (^{13}C and ^{18}O) from the NOAA ESRL Carbon Cycle Cooperative Global Air Sampling Network, 1990–2014, Version: 2015-10-26, Path: http://aftp.emdl.noaa.gov/data/trace_gases/co2e13/flask/, 2015.

White et al.: Parameterization and Sensitivity Analysis of the Biome-BGC Terrestrial Ecosystem Model: Net Primary Production Controls, [online] Available from: http://secure.ntsg.unt.edu/publications/2000/WTRN00/White_2000.pdf, 2000.

Wingate, L., Ogee, J., Burlett, R., Bosc, A., Devaux, M., Grace, J., Loustau, D. and Gessler, A.: Photosynthetic carbon isotope discrimination and its relationship to the carbon isotope signals of stem, soil and ecosystem respiration, *New Phytol.*, 188(2), 576–589, 2010.

Yohe, G.W., R.D. Lasco, Q.K. Ahmad, N.W. Arnell, S.J. Cohen, C. Hope, A.C. Janetos and R.T. Perez, 2007: Perspectives on climate change and sustainability. *Climate Change 2007: Impacts, Adaptation and Vulnerability. Contribution of Working Group II to the Fourth Assessment Report of the Intergovernmental Panel on Climate Change*, M.L. Parry, O.F. Canziani, J.P. Palutikof, P.J. van der Linden and C.E. Hanson, Eds., Cambridge University Press, Cambridge, UK, Section 20.6, pgs. 821–825

Zaehle, S., Medlyn, B. E., De Kauwe, M. G., Walker, A. P., Dietze, M. C., Hickler, T., Luo, Y., Wang, Y. P., El Masri, B., Thornton, P., Jain, A., Wang, S., Warland, D., Weng, E., Parton, W., Iversen, C. M., Gallet-Budynnek, A., McCarthy, H., Finzi, A., Hanson, P. J., Prentice, I. C., Oren, R. and Norby, R. J.: Evaluation of 11 terrestrial carbon–nitrogen cycle models against observations from two temperate Free Air CO₂ Enrichment studies, *New Phytol.*, 202(3), 803–822, doi:10.1111/nph.12697, 2014.

Zarter, C. R., Demmig-Adams, B., Ebbert, V., Adamska, I. and Adams, W. W.: Photosynthetic capacity and light harvesting efficiency during the winter to spring transition in subalpine conifers, *New Phytol.*, 172(2), 283–292, doi:10.1111/j.1469-8137.2006.01816.x, 2006.

Zeng, X.: Global Vegetation Root Distribution for Land Modeling, *J. Hydrometeorol.*, 2(5), 525–530, doi:10.1175/1525-7541(2001)002<0525:GVRDFL>2.0.CO;2, 2001.

Zeng, X. and Decker, M.: Improving the Numerical Solution of Soil Moisture Based Richards Equation for Land Models with a Deep or Shallow Water Table, *J. Hydrometeorol.*, 10(1), 308–319, doi:10.1175/2008JHM1011.1, 2009.

Table 1. List of symbols used.

| Symbol | Description | Unit or Unit Symbol |
|-------------------|--|--------------------------------------|
| α | Fractionation factor (R_a/R_{GPP}) | dimensionless |
| β_t | Soil water stress parameter (BTRAN) | dimensionless |
| Δ_{canopy} | photosynthetic carbon isotope discrimination | ‰ |
| $\delta^{13}C$ | $^{13}C/^{12}C$ isotope composition (relative to VPDB) | ‰ |
| δ_{atm} | $\delta^{13}C$ of atmospheric CO ₂ | ‰ |
| δ_{ER} | $\delta^{13}C$ of ecosystem respiration | ‰ |
| δ_{GPP} | $\delta^{13}C$ of net photosynthetic assimilation | ‰ |
| Γ^* | CO ₂ compensation point | Pa |
| A_c | Enzyme-limiting rate of photosynthetic assimilation | $\mu\text{mol m}^{-2} \text{s}^{-1}$ |
| A_j | Light-limiting rate of photosynthetic assimilation | $\mu\text{mol m}^{-2} \text{s}^{-1}$ |
| A_p | Product-limiting rate of photosynthetic assimilation | $\mu\text{mol m}^{-2} \text{s}^{-1}$ |
| A_n | net photosynthetic assimilation | $\mu\text{mol m}^{-2} \text{s}^{-1}$ |
| Resp_d | Leaf-level respiration | $\mu\text{mol m}^{-2} \text{s}^{-1}$ |

| | | |
|------------------------|--|--|
| a_{R25} | Specific activity of Rubisco at 25°C | $\mu\text{mol g}^{-1} \text{Rubisco s}^{-1}$ |
| b | Minimum stomatal conductance | $\mu\text{mol m}^{-2} \text{s}^{-1}$ |
| CF_{alloc} | Actual carbon allocated to biomass (N-limited) | $\text{gC m}^{-2} \text{s}^{-1}$ |
| $CF_{\text{av.alloc}}$ | Maximum carbon available for allocation to biomass | $\text{gC m}^{-2} \text{s}^{-1}$ |
| CF_{GPPpot} | Potential gross primary production (non N-limited) | $\text{gC m}^{-2} \text{s}^{-1}$ |
| c_a | Atmospheric CO ₂ partial pressure | Pa |
| c_i | Leaf intercellular CO ₂ partial pressure | Pa |
| c_i^* | Leaf intracellular CO ₂ partial pressure, (N-limited) | Pa |
| c_s | Leaf surface CO ₂ partial pressure | Pa |
| e_l | Saturation vapor pressure | Pa |
| e_s | Water vapor pressure at leaf surface | Pa |
| E_T | Ecosystem Transpiration | $\mu\text{mol m}^{-2} \text{s}^{-1}$ |
| ER | Ecosystem respiration | $\mu\text{mol m}^{-2} \text{s}^{-1}$ |
| GPP | Gross primary productivity (photosynthesis) | $\mu\text{mol m}^{-2} \text{s}^{-1}$ |
| F_{LNR} | Fraction of leaf nitrogen within Rubisco | $\text{gN Rubisco g}^{-1} \text{N}$ |
| F_{NR} | Total Rubisco mass per nitrogen mass within Rubisco | $\text{g Rubisco g}^{-1} \text{N Rubisco}$ |
| f_{df} | V_{cmax} scaling factor | dimensionless |
| f_{dreg} | Nitrogen photosynthetic downregulation factor | dimensionless |
| g_b | Leaf boundary layer conductance | $\mu\text{mol m}^{-2} \text{s}^{-1}$ |
| g_s | Leaf stomatal conductance | $\mu\text{mol m}^{-2} \text{s}^{-1}$ |
| h_s | Leaf surface relative humidity | Pa Pa ⁻¹ |
| K_c | CO ₂ Michaelis-Menten constant | Pa |
| K_o | O ₂ Michaelis-Menten constant | Pa |
| LE | Latent heat flux | W m^{-2} |
| m | Stomatal slope (Ball Berry conductance model) | dimensionless |
| Na | Leaf nitrogen concentration | $\text{gN m}^{-2} \text{leaf area}$ |
| NEE | Net ecosystem exchange | $\mu\text{mol m}^{-2} \text{s}^{-1}$ |
| NPP | Net primary production | $\mu\text{mol m}^{-2} \text{s}^{-1}$ |
| o_i | O ₂ atmospheric partial pressure | Pa |
| PFT | Plant functional type | N/A |
| P_{atm} | Atmospheric pressure | Pa |
| R_a | Isotopic ratio of canopy air | $^{13}\text{C}/^{12}\text{C}$ |
| R _{GPP} | Isotopic ratio of net photosynthetic assimilation | $^{13}\text{C}/^{12}\text{C}$ |
| R _{VPDB} | Isotopic ratio of Vienna Pee Dee Belemnite standard | $^{13}\text{C}/^{12}\text{C}$ |
| r | Fraction of roots (for β_i) | dimensionless |
| $V_{\text{cmax}25}$ | Maximum carboxylation rate at 25°C | $\mu\text{mol m}^{-2} \text{s}^{-1}$ |
| V_{cmax} | Maximum carboxylation rate at leaf temperature | $\mu\text{mol m}^{-2} \text{s}^{-1}$ |
| VPD | Vapor pressure deficit | Pa |
| w | Plant wilting factor (for β_i) | dimensionless |
| WUE | Water use efficiency, ground area basis | $\mu\text{mol C mol H}_2\text{O}^{-1}$ |
| iWUE | Intrinsic water use efficiency, leaf area basis | $\mu\text{mol C mol H}_2\text{O}^{-1}$ |

1 Table 2. CLM 4.5 model formulation description based upon timing of nitrogen limitation.
2 Pre-photosynthetic and post-photosynthetic nitrogen limitation are achieved through $V_{\text{cmax}25}$
3 calibration (equation 17) and f_{dreg} (equation 8) respectively.

| Formulation | Pre-Photosynthetic Nitrogen Limitation | Post-Photosynthetic Nitrogen Limitation | Impacts c_i^*/c_a & discrimination | Impacts g_s and A_n |
|---|--|---|--------------------------------------|-------------------------|
| <i>Limited nitrogen (default)</i> | Yes (weak) | Yes, $f_{\text{dreg}} > 0$ | Yes | No |
| <i>Unlimited nitrogen</i> | Yes (strong) | No, $f_{\text{dreg}} = 0$ | Yes | Yes |
| <i>No downregulation discrimination</i> | Yes (weak) | Yes, $f_{\text{dreg}} > 0$ | No | No |

1 Table 3. CLM 4.5 key parameter values for all model formulations

| Parameter | Description | Value | Units |
|-------------------------------|--|--------|---------------------------------|
| <i>froot_leaf</i> | new fine root C per new leaf C | 0.5 | gC gC ⁻¹ |
| <i>froot_cn</i> | fine root (C:N) | 55 | gC gN ⁻¹ |
| <i>leaf_long</i> | leaf longevity | 5 | years |
| <i>leaf_cn</i> | leaf (C:N) | 50 | gC gN ⁻¹ |
| <i>lflitcn</i> | leaf litter (C:N) | 100 | gC gN ⁻¹ |
| <i>slatop</i> | specific leaf area (top canopy) | 0.007 | m ² gC ⁻¹ |
| <i>stem_leaf</i> | new stem C per new leaf C | 2 | gC gC ⁻¹ |
| <i>mp</i> | stomatal slope | 9 | |
| <i>croot_stem</i> | coarse root: stem allocation | 0.3 | gC gC ⁻¹ |
| <i>deadwood_cn</i> | dead wood (C:N) | 500 | gC gN ⁻¹ |
| <i>livewood_cn</i> | live wood (C:N) | 50 | gC gN ⁻¹ |
| <i>flnr</i> | fraction of leaf nitrogen within Rubisco enzyme | 0.0509 | gN gN ⁻¹ |
| <i>decomp_depth_e_folding</i> | controls soil decomposition rate with depth | 20 | m |

2

3

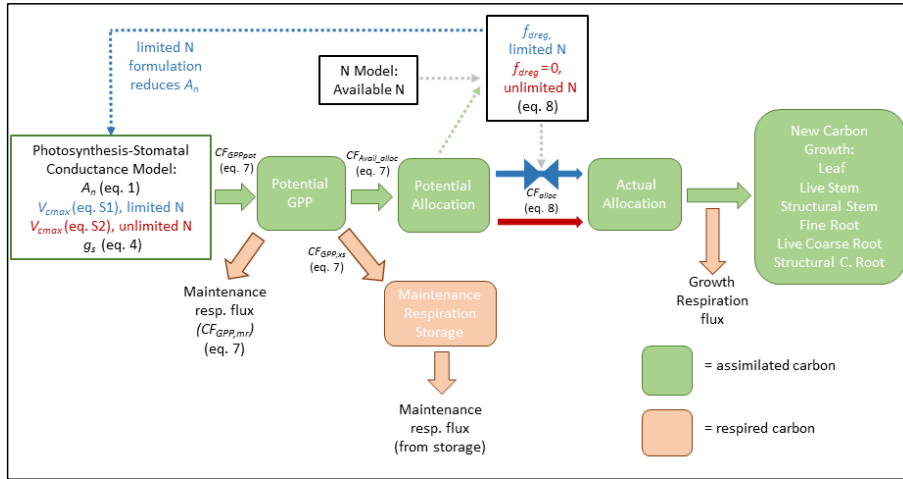


Figure 1: A simplified representation within CLM 4.5 of assimilation and allocation of carbon for conifer species. The colored boxes and solid arrows represent carbon pools and carbon fluxes respectively. The clear background boxes represent CLM sub-models. Nitrogen limitation is applied if the available N cannot meet the demand determined by the available carbon for allocation demand from C:N ratio based on (CF_{Avail_alloc}) and the C:N biomass ratio. The blue and red text and arrows represent the limited and unlimited nitrogen formulations respectively. The no-downregulation discrimination formulation is exactly the same as the limited N formulation in this schematic.

Formatted: Line spacing: 1.5 lines

Formatted: Not Superscript/ Subscript

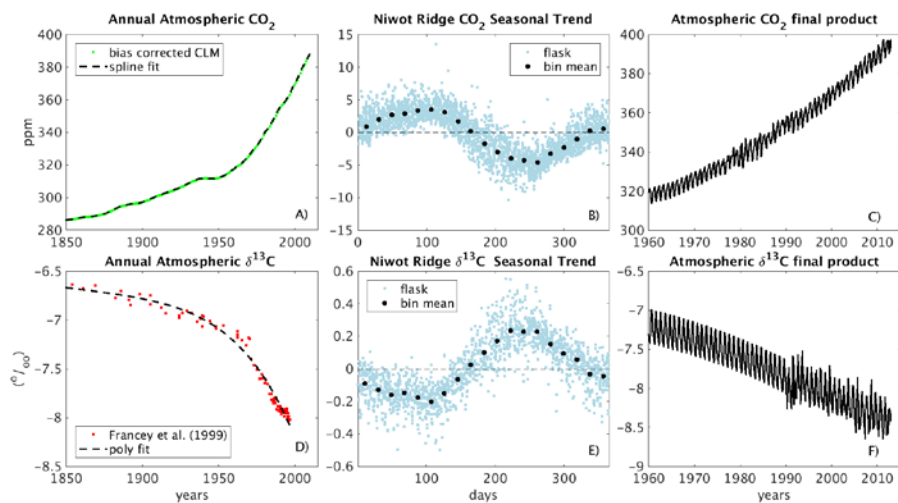
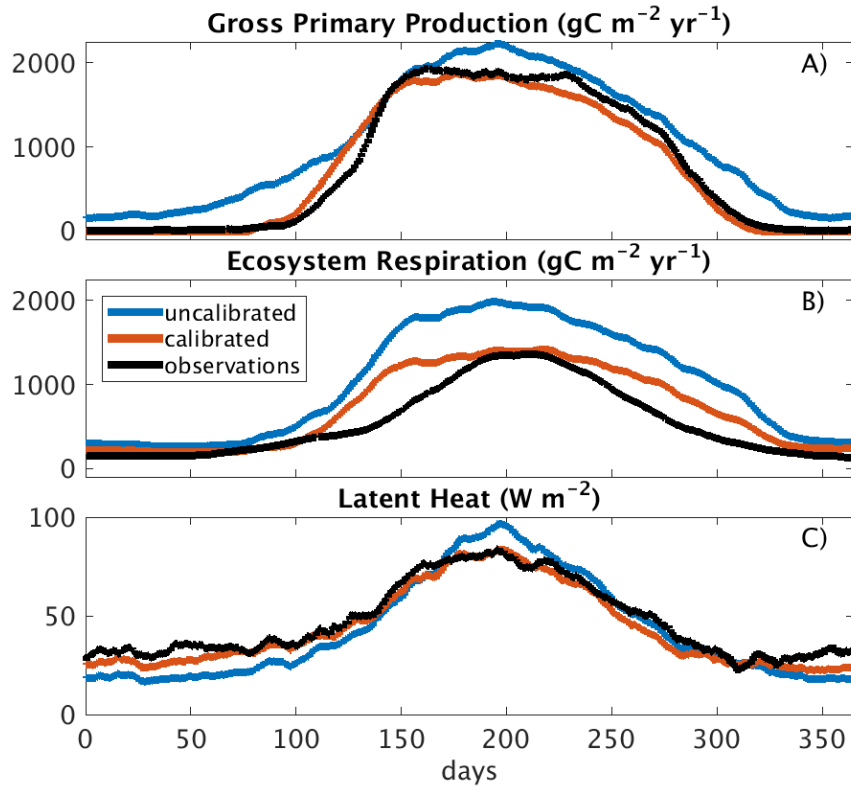
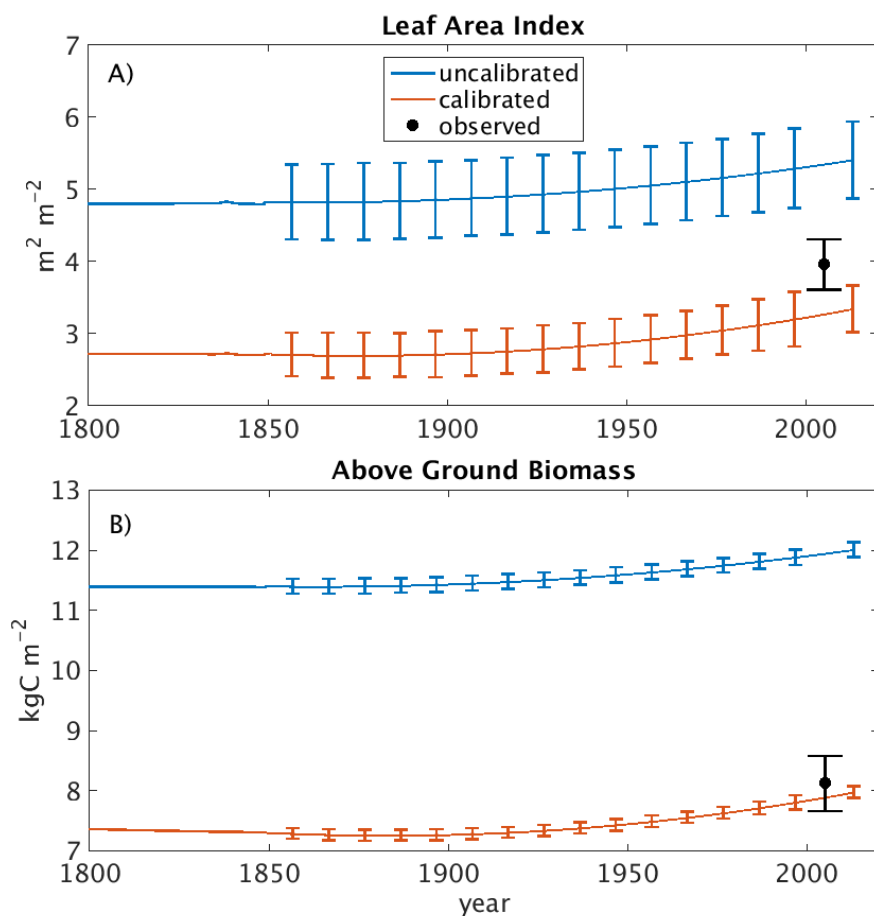


Figure 2. Niwot Ridge synthetic data product for atmospheric CO₂ concentration (c_a) (panels A, B and C top row) and $\delta^{13}\text{C}$ of CO₂ (δ_{atm}) (panels D, E and F bottom row). The final time series (panels C and F right column) was used as a boundary condition for CLM, and created by combining the annual trends reported by Francey et al. (1999) adjusted for Niwot Ridge (left column) with the mean seasonal cycles measured at Niwot Ridge (panels B and E middle column).



1
2 Figure 3. Seasonal averages (1999-2013) of simulated and observed land-atmosphere fluxes
3 for A) gross primary production (GPP) B) ecosystem respiration (ER) and C) latent heat (LE)
4 for the *limited nitrogen* simulation. The ‘observations’ are taken from the Ameriflux L2
5 processed eddy covariance flux tower data, partitioned into GPP and ER using the method of
6 Reichstein et al. (2005). The *uncalibrated* simulation represents the CLM simulation without
7 V_{max} scaling and the *calibrated* simulation represents the CLM run using the V_{max} scaling
8 approach.
9



1
2 Figure 4. Simulation of A) leaf area index and B) above ground biomass for both uncalibrated
3 and calibrated (V_{cmax} downscaled, *limited nitrogen*) simulation. Observations are from
4 Bradford et al. (2008) with uncertainty bars representing standard error. Uncertainty bars on
5 simulated runs represent 95% confidence of biomass variation as a result of cycling the site
6 level meteorology observations.

7

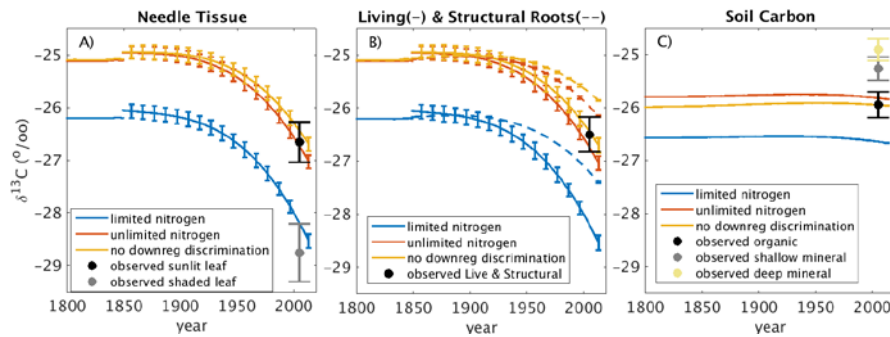
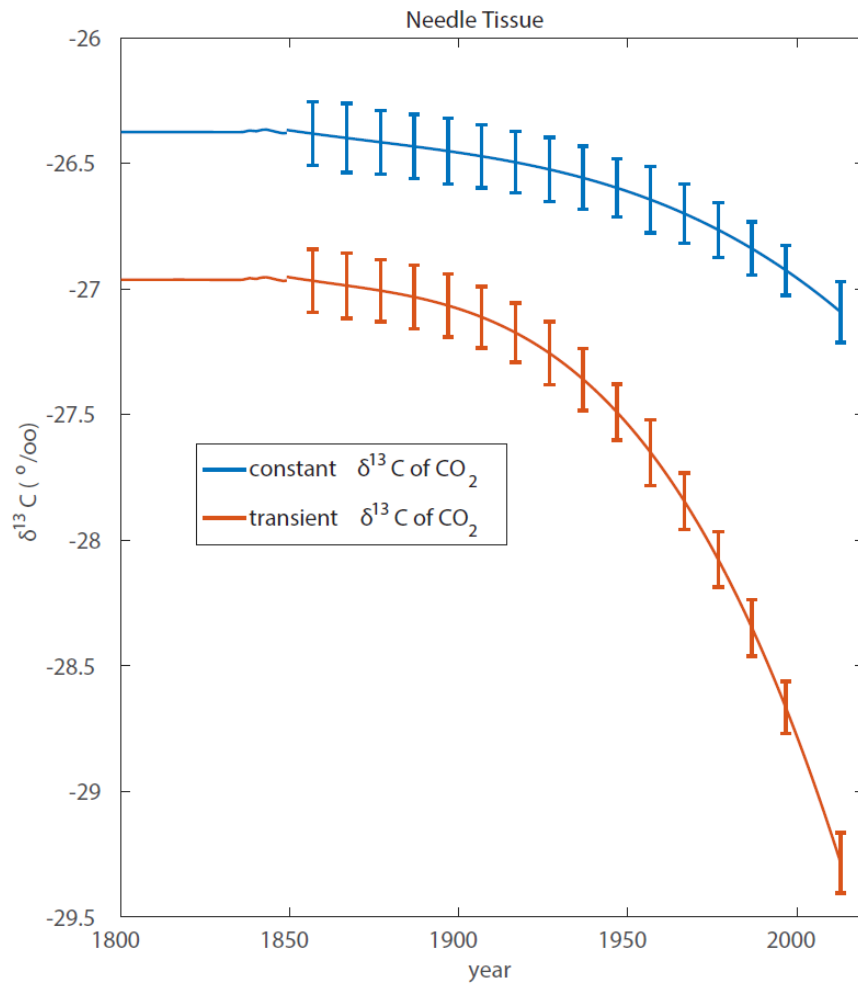


Figure 5. Simulation of $\delta^{13}\text{C}$ of **A)** bulk needle tissue, **B)** bulk roots and **C)** bulk soil carbon. A description of model formulations are provided in Table (2). Uncertainty bars for simulations represent 95% confidence intervals of $\delta^{13}\text{C}$ variation as a result of cycling the site level meteorology observations. The observed values are from Schaeffer et al. (2008) with uncertainty bars representing standard error. Solid lines and dashed lines in middle panel represent living roots and structural roots respectively.



1
2 Figure 6. Simulation of $\delta^{13}\text{C}$ of needle tissue using the *limited nitrogen* (default) CLM run. In
3 the *constant $\delta^{13}\text{C}$ of CO_2* (δ_{atm}) simulation the model boundary condition was -6 ‰, whereas
4 the *transient δ_{atm}* simulation varied over time (Figure 2).

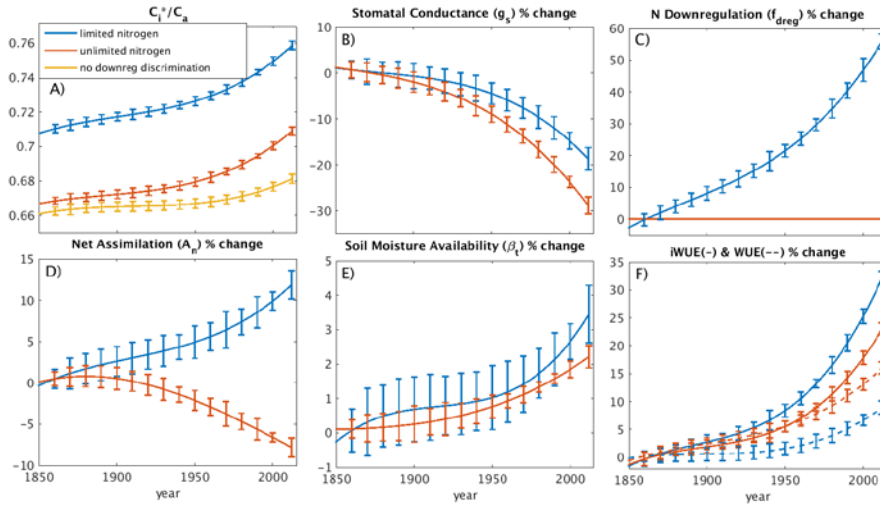


Figure 7. Diagnostic model variables that explain the discrimination trends (Figure 5) for the three model formulations as described in Table (2) for A) c_i^*/c_a , B) g_s , C) f_{dreg} , D) A_n , E) β_s , and F) the water use efficiency (WUE) and intrinsic water use efficiency (iWUE). Where the *no downregulation discrimination* simulation is not shown, it was identical to the *limited nitrogen* simulation. Uncertainty bars represent 95 % confidence intervals of diagnostic variable variation as a result of cycling the site level meteorology observations. The dashed lines represent WUE and the solid lines represent iWUE in panel F.

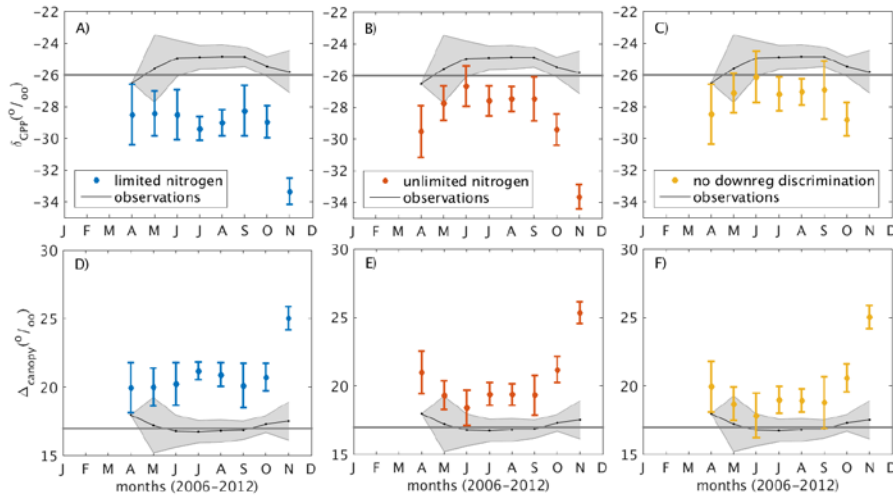


Figure 8. The seasonal pattern of photosynthetic discrimination as shown through δ_{GPP} (panels A, B and C top row) and Δ_{canopy} (panels D, E, and F bottom row). Uncertainty bars represent 95% confidence bounds of simulated monthly average values from 2006-2012. Gray-shaded observation bounds represent 95% confidence intervals of 'observed' monthly average values based upon isotopic mixing model using Reichstein et al. (2005) partitioning of net ecosystem exchange flux described by (Bowling et al. 2014). The horizontal lines at $\delta^{13}C$ of -26 ‰ (panels A, B and C top row) and 17 ‰ (panels A, B and C bottom row) are included for reference.

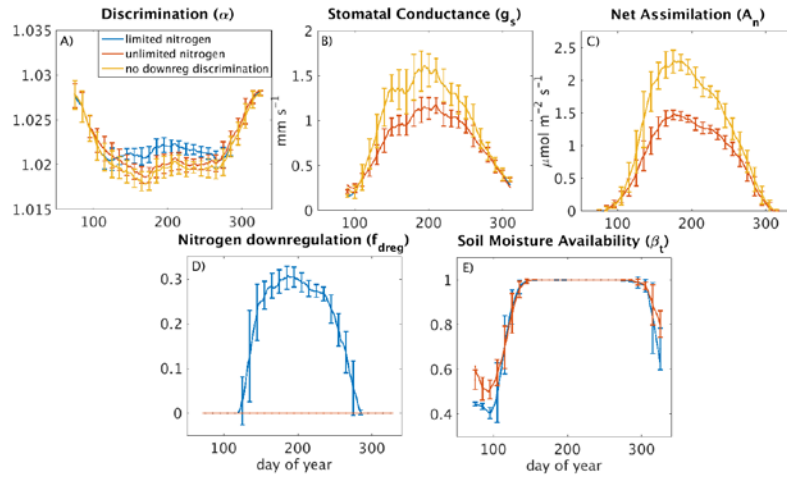


Figure 9. The seasonal pattern of discrimination (panel A) and diagnostic variables that explain the discrimination pattern in Figure (8). The individual tiles provide behavior from days 75-325 for A) α , B) g_s , C) A_n , D) f_{dreg} , and E) β_s . Where the *no downregulation discrimination* model simulation is not shown, it is identical to the *limited nitrogen* simulation. Uncertainty bars represent 95 % confidence intervals of inter-annual variation from 2006-2012.

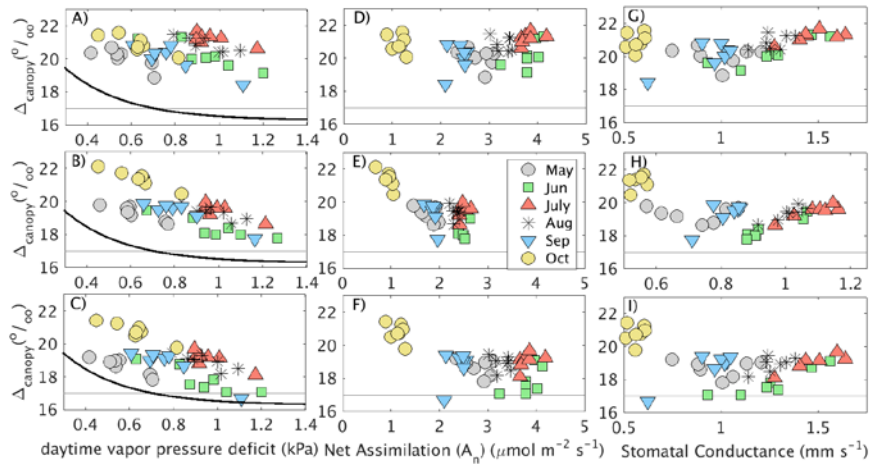


Figure 10. Relationship between monthly average photosynthetic discrimination and monthly average vapor pressure deficit (panels A, B and C^{1st}-column), A_n (panels D, E and F^{2nd}-column) and g_s (G, H and I^{3rd}-column) from 2006-2012. The rows represent the limited nitrogen (panels A, D and G^{row-1}), unlimited nitrogen (panels B, E and H^{row-2}), and no downregulation discrimination (panels C, F and I^{row-3}) simulations. The black lines in panels A, B and C^{1st}-column are based on an exponential fitted line from the observed relationship at Niwot Ridge (Bowling et al. 2014). The horizontal lines represent $\delta^{13}\text{C}$ of 17 ‰ and are included for reference.